Gator Locator

NASA Student Launch 2022 Preliminary Design Review

University of Florida
Swamp Launch Rocket Team

MAE-A 324
November 1, 2021

Table of Contents

Table of Figures

Table of Tables

1. Summary of Report

1.1 Team Summary

Swamp Launch Rocket Team
University of Florida – MAE-A 324
939 Center Drive
Gainesville, FL 32611

1.1.1 Team Mentor

Jimmy Yawn
NAR #85660, TRA #09266 Level 3 Certified
jimmy.yawn@sfcollege.edu
(352) 281-2025

1.1.2 Hours

The total number of hours spent on the design, planning, meeting, and writing of the Preliminary Design Review was 405 hours.

1.2 Launch Vehicle Summary

The launch vehicle consists of a 4 in. diameter airframe and has an overall length of 114 in. There are three main sections: the nosecone section, forward section, and aft section (Table 1). The forward section includes an avionics bay. The aft section houses a payload bay. A payload remains securely contained in the aft section throughout the duration of flight. The launch vehicle has a dual deploy recovery system comprised of two parachutes: a 72 in. main parachute and a 24 in. drogue parachute. The launch vehicle has a total weight of 434 oz. including the motor. The center of gravity is located 6.5 ft. from the tip of the nosecone and the center of pressure is located 7.6 ft. from the tip of the nosecone, as calculated in OpenRocket. The resulting stability margin is 3.26. A 12 ft. 1515 launch rail will be used. The Aerotech L1090W is the selected motor. The overall lengths and masses of each of the three main sections of the launch vehicle were tabulated (Table 1).

Section	Exterior Length (in.)	Overall Mass (oz.)
Nosecone	20	27
Forward Section	38	118
Aft Section	56	281
Total	**114**	**426**

Table 1: Masses and lengths of launch vehicle.

1.3 Payload Summary

Payload Title: Land-Mark Watney

The payload uses a hybrid inertial and image-based navigation system. Two downward-facing cameras capture images of the terrain during ascent, which are then compared to the pre uploaded image of the field using the SIFT algorithm to determine the vehicle's mid-flight location relative to known landmarks. The offset between the vehicle's last determined mid-flight position and final landing location is calculated using Inertial Measurement Unit (IMU) data. This helps determine the final landing location of the rocket.

2. Changes Made Since Proposal

2.1 Changes Made to Launch Vehicle

2.1.1 Changes Made to Vehicle Design

There have been changes to the vehicle design to improve the overall structure.

- The bulkhead material has been changed from plywood to Type II PVC based on the results of the material selection decision matrices (3.1.3.4). The change was made to improve the design of the bulkheads since Type II PVC received the highest score of the materials considered. Type II PVC has the best assembly since only one component needs to be manufactured. While the other materials perform better in other objectives, the objectives were either not weighted highly or Type II PVC still performs sufficiently well.

2.1.2 Changes Made to Avionics and Recovery Subsystem

There have been changes made to the selected parachutes and altimeters. The parachute changes were made to stay within the kinetic energy requirements of the launch vehicle, as the parachutes used during the proposal were no longer able to reach satisfactory descent rates in OpenRocket.

- The main parachute has changed to the 72 in. Iris Ultra made by Fruity Chutes due to the decision matrices presented in 3.2.2.5.
- The drogue parachute has changed to the 24 in. Skyangle C3 Drogue due to the decision matrices presented in 3.2.2.6.
- The primary altimeter has changed to a Stratologger CF due to the decision matrices presented in 3.2.2.3.
- The secondary altimeter has changed to an Entacore AIM altimeter due to the decision matrices presented in 3.2.2.3.

2.2 Changes Made to Payload

2.2.1 Changes Made to Electronics

There have been changes made to the payload electronics to allow for easier implementation.

- A digital signal processor was replaced with a Raspberry Pi to reduce the complexity of software development.

2.2.2 Changes Made to Mechanical Structure

There have been changes made to the different mechanical systems to better improve the functionality of the payload. These changes were made to better suit the payload sled and support the onboard electronics.

- PCB attachment method was changed to threaded inserts to fasten a Raspberry Pi to a payload sled.
- Battery compartment dimensions were changed to sustain a tighter fit around batteries.
- Camera housings were altered to allow updated camera lenses to take images of the launch field.
- A new latch system with increased thread engagement was designed to retain the payload sled to a rail system.

2.2.3 Changes Made to Software Design

There have been changes made to software design to reduce development time.

- The software algorithm was changed from using a modified CNN to using SIFT algorithm.

2.3 Changes Made to Project Plan

There have been changes made to the project plan schedule to improve the timeline of the project.

- The Subscale and payload prototype purchase order timeframe was changed. Instead of being in early November, the new timeframe was from October 5th to October 18th. This allowed more time for the required hardware to be shipped and increased manufacturing time.

3. Vehicle Criteria

3.1 Selection, Design, and Rationale of Launch Vehicle

3.1.1 Mission Statement

The mission is to perform a successful flight that meets the team defined criteria (6.1.1). The mission success criteria of the flight includes a flight path within the altitude range of 4100 ft to 4700 ft and a recoverable launch vehicle that successfully carries the payload. The launch vehicle must be able to be relaunched and must not sustain irreparable damage in order to be considered recoverable. In order to successfully carry the payload, the launch vehicle must not interfere with the payload performance.

3.1.2 Design Alternatives

The alternate design that was considered included two payload bays, resulting in an overall alternative launch vehicle design (Figure 1).

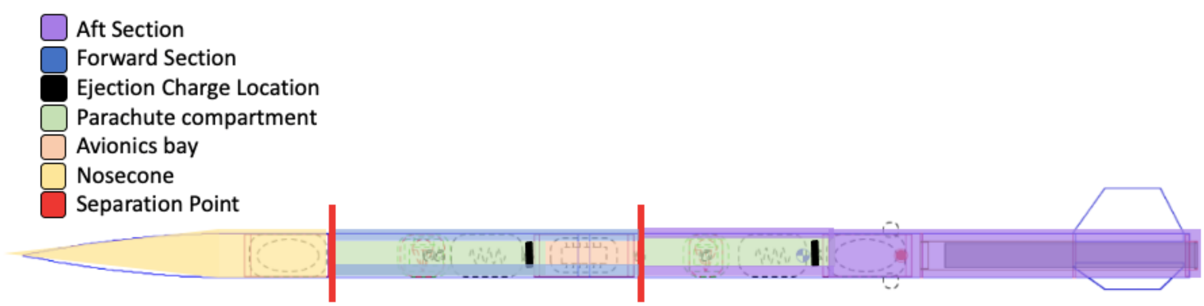

Figure 1: Alternative launch vehicle design.

This design involved mounting cameras on the forward section in addition to the aft section, which resulted in the need for two separate payload bays. One payload was located in the nosecone coupler and the other was located in the aft section. However, the cameras located on the forward section would not be able to collect useful data due to the amount of movement the forward section would undergo during descent. As a result, the design with the cameras mounted on the forward section was not selected. Since the design was altered to remove the cameras mounted on the forward section, the payload bay was no longer required in the nosecone coupler.

A separation point is the point where two sections of the launch vehicle that are connected during flight via a coupler and shear pins meet. During descent, the shear pins will be sheared with the use of ejection charges set off by a programmed altimeter to deploy either the drogue or main parachute. The portion of the payload located in the nosecone coupler of the launch vehicle was included as a part of the nosecone section during separation. The main parachute was still located in the forward section, and the drogue parachute was located in the aft section.

3.1.3 Material Selection

Objectives and decision matrices were used to evaluate alternative materials for each component. The following qualitative score assignment table was used when evaluating objectives based on qualitative parameters (Table 2).

Qualitative Score Assignments:	
Great	10
Good	8
Okay	6
Fair	4
Poor	2

Table 2: Qualitative scoring assignments.

3.1.3.1 Nosecone

Potential nosecone materials were evaluated with defined evaluation criteria in order to select a final material.

3.1.3.1.1 Evaluation Criteria

Decision matrices were used to evaluate the nosecone material (Table 3). The scores were calculated using linear scoring. The best concept was assigned a score of 10 out of 10 points.

Nosecone			**Polypropylene**			**G12 Fiberglass**		
Objective	Weighting Factor	Parameter	Mag.	Score	Value	Mag.	Score	Value
Cost	0.20	USD/lb	48.35	10.0	2.00	79.95	6.05	1.21
Density	0.35	lb/in^3	0.033	4.93	1.72	0.067	10.0	3.50
Tensile strength	0.45	ksi	6.5	0.57	0.25	115.0	10.0	4.50
Overall value					**3.98**			**9.21**

Table 3: Nosecone material decision matrix.

Cost is the total price (USD/lb) of a 4 in. diameter nosecone. Cost was taken into consideration because it is unnecessary to purchase expensive materials if sufficient materials are available at a lower price. Since the price of the nosecone was relatively low in comparison to the overall cost of the launch vehicle, the cost was weighted at only 20%. Therefore, the material with the lowest cost received a score of 10 out of 10.

Density is the measurement of mass per unit of volume (lb/in^3) of the material. In high powered rockets, the center of gravity helps keep the body stable during flight, especially if it is further in front of the center of pressure. The nosecone's density can raise the center of gravity of the rocket and increase the stability, ensuring that it will fly its predicted path. Since a higher density nosecone was needed to help increase the stability, the density was weighted at 35%. Therefore, the material with the highest density received a score of 10 out of 10.

Tensile strength is the maximum stress (ksi) the nosecone can withstand before breaking. The nosecone needs to be able to withstand the stresses it experiences from going against the drag of the air, the ejection charges, the shock cord, the impact on the ground. A failure of the nosecone could not only throw the rocket off course, but also result in a failure in recovery and payload development. Therefore, this could result in a failure of completing the mission. As a result, tensile strength was weighted at 45%. Therefore, the design with the highest tensile strength received a score of 10 out of 10.

3.1.3.1.2 Alternative Materials

A polypropylene nosecone was considered. However, it had a much lower tensile strength in comparison to fiberglass, which resulted in a score of 0.57 for the tensile strength objective. In addition, it also had a lower density compared to fiberglass, and as a result, polypropylene received a lower score for the density objective. While polypropylene received a higher score in terms of cost, the cost was not weighted as highly as the other objectives. Therefore, polypropylene had a lower overall score and was not selected for the nosecone material.

3.1.3.1.3 Selected Material

A G12 fiberglass nosecone was selected since it had the highest density and tensile strength. The higher density was ideal since it would raise the center of gravity, and by extension, the stability would also increase. Furthermore, fiberglass also had the advantage of being stronger than polypropylene and more suited to withstanding the forces experienced during flight. Since these factors were weighted the highest, the fiberglass nosecone received the highest overall score of 9.21.

3.1.3.2 Airframe and Couplers

Potential materials were evaluated with defined evaluation criteria (3.1.3.2.1 Evaluation Criteria) in order to select a final material for the airframe and couplers.

3.1.3.2.1 Evaluation Criteria

Decision matrices were used to evaluate the airframe and coupler material (Table 4). The scores were calculated using linear scoring. The best concept was assigned a score of 10 out of 10 points.

Airframe			**G12 Fiberglass**			**Blue tube**		
Objective	Weighting Factor	Parameter	Mag.	Score	Value	Mag.	Score	Value
Cost	0.20	USD/in	1.95	3.54	0.71	0.83	8.31	1.66
Density	0.25	lb/in^3	0.067	6.87	1.72	0.059	7.80	1.95
Compressive strength	0.40	ksi	37.1	10.0	4.00	5.08	1.37	0.55
Machinability	0.15	resources required	Okay	6.00	0.90	Good	8.00	1.20
Overall value					**7.33**			**5.36**
Airframe			**Quantum tube**			**Phenolic**		
Objective	Weighting Factor	Parameter	Mag.	Score	Value	Mag.	Score	Value
Cost	0.20	USD/in	0.81	8.52	1.70	0.69	10.0	2.00
Density	0.25	lb/in^3	0.048	9.65	2.41	0.046	10.0	2.50
Compressive strength	0.40	ksi	18.2	4.92	1.97	13.5	3.63	1.45
Machinability	0.15	resources required	Good	8.00	1.20	Good	8.00	1.20
Overall value					**7.28**			**7.15**

Table 4: Airframe and coupler material decision matrix.

Cost is the price (USD/in) of the material. Cost was taken into consideration because it is unnecessary to purchase expensive materials if sufficient materials are available at a lower price. Although the cost of the airframe was higher than the cost of other components, the budget was not heavily limited. Therefore, cost was weighted at 20%. The material with the lowest cost received a score of 10 out of 10.

Density is the mass per unit volume (lb/in^3) of a material. It was weighted at 20% because the rocket must minimize weight to optimize its flight. Since the airframe contributed significantly to the overall weight of the launch vehicle, it was weighted at 25%. The material with the lowest density received a score of 10 out of 10.

Compressive strength is the maximum amount of compressive stress (ksi) a material can withstand before it fractures. It was weighted at 25% because the airframe and couplers must be able to withstand significant compressive stresses. For instance, after takeoff, the motor pushes upward on the airframe, compressing the body of the rocket. Furthermore, when the rocket lands there are often significant compressive stresses that the airframe and couplers must be able to withstand to complete multiple flights and remain in the competition. The material with the highest compressive strength received a score of 10 out of 10.

Machinability is the ease at which the material can be manufactured based on the safety concerns that each material presented, and the resources required for safe manufacturing. Materials that presented greater safety concerns had a lower ease of machinability because the hazards must be mitigated and required more resources. The machinability scoring was determined using a qualitative scale of poor, fair, okay, good, and great. The corresponding quantitative values were 2, 4, 6, 8, and 10. Since the team has the capability to manufacture all the materials, machinability was weighted at 15%. Therefore, the material with the best machinability received a score of 10 out of 10.

3.1.3.2.2 Alternative Materials

Blue tube, quantum tube, and phenolic were considered for the airframe and couplers; however, they were not selected due to their lower compressive strength in comparison to fiberglass. Blue tube had a significantly lower compressive strength in comparison to fiberglass, and as a result, received a much lower score of 1.37. Quantum tube and phenolic also had lower compressive strengths, and received scores of 4.92 and 3.63, respectively. Although blue tube, quantum tube, and phenolic received higher scores in terms of cost, density, and machinability, the compressive strength was the highest weighted objective. Therefore, blue tube, quantum tube, and phenolic had lower overall scores in comparison to fiberglass and were not selected as the material for the airframe and couplers.

3.1.3.2.3 Selected Material

G12 fiberglass was selected as the airframe and couplers material (Table 4: Airframe and coupler material decision matrix.Table 4). Fiberglass was the ideal material for the airframe and couplers due to its strength and durability. Additionally, it was important that the selected coupler material matched that of the airframe, as it ensured a proper fit between sections of the launch vehicle. The higher compressive strength was ideal because the airframe and couplers must withstand significant stresses over the duration of flight and across multiple flights. While fiberglass received a lower score in terms of cost, density, and machinability, the most significant objective was compressive strength to produce a recoverable launch vehicle.

3.1.3.3 Motor Tube

Potential motor tube materials were evaluated with defined evaluation criteria (3.1.3.3.1 Evaluation Criteria) in order to select a final material.

3.1.3.3.1 Evaluation Criteria

Decision matrices were used to evaluate the motor tube material (Table 5). The scores were calculated using linear scoring. The best concept was assigned a score of 10 out of 10 points.

Motor tube			G12 Fiberglass			Blue tube		
Objective	Weighting Factor	Parameter	Mag.	Score	Value	Mag.	Score	Value
Cost	0.20	USD/in	1.20	3.33	0.67	0.40	10.0	2.00
Density	0.25	lb/in^3	0.067	6.87	1.72	0.059	7.80	1.95
Compressive Strength	0.40	ksi	37.1	10.0	4.00	5.08	1.37	0.55
Machinability	0.15	resources required	Fair	4.00	0.60	Good	8.00	1.20
Overall value					**6.32**			**3.70**
Motor tube			**Quantum tube**			**Phenolic**		
Objective	Weighting Factor	Parameter	Mag.	Score	Value	Mag.	Score	Value
Cost	0.20	USD/in	0.96	4.17	0.830	0.71	5.63	1.13
Density	0.25	lb/in^3	0.048	9.58	2.40	0.046	10.0	2.50
Compressive Strength	0.40	ksi	18.2	4.92	1.97	13.5	3.63	1.45
Machinability	0.15	resources required	Good	8.00	1.20	Good	8.00	1.20
Overall value					**5.57**			**5.15**

Table 5: Motor tube material decision matrix.

Cost is the price (USD/in) of the material. Cost was taken into consideration because it is unnecessary to purchase expensive materials if sufficient materials are available at a lower price. Although the cost of the motor tube was higher than the cost of many of the other components, the budget was not heavily limited. Therefore, cost was weighted at 20%. The material with the lowest cost received a score of 10 out of 10.

Density is the mass per unit volume (lb/in^3) of a material. It was weighted at 20% because the rocket must minimize weight to optimize its flight. Since the motor tube contributed significantly to the overall weight of the launch vehicle, it was weighted at 25%. The material with the lowest density received a score of 10 out of 10.

Compressive strength is the maximum amount of compressive stress (ksi) a material can withstand before it fractures. It was weighted at 25% because the motor tube must be able to withstand significant compressive stresses. For instance, after takeoff, the motor created compressive forces by pushing upward on the motor tube. The material with the highest compressive strength received a score of 10 out of 10 possible points.

Machinability is the ease at which the material can be manufactured based on the safety concerns that each material presented, and the resources required for safe manufacturing. Materials that presented greater safety concerns had a lower ease of machinability because the hazards must be mitigated and required more resources. The machinability scoring was determined using a qualitative scale of poor, fair, okay, good, and great. The corresponding quantitative values were 2, 4, 6, 8, and 10. Since the team has the capability to manufacture all the materials, machinability was weighted at 15%. Therefore, the material with the best machinability received a score of 10 out of 10.

3.1.3.3.2 Alternative Materials

Blue tube, quantum tube, and phenolic were considered for the motor tube; however, they were not selected due to their lower compressive strength in comparison to fiberglass. Blue tube had a significantly lower compressive strength in comparison to fiberglass, and as a result, received a much lower score of 1.37. Quantum tube and phenolic also had lower compressive strengths, and received scores of 4.92 and 3.63, respectively. Although blue tube, quantum tube, and phenolic received higher scores in terms of cost, density, and machinability, the compressive strength was the highest weighted objective. Therefore, blue tube, quantum tube, and phenolic had lower overall scores in comparison to fiberglass and were not selected as the material for the motor tube.

3.1.3.3.3 Selected Material

G12 fiberglass was selected as the motor tube. Fiberglass was the ideal material for the motor tube due to its strength and durability. The higher compressive strength was ideal because the motor tube must withstand significant stresses over the duration of flight and across multiple flights. While fiberglass received a lower score in terms of cost, density, and machinability, the most significant objective was compressive strength to produce a recoverable launch vehicle.

3.1.3.4 Bulkheads

Potential bulkhead materials were evaluated with defined evaluation criteria (3.1.3.4.1 Evaluation Criteria) to select a final material.

3.1.3.4.1 Evaluation Criteria

The decision matrices were used to evaluate the bulkhead material (Table 6). The scores were calculated using linear scoring. The best concept was assigned a score of 10 out of 10 points.

Bulkheads			**Structural FRP Fiberglass**			**Plywood**		
Objective	Weighting Factor	Parameter	Mag.	Score	Value	Mag.	Score	Value
Density	0.10	lb/in^3	0.065	3.23	0.32	0.021	10.0	1.00
Tensile Strength	0.40	ksi	13.5	10.0	4.00	4.50	3.33	1.33
Manufacturing time	0.15	min	16.00	4.38	0.66	7.00	10.0	1.50
Assembly	0.35	experience	fair	4.00	1.40	Fair	4.00	1.40
Overall value					**6.38**			**5.23**

Bulkheads			**Type II PVC**		
Objective	Weighting Factor	Parameter	Mag.	Score	Value
Density	0.10	lb/in^3	0.049	4.29	0.43
Tensile Strength	0.40	ksi	7.54	5.59	2.23
Manufacturing time	0.15	min	40.0	1.75	0.26
Assembly	0.35	ease of assembly	Great	10.00	3.50
Overall value					**6.43**

Table 6: Bulkhead material decision matrix.

Density is the measurement of the mass per unit of volume (lb/in^3) of the material. The weight of the bulkheads was an important consideration because it needed to be minimized where possible to reduce the overall weight of the launch vehicle. However, since the weight of the bulkheads was relatively low in comparison to the overall weight of the launch vehicle, density was weighted at 10%. The material with the lowest density received a score of 10 out of 10.

Tensile strength is the maximum amount of stress (ksi) a material can withstand before failure. Tensile strength was an important consideration because the bulkheads need to be able to withstand the forces it will experience during flight. Since bulkhead failure may result in an overall recovery failure, tensile strength was weighted at 40%. The material with the highest tensile strength received a score of 10 out of 10.

Manufacturing time is the total amount of time (min) required to machine the centering rings. Since the waterjet was selected for manufacturing the centering rings, the manufacturing time was calculated using the material and material thickness. The machinability of the centering ring material was only evaluated based on time because the ease of machinability was very similar for each material. Therefore, it did not effectively evaluate the materials. However, the required time for manufacturing varied by material. Since the centering rings are relatively simple components that do not require a significant amount of time to machine, manufacturing time was weighted at 15%. Therefore, the material with the lowest manufacturing time received a score of 10 out of 10.

Assembly is the ease at which the material can be assembled. Assembly was considered because the bulkheads are assembled differently depending on the material used and have varying levels of complexity. Some materials required manufacturing two components that need to be epoxied together while other materials do not require this process. As a result, the assembly process differed between materials. The assembly scoring was determined using the defined qualitative scale (Table 2). Since bulkheads require precise assembly in order to fulfill its purpose, assembly was weighted at 35%. Therefore, the material with the best assembly received a score of 10 out of 10.

The durability of the materials was also taken into consideration because the bulkheads need to be able to withstand repeated uses. Some materials, like plywood, may have defects, which reduce the strength and durability of the material.

3.1.3.4.2 Alternative Materials

Structural FRP fiberglass and plywood were potential bulkhead materials. However, they were not selected due to their performance in the decision matrices. While each material scored the highest in at least one objective, the overall scores of FRP fiberglass and plywood were lower than the score of Type II PVC. Furthermore, they would each require manufacturing of two pieces to construct the bulkhead. Since these pieces would be epoxied together, the bulkhead could fail if the epoxy failed.

3.1.3.4.3 Selected Material

Type II PVC was the selected material for the bulkheads. Type II PVC performed the best in the decision matrices (Table 6). While PVC only scored the highest in one objective, it still scored highly in other objectives, which is why it had the highest overall score. PVC has the advantage of only consisting of one piece to construct the bulkhead. The alternative materials would require epoxying two separate components together to construct the bulkhead. Furthermore, PVC is unlikely to have defects and can sufficiently seal the coupler from the rest of the launch vehicle. Therefore, Type II PVC was selected as the bulkhead material.

3.1.3.5 Centering Rings

Potential bulkhead materials were evaluated with defined evaluation criteria (3.1.3.5.1 Evaluation Criteria) to select a final material.

3.1.3.5.1 Evaluation Criteria

Decision matrices were used to evaluate the centering ring material (Table 7). The scores were calculated using linear scoring. The best concept was assigned a score of 10 out of 10 points.

Centering rings			**Structural FRP Fiberglass**			**Plywood**		
Objective	Weighting Factor	Parameter	Mag.	Score	Value	Mag.	Score	Value
Density	0.25	lb/in^3	0.065	3.23	0.81	0.021	10.0	2.50
Shear strength	0.45	ksi	21.5	10.0	4.50	5.00	2.33	1.05
Manufacturing time	0.30	min	13.0	3.85	1.15	5.00	10.0	3.00
Overall value					**6.46**			**6.55**

Centering rings			**Type II PVC**		
Objective	Weighting Factor	Parameter	Mag.	Score	Value
Density	0.25	lb/in^3	0.049	4.29	1.07
Shear strength	0.45	ksi	1.50	0.70	0.31
Manufacturing time	0.30	min	25.0	2.00	0.60
Overall value					**1.98**

Table 7: Centering rings decision matrix.

Density is the measurement of the mass per unit of volume (lb/in^3) of the material. The weight of the centering rings was considered because it needed to be minimized where possible to reduce the overall weight of the launch vehicle. However, since the centering rings did not contribute significantly to the overall weight, density is weighted at 20%. The material with the lowest density received a score of 10 out of 10.

Shear strength is the maximum amount of stress (ksi) a material can withstand against forces that cause the material's internal structure to slide against itself or shear. Shear strength was considered because the centering rings experience a high amount of shear stress. Therefore, shear strength was weighted at 40%. The material with the greatest shear strength received a score of 10 out of 10.

Manufacturing time is the total amount of time (min) required to machine the centering rings. Since the waterjet will be used to manufacture the centering rings, the manufacturing time is calculated using the material and material thickness. The machinability of the centering ring material is only evaluated based on time because the ease of machinability is very similar for each material. Therefore, machinability does not effectively evaluate the materials. However, the required time for manufacturing varies by material and material thickness. Since the centering rings are relatively simple components that do not require a significant amount of time to machine, manufacturing time is weighted at 10%. Therefore, the material with the lowest manufacturing time will receive a score of 10 out of 10.

3.1.3.5.2 Alternative Materials

Structural FRP fiberglass and Type II PVC were considered for the centering ring material. However, based on the evaluation criteria and decision matrices (Table 7), they were not selected. While structural FRP fiberglass had the highest strength, it did not score as well as plywood in terms of density and manufacturing time. Although Type II PVC had a relatively low density and manufacturing time, it did not perform as well as the other materials in the decision matrices. Therefore, Structural FRP and Type II PVC were not selected.

3.1.3.5.3 Selected Material

Plywood was selected as the material for the centering rings based on the evaluation criteria. Plywood scored the highest in terms of both density and manufacturing time, which makes it the ideal material for the centering rings. Although it has a lower shear strength than fiberglass, plywood is sufficiently strong. The centering rings were designed with two holes for the electronics tubes to pass through, which would create stress concentrations in those areas. However, since the holes were only designed in the forward and central centering rings, the stress concentrations were not a concern because the motor transfers most of the force to the airframe through the aft centering ring. Furthermore, since plywood is less dense than fiberglass, it needed to be slightly thicker to have a similar strength. As a result, the higher thickness of the plywood design had a greater area of contact with the airframe and a stronger epoxy bond. Therefore, plywood was the optimal material for the centering rings.

3.1.3.6 Fins

Potential bulkhead materials were evaluated with defined evaluation criteria (3.1.3.6.1 Evaluation Criteria) to select a final material.

3.1.3.6.1 Evaluation Criteria

Decision matrices were used to evaluate the fin material (Table 8). The scores were calculated using linear scoring. The best concept was assigned a score of 10 out of 10 points.

Fins			**Structural FRP Fiberglass**			**Plywood**		
Objective	Weighting Factor	Parameter	Mag.	Score	Value	Mag.	Score	Value
Cost	0.15	USD/ft^2	14.39	2.85	0.43	4.10	10.0	1.50
Density	0.20	lb/in^3	0.065	3.23	0.65	0.021	10.0	2.00
Shear strength	0.45	ksi	21.5	10.0	4.50	5.00	2.33	1.05
Manufacturing time	0.10	min	8.20	7.34	0.73	6.02	10.0	1.00
Overall value					**6.31**			**5.55**

Table 8: Fin material decision matrix.

Cost is the total price (USD/ft^2) of a nosecone with a 4 in diameter base. Cost was taken into consideration because it is unnecessary to purchase expensive materials if there are sufficient materials available at a lower price. Since the cost of the fins is relatively low in comparison to the overall cost of the launch vehicle, the cost was weighted at 15%. Therefore, the material with the lowest cost will receive a score of 10 out of 10.

Density is the measurement of mass per unit of volume (lb/in^3) of the material. The weight of a component is an important consideration because it needs to be minimized where possible to reduce the overall weight of the launch vehicle. However, since the fins do not contribute significantly to the overall weight, density is weighted at 20%. The material with the lowest density will receive a score of 10 out of 10.

Shear strength is the maximum amount of stress (ksi) a material can withstand against forces that cause the material's internal structure to slide against itself or shear. Since the fins are often the first point of contact upon landing, it is important to ensure that the fins can withstand the force from impacting the ground. Therefore, shear strength is weighted at 45%. The material with the greatest shear strength will receive a score of 10 out of 10.

Manufacturing time is the total amount of time (min) required to machine the fins. Since the waterjet will be used to manufacture the fins, the manufacturing time is calculated based on the material and material thickness. Since the fins are relatively simple components, manufacturing time is weighted at 10%. Therefore, the material with the lowest manufacturing time will receive a score of 10 out of 10.

3.1.3.6.2 Alternative Materials

Plywood was the alternative material considered for fins. Although plywood scored well in terms of density, cost, and manufacturing time, plywood was not sufficiently strong enough given that the fins are often the first point of contact with the ground. Therefore, plywood was not selected as the fin material.

3.1.3.6.3 Selected Material

Structural FRP fiberglass was selected for the fin material (Table 8) since it had the greatest shear strength. While it did not score as well as plywood in the other objectives, the shear strength had the greatest weight since a sufficiently strong material was needed in order to prevent the component from failing. As a result, Structural FRP fiberglass was determined to be the most suitable material for the fins.

3.1.3.7 Epoxy

Potential epoxy options were evaluated using defined evaluation criteria (3.1.3.6.1 Evaluation Criteria).

3.1.3.6.1 Evaluation Criteria

Epoxy must have a high tensile strength due to the forces it experiences during launch. Failure of the epoxy may result in failure of the launch vehicle. Since epoxy is used near the motor tube to attach the centering rings and fins to the launch vehicle, it must also be able to withstand high temperatures.

3.1.3.6.2 Selected Components

JBWeld was selected to epoxy the centering rings to the motor tube and inside of the airframe. It was also selected for the interior fillets. JBWeld was chosen due to its high tensile strength of 5.0 ksi and high maximum temperature threshold of 550° F. While RocketPoxy has a lower temperature threshold of 225° F, it was selected for the exterior fin fillets due to its higher tensile strength. While RocketPoxy has a higher tensile strength of 7.6 ksi, it was only used for the exterior fillets due to its poor heat threshold.

3.1.4 Leading Vehicle Design

The leading vehicle design was modeled using OpenRocket (Figure 2).

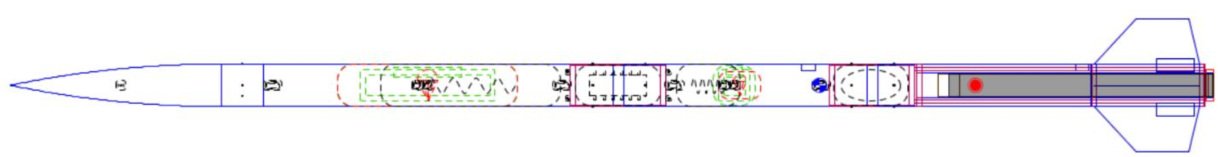

Figure 2: Launch vehicle OpenRocket design.

Additionally, the leading vehicle design was modeled in SolidWorks and each section was labeled (Figure 3).

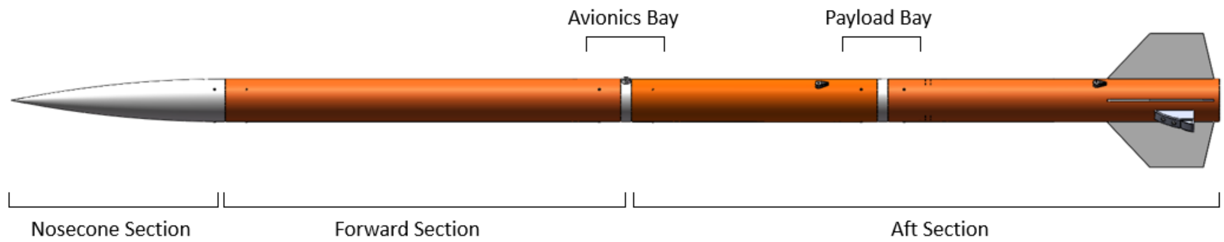

Figure 3: Launch vehicle SolidWorks design.

3.1.4.1 Nosecone Section

The nosecone section includes a nosecone, nosecone bulkhead, and an eyebolt (Figure 4).

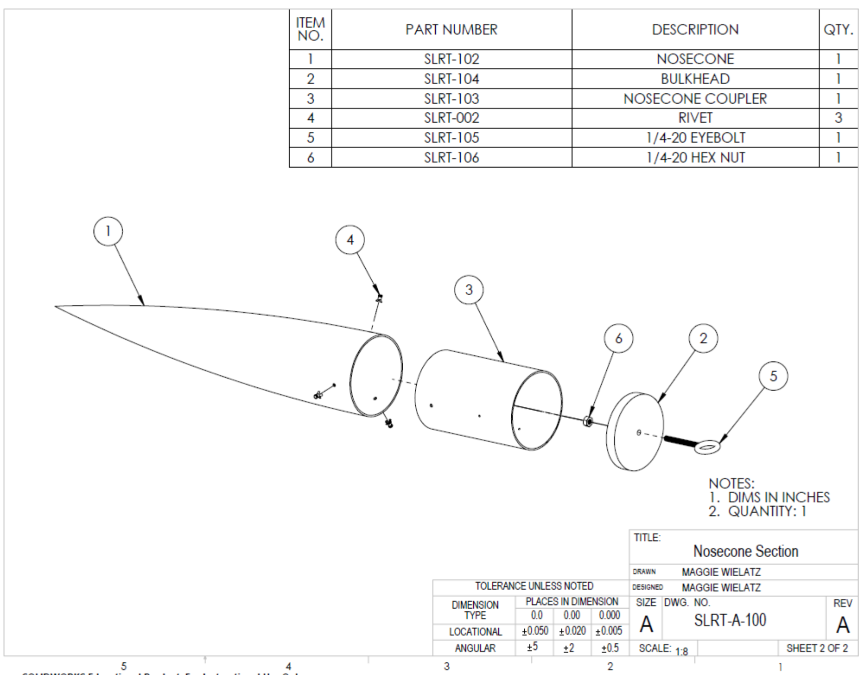

Figure 4: Nosecone section assembly drawing.

The selected nosecone was a 5:1 ogive nosecone made of G12 fiberglass (Figure 5). The selected nosecone was 20 in. long with a 4 in. diameter and a 4 in. shoulder. The nosecone was designed to connect with the shoulder using three plastic rivets with 0.154 in. diameters. The shoulder was designed to connect with the forward section with three nylon shear pins with 0.086 in.

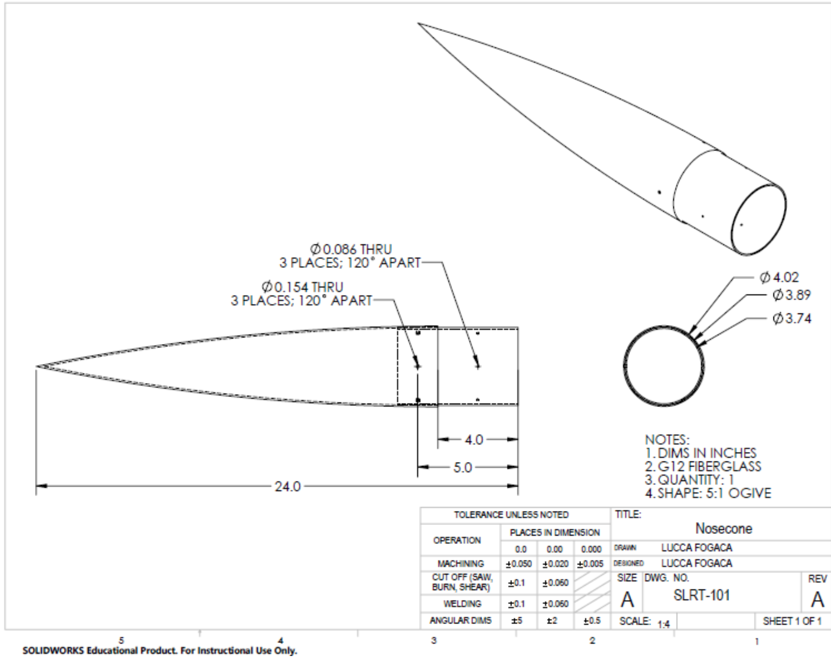

Figure 5: Nosecone drawing.

Type II PVC was selected as the nosecone bulkhead material. It was designed with a 3.8 in. diameter so that it could be epoxied into the nosecone shoulder. The bulkhead was designed to connect to an eyebolt that connects the nosecone section to the forward section using the recovery harness.

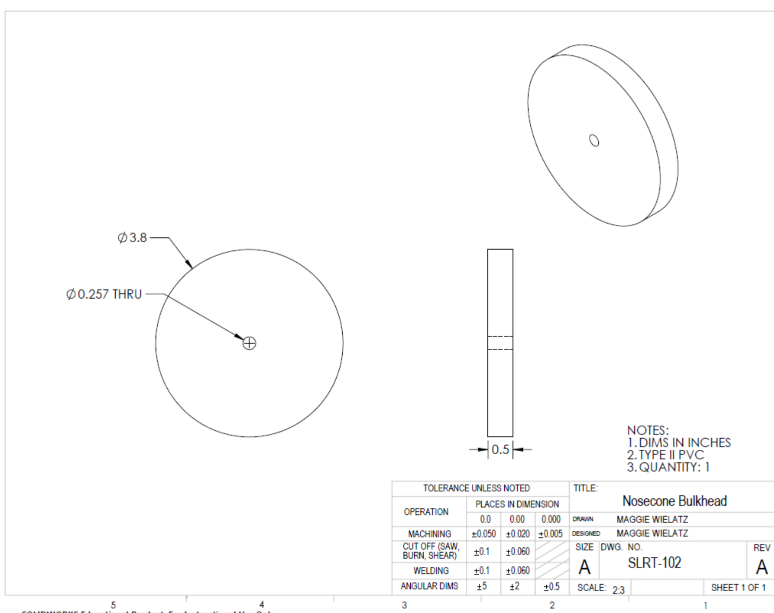

Figure 6: Bulkhead drawings.

3.1.4.2 Forward Section

The forward section consists of a forward airframe and an avionics bay (Figure 7).

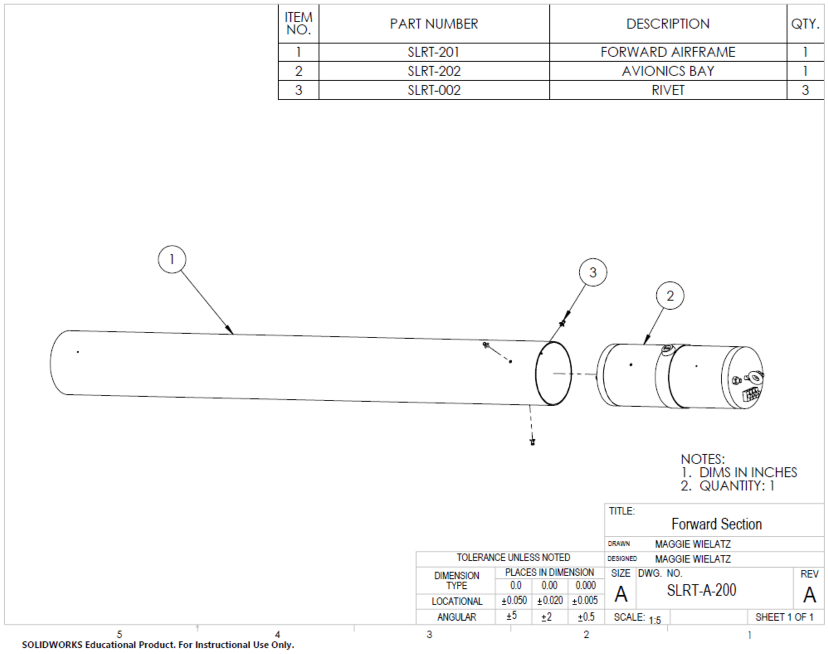

Figure 7: Forward section assembly drawings.

G12 fiberglass was selected as the material for the airframe. The forward airframe was designed with a nominal diameter of 4 in. and a length of 37 in (Figure 8). The forward airframe was designed with three shear pin holes where the forward airframe connects to the nosecone section. The forward airframe was designed to be secured to the avionics bay with three rivets.

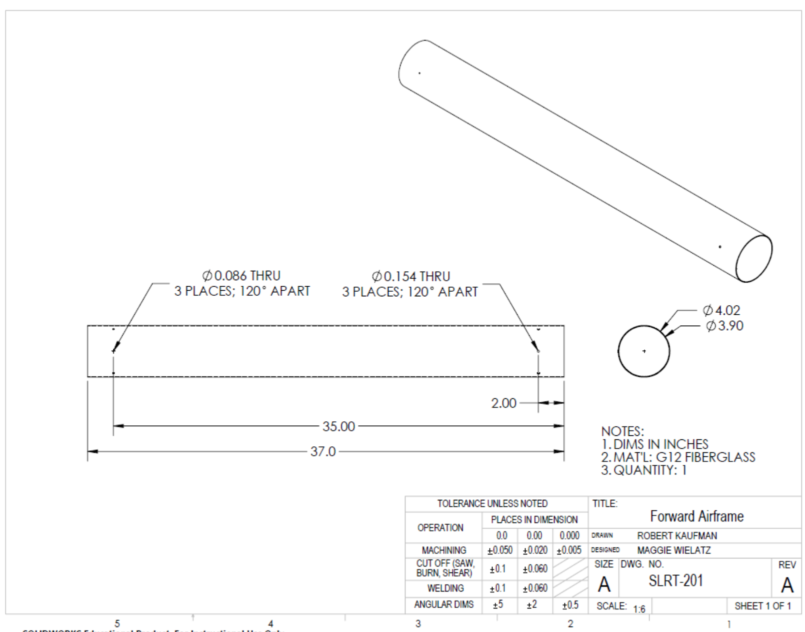

Figure 8: Forward airframe drawing.

Avionics bulkheads were designed with an outer diameter of 3.9 in. and an inner diameter of 3.7 in. and an overall thickness of 1 in. (Figure 9). The bulkheads were designed to seal the avionics bay. The bulkheads were also designed for steel ¼-20 eyebolt with no shoulder to fasten to the center hole. The eyebolts were necessary in order to connect both sides of the avionics bay to the recovery harnesses.

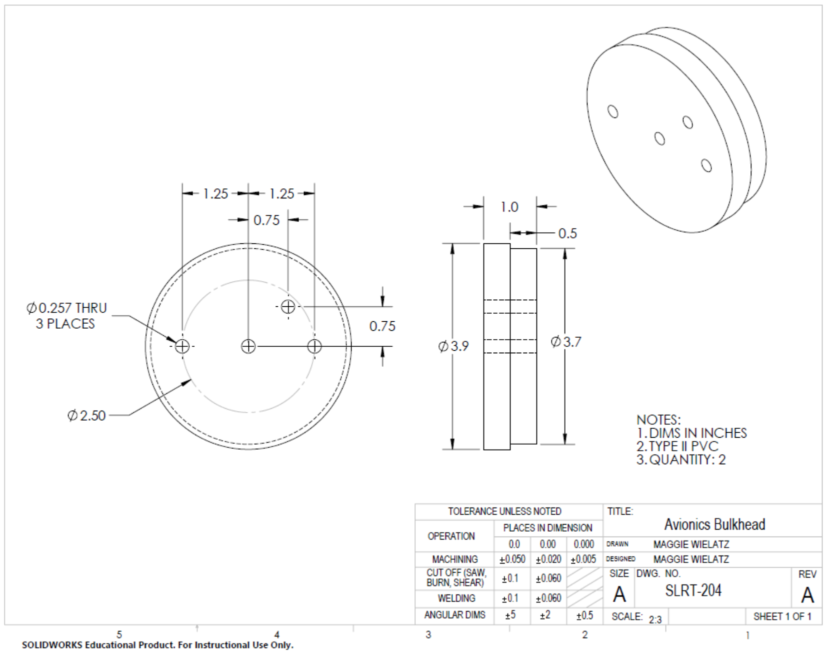

Figure 9: Avionics bulkhead drawings.

G12 fiberglass was selected as coupler material. An avionics coupler was designed to have a length of 9.0 in., an outer diameter of 3.90 in., and an inner diameter of 3.76 in. (Figure 10). A 9.0 in. long coupler was selected to provide sufficient space to house the avionics components.

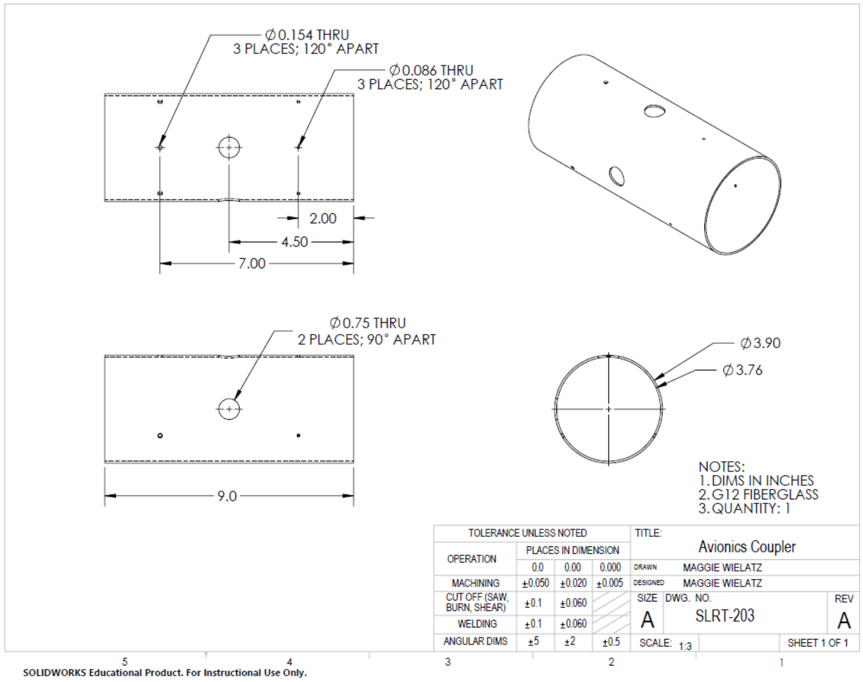

Figure 10: Avionics coupler drawing.

3.1.4.3 Aft Section

The aft section includes aft airframes, payload bay, motor tube, centering rings, and fins (Figure 11). Structural payload components are also present.

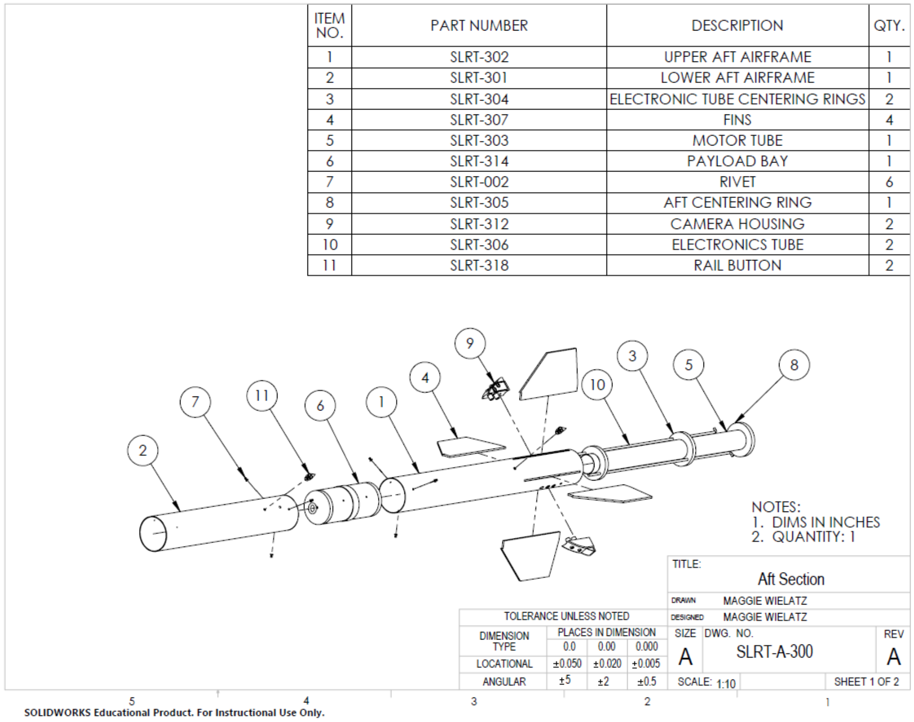

Figure 11: Aft section assembly drawing.

Upper and lower aft airframes were designed with a nominal diameter of 4.0 in. and lengths of 23.0 in. and 31.0 in., respectively (Figure 12, Figure 13, Figure 14). Three nylon shear pins connect the upper aft airframe to the avionics bay. The lower aft airframe was designed for payload camera mounts to be secured between two fins on opposite sides of the launch vehicle. The lower aft airframe also had four fin slots that were equally spaced apart.

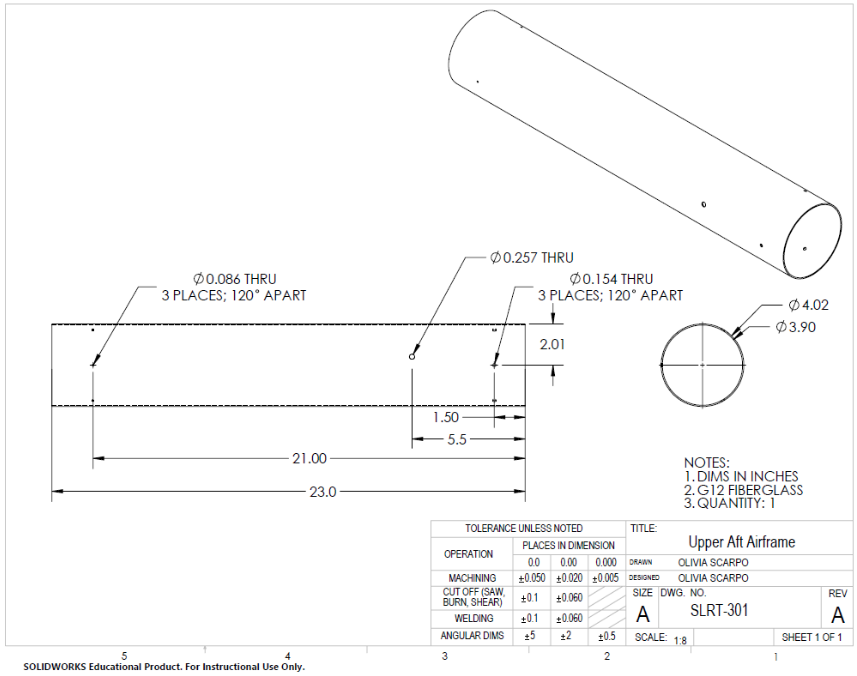

Figure 12: Upper aft airframe drawing.

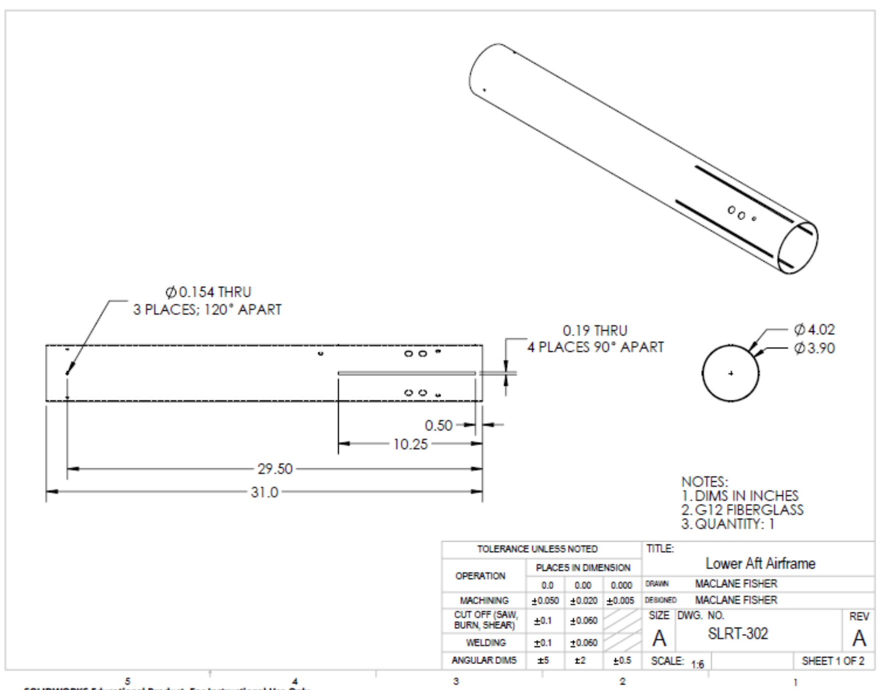

Figure 13: Lower aft airframe drawing.

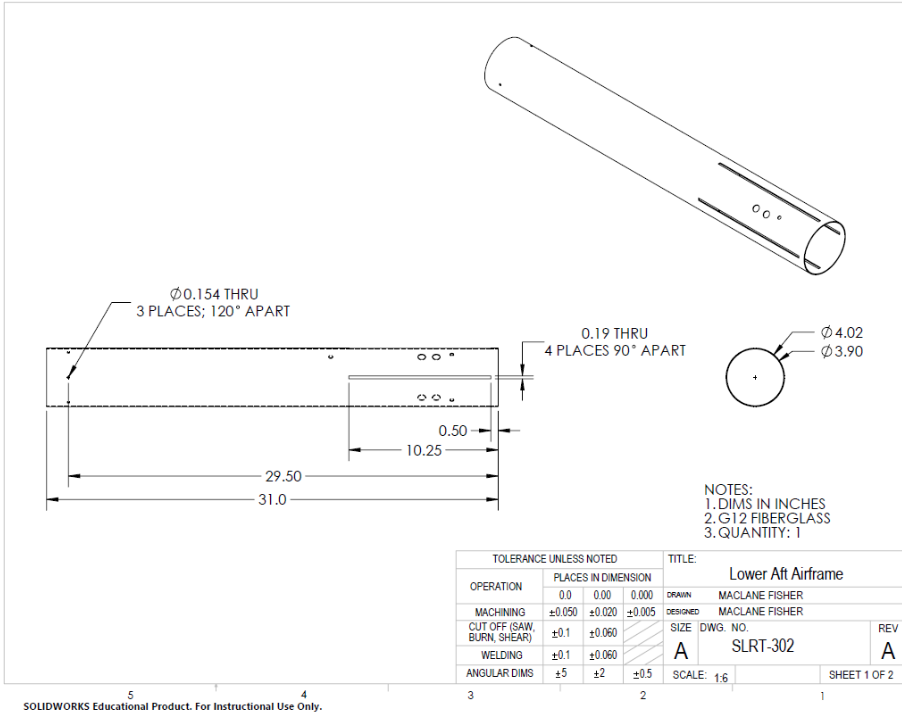

Figure 14: Lower aft airframe drawing.

The payload bay was designed with an 8.0 in. long coupler and two bulkheads. The coupler length was selected to provide sufficient space to house the payload components. The coupler was designed with an outer diameter of 3.90 in. and an inner diameter of 3.76 in. (Figure 15). The coupler was also designed with three rivet holes on each side of the coupler in order to secure the payload bay between the upper and lower aft airframes.

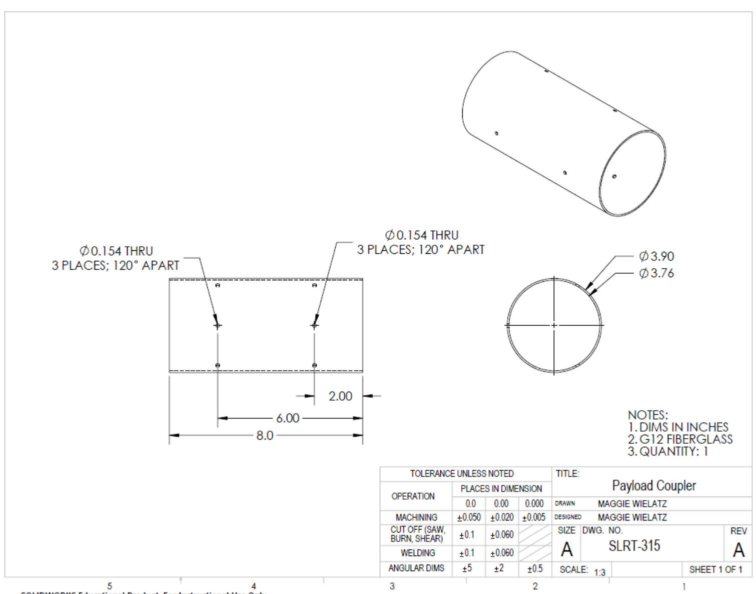

Figure 15: Payload coupler drawing.

Bulkheads were used to seal the payload bay from the other sections of the launch vehicle. The bulkheads were designed with an outer diameter of 3.9 in. and an inner diameter of 3.8 in. (Figure 16, Figure 17). Type II PVC was the selected material. The forward bulkhead was designed for an eyebolt to fasten to the component and connect the aft section to the recovery harness.

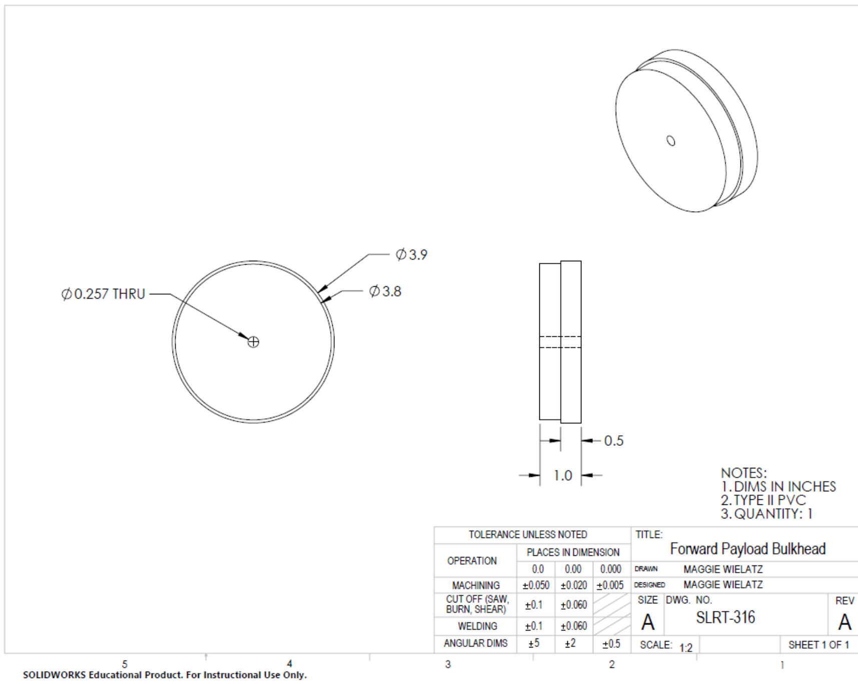

Figure 16: Forward payload bulkhead drawing.

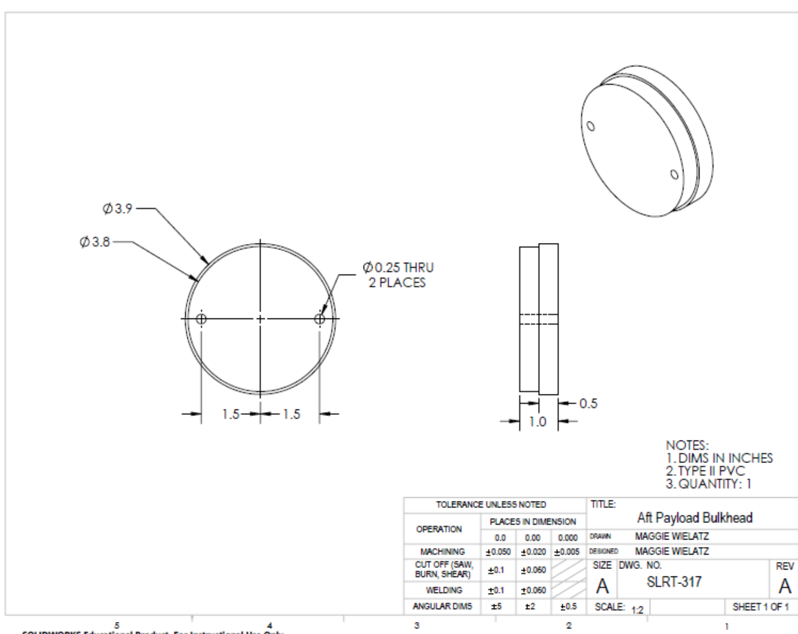

Figure 17: Aft payload bulkhead drawing.

Electronic tubes were designed to house the wires that travel from the payload bay, through the forward and central centering rings, to the cameras on the outside of the lower aft airframe (Figure 18). The selected material was reinforced kraft paper tubes since the components needed to be flexible and have a small diameter. The tubes were designed with a diameter of 0.25 in. and an overall length of 25.0 in.

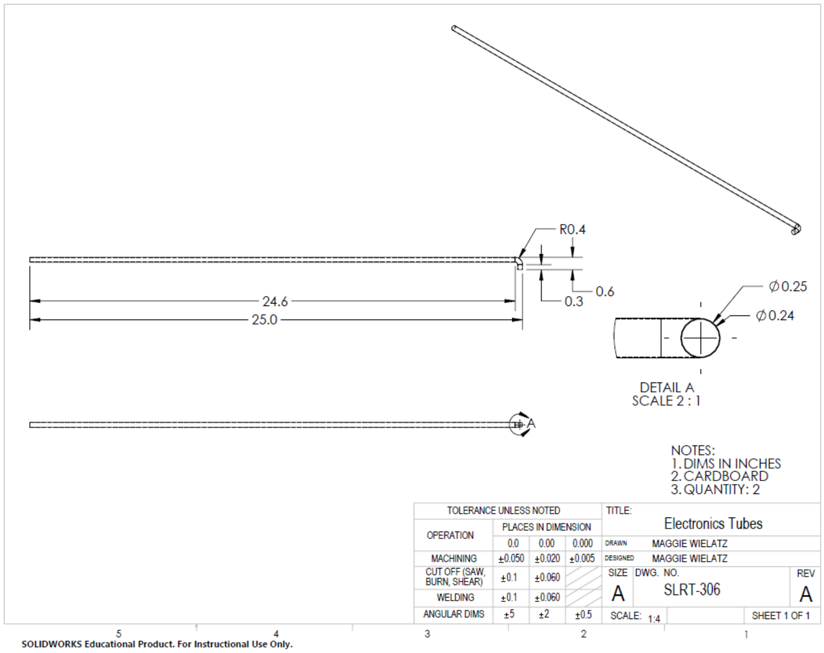

Figure 18: Electronics tubes drawing.

The motor tube was designed with a length of 27.0 in., an outer diameter of 2.24 in., and an inner diameter of 2.15 in. (Figure 19). G12 fiberglass was selected as the material for the motor tube.

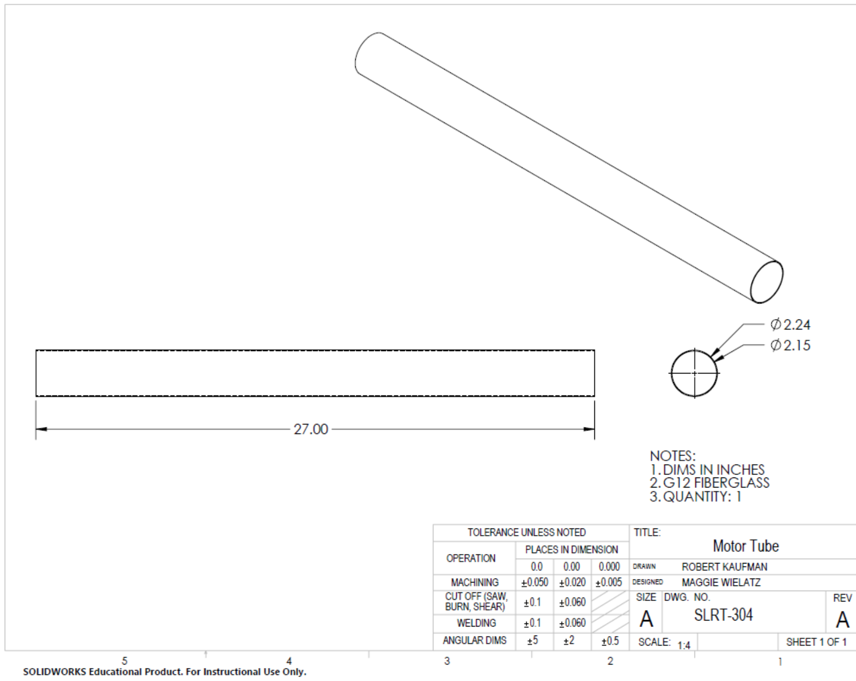

Figure 19: Motor tube drawing.

The centering rings were designed to keep the motor tube aligned in the aft section. The launch vehicle was designed with three centering rings. The forward and central centering rings were designed with two 0.25 in. holes that the electronics tubes pass through (Figure 20). The selected material was 0.5 in. thick plywood. The aft centering ring was designed with 0.5 in. thick plywood. However, it was not designed with holes for the electronics tubes since the tubes did not need to pass through the aft centering ring (Figure 21). The aft centering ring was designed to be flush with the end of the lower aft airframe. The centering rings were designed to be epoxied to the outside of the motor tube and the inside of the lower aft airframe.

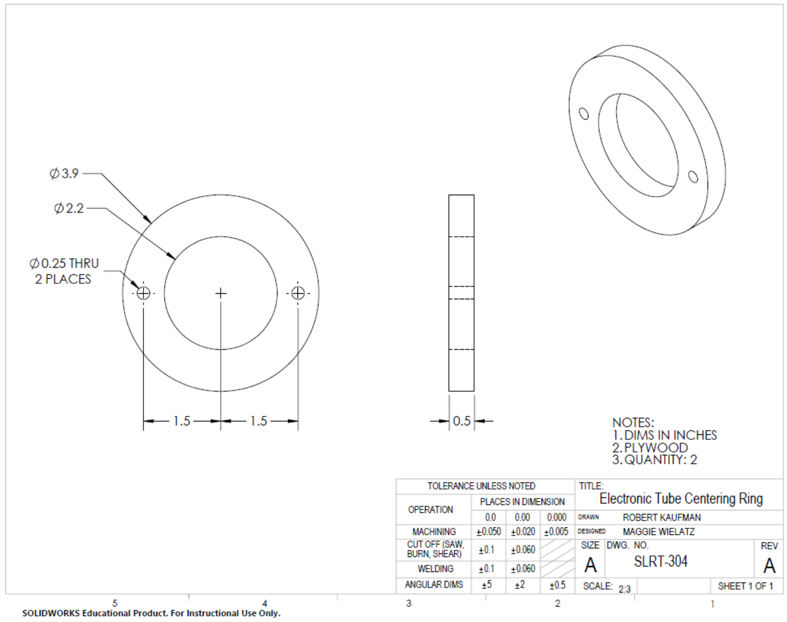

Figure 20: Electronic tube centering ring drawing.

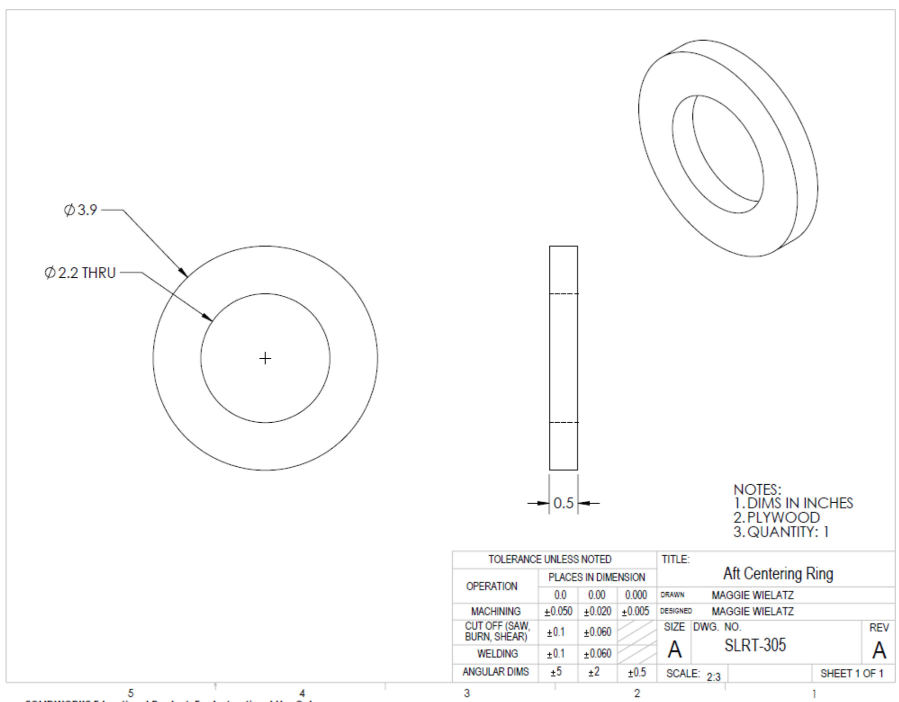

Figure 21: Aft centering ring drawing.

The launch vehicle was designed to have four fins made of 3/16 in. thick structural FRP fiberglass. The fins were designed to be 0.5 in. from the end of the lower aft airframe (Figure 22). The fins were designed to be attached through the wall of the airframe and epoxied to the outside of the motor tube, inside of the lower aft airframe, and outside of the lower aft airframe.

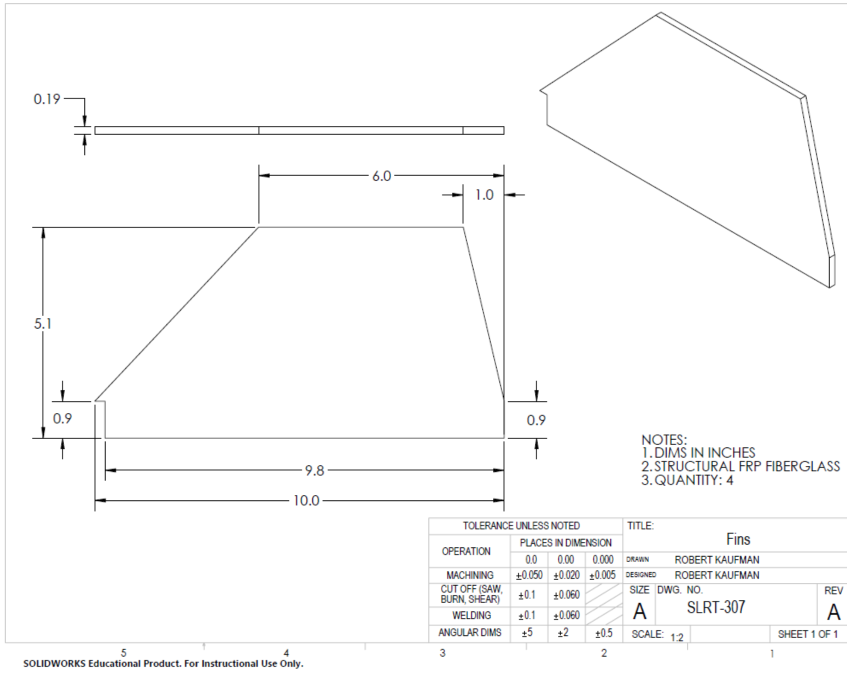

Figure 22: Fins drawing.

3.1.4.4 Component Masses

The following table lists the masses of each component within each section of the launch vehicle. The masses of the payload components are not included (Table 9).

Nosecone Section		
Subteam	**Component**	**Mass (oz)**
Structures	Nosecone	20
Avionics and Recovery	GPS	0.8
Structures	Nosecone bulkhead	4.8
Structures	U-bolt	1.0
Total		**27**
Forward Section		
Subteam	**Component**	**Mass (oz)**
Structures	Airframe	32
Avionics and Recovery	Parachute protector	5.0
Avionics and Recovery	Main parachute	30
Avionics and Recovery	Recovery harness	16
Structures	Coupler and switchband	9.9
Structures	Bulkheads	9.6
Avionics and Recovery	Threaded rods	6.1
Avionics and Recovery	Altimeters	0.80
Avionics and Recovery	U-bolts	2.0
Avionics and Recovery	Electronics sled	4.0
Avionics and Recovery	9-V batteries	2.4

Total		118
Aft Section		
Subteam	**Component**	**Mass (oz)**
Structures	Airframe	47
Structures	Rail Buttons	0.7
Avionics and Recovery	Drogue parachute	1.1
Avionics and Recovery	Parachute protector	1.0
Avionics and Recovery	Recovery harness	16
Payloads	Electronics tubes	0.6
Structures	Epoxy	22
Structures	Motor tube	10
Structures	Centering rings	4.4
Structures	Forward closure	3.1
Structures	Aft closure	2.0
Structures	Motor casing	14
Structures	Thrust plate	4.8
Structures	Motor retainer	2.3
Flight Dynamics	Motor	80
Structures	Fins	33
Structures	Coupler and switchband	8.9
Structures	Bulkheads	9.6
Payloads	Hardware	20
Payloads	U-bolt	1.0
Total		**281**
Overall Total		**426**

Table 9: Mass table.

3.2 Avionics and Recovery Subsystem

The Avionics and Recovery Subsystem consists of parachutes, recovery connection hardware, recovery harness, altimeters, ejection charges, and GPS. The team will use one avionics bay and two parachutes to recover the launch vehicle. The avionics bay will store two altimeters wired independently from each other. The altimeters will control ejection charges that will cause the launch vehicle to separate into three sections. The launch vehicle will first separate into the forward and aft sections to deploy the drogue parachute, then separate the nosecone section from the rest of the forward section to deploy the main parachute. The Avionics and Recovery Subteam used decision matrices to select the subsystem components.

3.2.1 Estimated Parachute Sizing

OpenRocket simulations were used to estimate the size of parachute needed to match target descent rates. Target descent rates were set at 80 ft/s for the drogue parachute and 18 ft/s for the main parachute. These descent rates were selected to ensure the launch vehicle would descend in less than 90 seconds and drift less than 2500 ft with constant wind speeds of 20 mph (6.1.1). The size of the parachute that will provide the target descent rate will change based on the coefficient of drag of the parachute. Various coefficient of drag values were input into the simulation to represent different makes or models of parachute (Table 10, Table 11). The descent rates were found using OpenRocket simulation when the simulation reached terminal velocity under the respective parachute.

Main Parachute Estimated Sizes		
C_D	Diameter (in)	Descent Rate (ft/s)
1	108	17
1.2	96	18
1.6	84	18
2.2	72	17

Table 10: Main parachute estimated sizes.

Drogue Parachute Estimated Sizes		
C_D	Diameter (in)	Descent Rate (ft/s)
0.75	24	92
1	24	80
1.2	24	72
1.6	18	84

Table 11: Drogue parachute estimated sizes.

3.2.2 Component Selection

Decision matrices were used to select the altimeters, main parachute, and drogue parachute. When possible, objectives were assessed quantitatively using values provided by the manufacturer. Qualitative scores were assigned using the defined values (Table 2).

3.2.2.1 Recovery Harness

A recovery harness is used to connect the separated sections to the parachutes. It is attached to the connection hardware within the bulkheads of the avionics bay, nosecone section, and payload bay.

3.2.2.1.1 Evaluation Criteria

The recovery harness must be close to 2.5 times the length of the fully assembled launch vehicle to ensure the separated sections don't collide during descent. The recovery harness must be approximately 23.75 ft. long to meet this requirement. It is also important for the recovery harness to be wide to avoid zippering during deployment. A thin recovery harness would increase the stress on the side of the airframe during deployment because of the smaller contact area for the same amount of force. Ideally, the recovery harness will also be heat resistant because it will be near the ejection charges when they go off. However, the recovery harness could be protected using insulation material or by coiling it in the parachute protector.

3.2.2.1.2 Alternative Component

A nylon recovery harness sold by Wildman Rocketry was considered to be the recovery harness for the launch vehicle. It was 20 ft long and 9/16 in. wide. The length is less than the targeted value, but still acceptable because it would be possible to position the parachutes such that the sections would not collide during descent. This harness is wider than the selected harness, but only by 1/8 in. Nylon is not very heat resistant and would need protecting from the hot ejection charge gasses during separation.

3.2.2.1.3 Selected Component

The selected recovery harness is a tubular Kevlar recovery harness sold by Wildman Rocketry. It is 25 ft. long and 7/16 in. wide. It is longer than the targeted value and will be able to position the separated sections such that they will not collide during descent. The width is smaller than the nylon recovery harness assessed however it is still sufficiently wide enough to avoid zippering the airframe during main parachute deployment. Kevlar is heat resistant and will need less protection from the ejection charge gasses during separation. This will improve the safety and reusability of the recovery harness.

3.2.2.2 Connection Hardware

The connection hardware is used to connect the recovery harness to the bulkheads of the nosecone section, the avionics bay, and the payload bay. Both eyebolts and U-bolts were assessed to determine which would be best for the launch vehicle. The bolt that is selected will be secured to the bulkhead using hex nuts and then epoxied into the bulkhead to ensure that ejection gasses can not pass through the clearance hole for the threaded shaft of the bolt. There will be a total of four bolts in use, one on the nosecone bulkhead, one per avionics bay bulkhead, and one on the forward bulkhead of the payload bay.

3.2.2.2.1 Evaluation Criteria

The connection hardware was assessed on their size and weight. The size of the bolt is important because it takes up valuable space inside of the launch vehicle. The more space the connection hardware takes up, the longer the launch vehicle will need to be to make up for lost space due to the protrusion of the bolt. The weight of the bolt is important because there will be multiple throughout the launch vehicle, and it will have an effect on the overall weight of the launch vehicle.

3.2.2.2.2 Alternative Components

A 1/4-20 threaded U-bolt from McMaster Carr was assessed. It has a height of 3.1875 in. and a width of 1.875 in. It has a load capacity of 425 lbs. With a threaded length of 2 in., the two threaded shafts would protrude one inch into the avionics bay for each bulkhead of the avionics bay. Having the two attachment points would disperse the load from the recovery harness more evenly across the bulkhead, but an eyebolt can perform similarly with a well sized washer. This U-bolt also weighs 2.2 oz. With four of these bolts in use it would total to 8.8 oz which is over half a pound.

Another U-bolt from McMaster Carr that was considered was a 1/4-20 thread U-bolt with a height of 2.9375 in. It was 1.375 in. wide and weighs 2.1 oz. This U-bolt also has a load capacity of 425 lbs. This U-bolt is not as tall or wide as the other U-bolt assessed. However, the portion of the U-bolt that is threaded is longer at 2.5 in. long. This would create two 1.5 inch obstructions in the avionics bay. This is a sizable amount of space in an avionics bay that only has 8 inches from bulkhead to bulkhead inside the avionics bay.

A 1/4”-20 threaded eyebolt with a shoulder from McMaster-Carr was assessed. It has a height of 2.875 in. and a width of 1.875 in. It has a load capacity of 500 lbs. The threaded portion of the eyebolt is 1.5 inches long. This would only protrude half an inch into the avionics bay. It weighs 2.3 oz. This is a smaller obstruction than the U-bolt, but it weighs more. The increased weight is due to the addition of the shoulder on the eyebolt. The shoulder adds additional strength, but this additional strength isn’t needed as all the components assessed have sufficiently high load capacities.

3.2.2.2.3 Selected Component

A 1/4-20 thread threaded eyebolt from McMaster-Carr without a shoulder was chosen. The chosen eyebolt has a total height of 3 inches and a shank length of 2 inches. It is 1 inch wide. Neither its height nor its width is the smallest of the bolts assessed, but together take up the least amount of space in the launch vehicle. The shank is 2 inches long and will protrude 1 inch into the avionics bay at most. It also weighs the least at 1 oz. This would only add a total of 4 oz to the launch vehicles total mass.

3.2.2.3 Altimeter

A decision matrix was used to evaluate altimeters. The scores were calculated using linear scoring. The best concept was assigned a score of 10 out of 10 points (Table 12).

Altimeter			**Entacore AIM Altimeter**			**Telemetrum Altimeter**		
Objective	Weighting Factor	Parameter	Mag.	Score	Value	Mag.	Score	Value
Volume	0.2	cubic inches	1.4	5.4	1.1	1.8	4.1	0.8
Weight	0.2	oz	0.4	7.5	1.5	0.7	4.2	0.8
Cost	0.3	USD	121.20	5.8	1.7	363.50	1.9	0.6
Resolution	0.3	ft	1	6.7	2.0	0.67	10.0	3.0
Overall Value					**6.3**			**5.2**
Stratologger CF			**EasyMega Altus Metrum**			**EasyMini Altimeter**		
Mag.	Score	Value	Mag.	Score	Value	Mag.	Score	Value
0.8	8.9	1.8	1.9	3.9	0.8	0.75	10.0	2.00
0.4	7.9	1.6	0.5	6.0	1.2	0.3	10.0	2.00
70.00	10.0	3.0	300.00	2.3	0.7	96.93	7.2	2.16
1	6.7	2.0	0.67	10.0	3.0	unknown	0.0	0.0
		8.4			**5.7**			**6.2**

Table 12: Altimeter decision matrix.

3.2.2.3.1 Objective Definitions and Weighting Factors

Volume was chosen as an objective because it is necessary to find an altimeter that fits inside the avionics bay of the launch vehicle. A small volume is significant because it would allow for more space for the batteries, wiring, and switches in the avionics bay. For this reason, it has a weighting factor of 20%. The smallest volume will receive a score of 10 out of 10.

Weight was chosen as an objective because it is important to find a weight that does not greatly affect the launch vehicle. Weight has a weighting factor of 20%. The smallest weight will receive a score of 10 out of 10.

Cost is the amount in USD that must be paid to obtain the bolt. There is a limited budget, so the price of the altimeters should be accounted for. The cost has a weighting factor of 30%. Altimeters are very expensive compared to their other traits, so it has a relatively high weight. The altimeter with the lowest price will receive a score of 10 out of 10.

Resolution was chosen as an objective because it is essential to utilize the altimeter that is the most accurate. An inaccurate altimeter may result in an early or late deployment of the parachutes. An early deployment of the parachutes could cause the launch vehicle to drift outside of the launch field, and a late deployment could cause zippering, tearing of the parachute, or a higher than expected ground hit velocity. Therefore, accuracy is one the most significant objectives. For this reason, accuracy has a weighting factor of 30%. Accuracy is assessed qualitatively because not all manufacturers provide accuracy in the same way.

3.2.2.3.2 Selected Component

The Stratologger CF was selected to be the primary altimeter for the launch vehicle. It had the highest overall value in the decision matrix, with a value of 8.9. It is the cheapest altimeters assessed, and one of the most accurate.

The Entacore AIM Altimeter was selected to be the secondary altimeter for the launch vehicle. It had the second highest overall value, with a value of 6.7. It is also a very accurate altimeter with very similar capabilities as the Stratologger CF. It will be used as the secondary altimeter to ensure that any failures that could arise due to the Perfectflite Stratologger brand of altimeter does not cause both the primary and secondary altimeters to fail.

3.2.2.4 GPS

The GPS is important for locating the launch vehicle. It is not connected to the payload system in any way, and is kept as far away as possible from the altimeters and ejection charges. The GPS will be located in the nosecone section of the launch vehicle, 32 in. from the nearest ejection charge.

3.2.2.4.1 Evaluation Criteria

The GPS was assessed on the accuracy of the GPS module, the cost, and the current draw. Accuracy is important so that the team can accurately find the launch vehicle on the field if the payload were to fail. GPS transmitters are among the more expensive items the team has to purchase, so the cost of the GPS is important. The current draw of the GPS transmitter is important because it is a requirement that the launch vehicle have at least a 2-hour pad time. The lower the current draw, the longer the GPS will last with the same battery.

3.2.2.4.2 Alternative Component

An alternative GPS that was assessed was the 70 cm 100mW GPS by Big Red Bee. It costs $259.00 and has a resolution of 6.7 ft. The current draw of this GPS is 112 mA. The resolution and current draw for this GPS are better than the selected GPS, but it costs much more without significant improvements.

3.2.2.4.3 Selected Component

The selected GPS is the Big Red Bee 900 MHz. It costs $199.99 and has a resolution of 8.2 ft. The current draw of this GPS is 115 mA. The resolution and current draw for this GPS are worse than the alternative GPS, but the difference between the two is not significant. This makes the cost the deciding factor on the selected component.

3.2.2.5 Main Parachute

A decision matrix was used to evaluate parachutes for the main parachute. The scores were calculated using linear scoring. The best concept was assigned a score of 10 out of 10 points (Table 13).

Main Parachute			**84" Iris Ultra Fruity Chutes**			**72" Irus Ultra Fruity Chutes**		
Objective	Weighting Factor	Parameter	Mag.	Score	Value	Mag.	Score	Value
cost	0.2	USD	297.00	3.9	0.8	246.80	4.7	0.9
descent rate	0.35	ft/s	15.4	1.2	0.4	17.7	10.0	3.5
weight	0.1	oz	19.0	5.2	0.5	13.3	7.4	0.7
shroud lines	0.35	qualitative	great	10	3.5	great	10	3.5

Overall Value					**5.2**			**8.7**
72" Rocketman Elliptical			**Large Skyangle C3**			**60" Rocketman Elliptical**		
Mag.	Score	Value	Mag.	Score	Value	Mag.	Score	Value
135.00	8.5	1.7	139.00	8.3	1.7	115.00	10.0	2.0
20.2	1.4	0.5	20.1	1.4	0.5	24.4	0.5	0.2
12.6	7.9	0.8	34.0	2.9	0.3	9.9	10.0	1.0
good	8	2.8	good	8	2.8	good	8	2.8
		5.8			**5.2**			**6.0**

Table 13: Main parachute decision matrix.

3.2.2.6.1 Objective Definitions and Justifications

Cost is the total price of the parachute. It is important to pick a parachute within budget. There are multiple sources to buy these parachutes, however the prices used in the matrix are those that are from the manufacturer. Price is weighted at 20% since the only requirement is being under budget, but the money saved here can be allocated to other parts of the design. The parachute with the lowest cost will receive a score of 10 out of 10 while the others will be evaluated on a linear scale by cost.

Descent Rate is the rate at which the launch vehicle will descend while using the main parachute. The descent rate is vital to this competition since there are specified descent rates in the guidelines. For the parachute, the target descent rate is 18 m/s. Descent rate is weighted at 35% since this is a crucial requirement of the competition. The descent rate of the parachutes will be evaluated using the program OpenRocket. The parachute that achieves a descent rate closest to the target value will receive a score of 10 out of 10 while others will be evaluated on a linear scale by their distance to the target value.

Weight is the relative mass contained by the parachute giving rise to a downward force of gravity. The parachute's weight is necessary to consider in the calculations as it can alter the flight dynamics of the launch vehicle and its descent speed. Weight is weighted at 10% since the parachute's weight is relatively small compared to the weight of the full launch vehicle, and therefore not as crucial. The parachute with the lowest weight will receive a score of 10 out of 10.

Shroud Lines is an evaluation of the effectiveness of the shroud lines and how they are attached to the parachute. This is done through inspection of the shroud lines and a qualitative analysis. How the shroud lines are attached and how many shroud lines are used are important factors in preventing damage to the parachute during deployment. The shroud lines will be counted and inspected and be given a qualitative score, which will be weighted at 35%. The way the lines are attached is more important than the number of shroud lines and will weigh more into the final score of the shroud lines. The parachute with the most effectively attached shroud lines and a decent amount of shroud lines will receive a score of 10 out of 10.

3.2.2.6.2 Selected Component

The 72 in. Fruity Chutes Irus Ultra parachute was selected to be the main parachute for the launch vehicle. It had the highest overall score in the decision matrix, with a score of 8.7. It also had the closest descent rate to the target value with a descent rate of 17.7 ft/s. It also has high quality shroud lines that are sewn well into the material of the parachute.

3.2.2.6 Drogue Parachute

A decision matrix was used to evaluate parachutes for the drogue parachute. The scores were calculated using linear scoring. The best concept was assigned a score of 10 out of 10 points (Table 14).

Drogue Parachute			18" Elliptical Fruity Chutes			24" Elliptical Rocketman			24" Elliptical Fruity Chutes			Skyangle C3 Drogue		
Objective	Weighting Factor	Parameter	Mag.	Score	Value	Mag.	Score	Value	Mag.	Score	Value	Mag.	Score	Value
cost	0.2	USD	62.30	4.4	0.9	50.00	5.5	1.1	64.00	4.3	0.9	27.50	10.0	2.0
descent rate	0.35	ft/s	85.7	2.3	0.8	64.2	0.8	0.3	66.3	0.9	0.3	78.7	10.0	3.5
weight	0.1	oz	2.1	10.0	1.0	2.1	10.0	1.0	2.2	9.5	1.0	3.1	6.8	0.7
shroud lines	0.35	qualitative	Good	8	2.8	Okay	6	2.1	Good	8	2.8	Great	10	3.5
Overall Value					**5.5**			**4.5**			**4.9**			**9.7**

Table 14: Drogue parachute decision matrix.

3.2.2.6.1 Objective Definitions and Justifications

Cost is the total price of the parachute. It is important to pick a parachute within budget. There are multiple sources to buy these parachutes, however the prices used in the matrix are those that are from the manufacturer. Price is weighted at 20% since the only requirement is being under budget, but the money saved here can be allocated to other parts of the design. The parachute with the lowest cost will receive a score of 10 out of 10 while the others will be evaluated on a linear scale by cost.

Descent Rate is the rate at which the launch vehicle will descend while using the main parachute. The descent rate is vital to this competition since there are specified descent rates in the guidelines. For the parachute, the target descent rate is 80 ft/s for the drogue parachute. Descent rate is weighted at 35% since this is a crucial requirement of the competition. The descent rate of the parachutes will be evaluated using the program OpenRocket. The parachute that achieves a rate of descent closest to the target value will receive a score of 10 out of 10 while others will be evaluated on a linear scale by their distance to the target value.

Weight is the relative mass contained by the parachute giving rise to a downward force of gravity. The parachute's weight is necessary to consider in the calculations as it can alter the flight dynamics of the launch vehicle and its descent speed. Weight is weighted at 10% since the parachute's weight is relatively small compared to the weight of the full launch vehicle, and therefore not as crucial. The parachute with the lowest weight will receive a score of 10 out of 10.

Shroud Lines is an evaluation of the effectiveness of the shroud lines and how they are attached to the parachute. This is done through inspection of the shroud lines and a qualitative analysis How the shroud lines are attached and how many shroud lines are used are important factors in preventing damage to the parachute during deployment. The shroud lines will be counted and inspected and be given a qualitative score, which will be weighted at 35%. The way the lines are attached is more important than the number of shroud lines and will weigh more into the final score of the shroud lines.

3.2.2.6.2 Selected Component

The Skyangle C3 Drogue was selected to be the drogue parachute for the launch vehicle. Unlike many smaller parachutes, this parachute was built to be a drogue parachute and there is no doubt that it will be able to hold the weight of the launch vehicle. It also had the descent rate that was closest to the target value, with a descent rate of 78.7 ft/s.

3.2.3 Recovery System Layout

The recovery system has two parachutes, one avionics bay, and a GPS. The main parachute is located in the forward section. The drogue parachute is located in the aft section. The main parachute deploys through the forward separation point between the nosecone section and the forward section. The drogue parachute deploys through the aft separation point between the avionics bay and aft section (Figure 23). Separation will be caused by black powder ejection charges controlled by a programmed altimeter (3.2.4). The GPS is located in the nosecone to keep it as far from the avionics bay as possible so as to avoid interference.

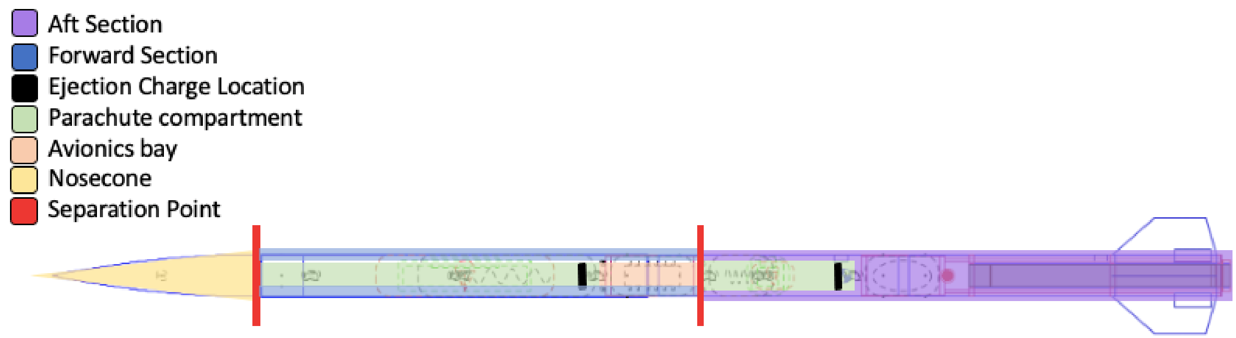

Figure 23: Launch vehicle separation points.

The first separation event will occur at apogee to deploy the drogue parachute from the aft section (Figure 24). The primary ejection charge for this separation will be programmed to detonate at apogee. The secondary ejection charge will be programmed to detonate 0.5 s. after apogee (6.1.1).

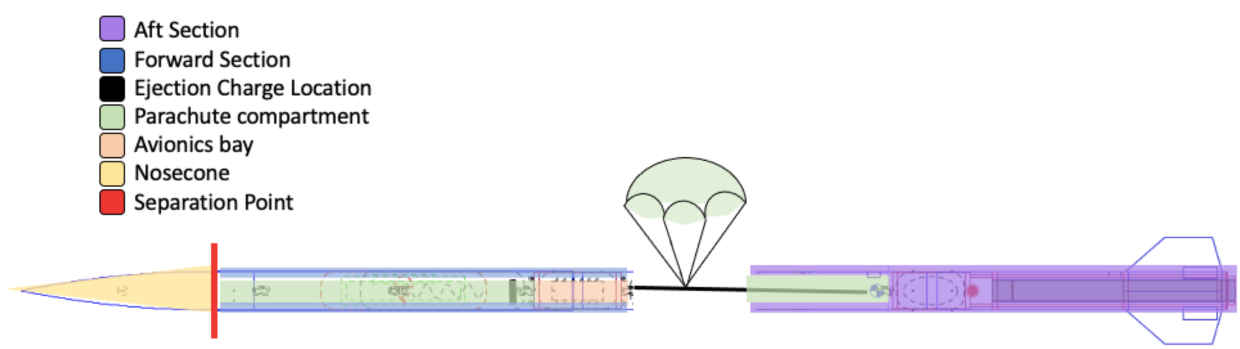

Figure 24: First separation event.

The second separation event will occur at 600 ft to deploy the main parachute from the forward section (Figure 25). The primary ejection charge for this separation will be programmed to detonate at 600 ft.

above ground level. The secondary ejection charge will be programmed to detonate at 550 ft. above ground level (6.1.1).

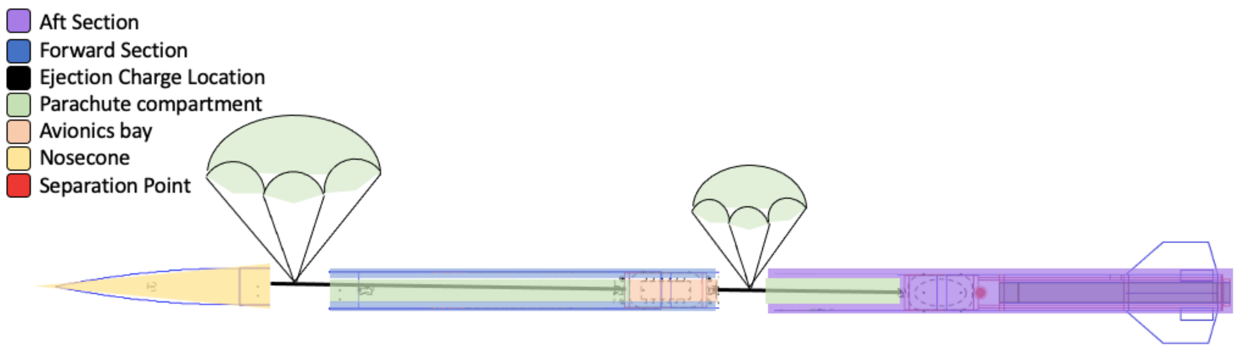

Figure 25: Second separation event.

3.2.4 Redundancy in the System

The Avionics and Recovery Subsystem will have a redundant set of ejection charges wired independently of the primary charges. The redundant ejection charges will be 25% larger than the primary ejection charges and be on a delay from the primary charges. The secondary aft ejection charges will be on a 0.5 second delay from the primary aft ejection charge. The secondary forward ejection charge will be on a 50 ft delay from the primary forward ejection charge (6.1.1). The primary and secondary ejection charges will be controlled by separate altimeters. The primary altimeter will be a Stratologger CF, and the secondary altimeter will be an Entacore AIM altimeter. Having the two different altimeters protects against a failure that could occur in any altimeter of the same make and model. The two altimeters will be powered by their own 9-volt batteries (Figure 26).

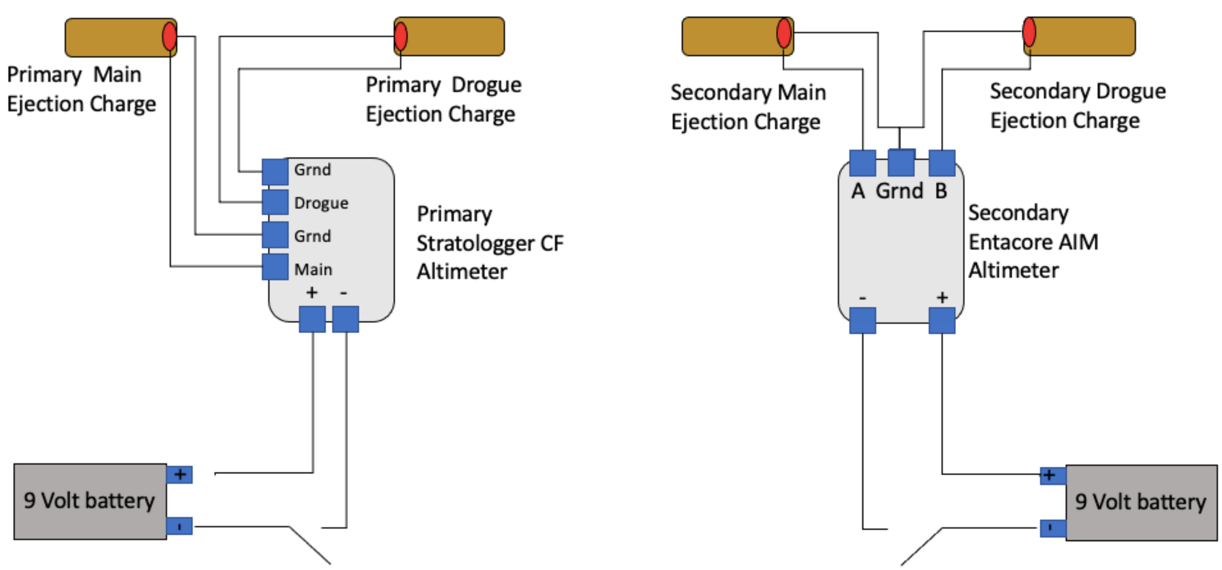

Figure 26: Avionics wiring diagram.

3.3 Mission Performance Predictions

3.3.1 Target Altitude Declaration

3.3.1.1 Sensitivity Analysis and Altitude Confirmation

A Monte Carlo Simulation was conducted in MATLAB to test the sensitivity of the launch vehicle to wind conditions and its effects on the apogee. To validate the target altitude, a total of 10,000 simulations were conducted with random values of wind profiles ranging from 0 mph to 20 mph (Figure 27). The data indicates the altitude is most likely to be in the range of 4550 ft to 4600 ft.

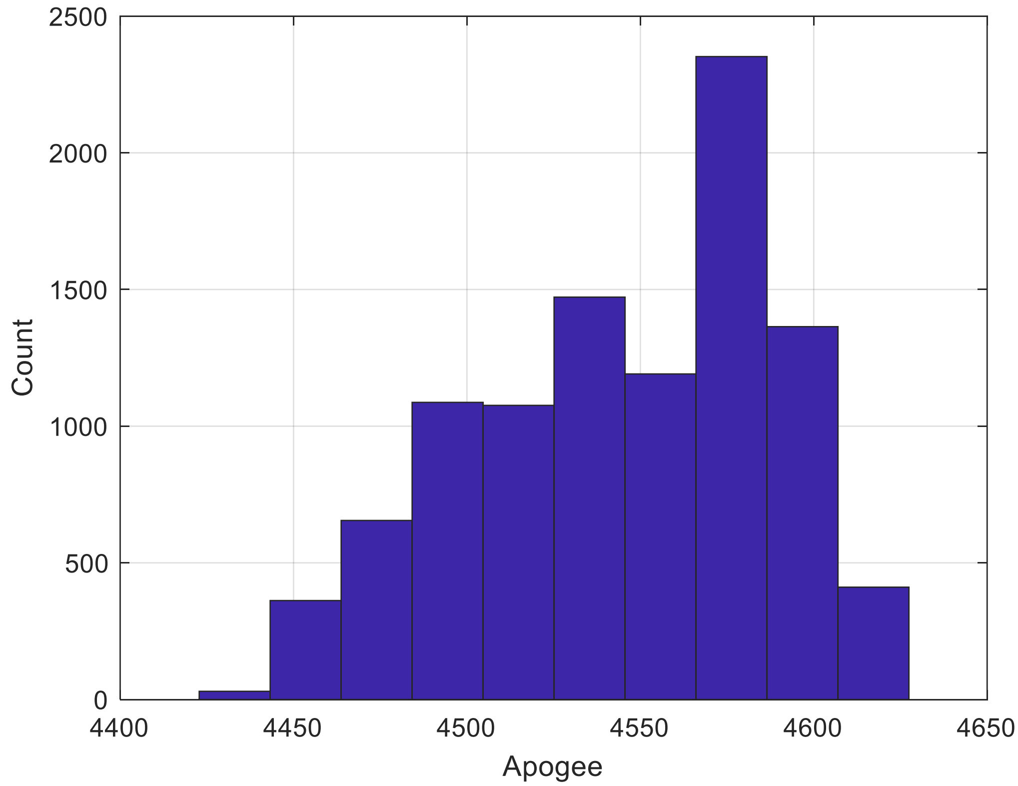

Figure 27: Monte Carlo simulation results.

3.3.1.2 Target Altitude

The official launch day target altitude is 4578 ft. The value was chosen to reflect launch conditions and is a result of the average predicted performance of the Gator Locator (Table 15). The probability weight is the percentage chance that the combination of launch angle and wind condition is likely to occur. The values were assigned by allocating the most likely condition with the largest probability and determining the rest accordingly. The values were allocated as results of sensitivity analyses, discussed in section 3.3.3, and considering the climate of the launch site. While the launch angles for the simulated conditions in the table include 0 and 2.5 degrees, the launch angle will be between 5 to 10 degrees on the launch day as the competition requires. However, the analysis uses these given angles to ensure proportional altitude changes between launch conditions.

Average Altitude			
Launch Angle	Wind Condition	Probability Weight	Predicted Altitude
0	0 mph	5%	4682 ft
2.5 deg	5 mph	10%	4655 ft
5 deg	10 mph	70%	4588 ft
7.5 deg	15 mph	10%	4480 ft
10 deg	20 mph	5%	4379 ft
Average Altitude			**4578 ft**

Table 15: Predicted altitude performance.

3.3.2 Flight Profile Simulations

3.3.2.1 Flight Simulations

The flight simulation assumes the predicted flight conditions in Huntsville, Alabama (Table 16). Based on simulations the launch vehicle achieves an apogee at 4588 ft given these conditions (Figure 28). The maximum velocity is 626 ft/s, and the maximum acceleration is 98.7 m/s^2 (Figure 29, Figure 30).

Launch Conditions in Huntsville, Alabama	
Wind	10 mph
Launch Angle	5 deg
Launch Rod Length	144 in
Latitude	34.6 °N
Longitude	-86.7 °E
Altitude	800 ft
Temperature	62 °F
Pressure	1 atm

Table 16: Launch conditions in Huntsville, AL

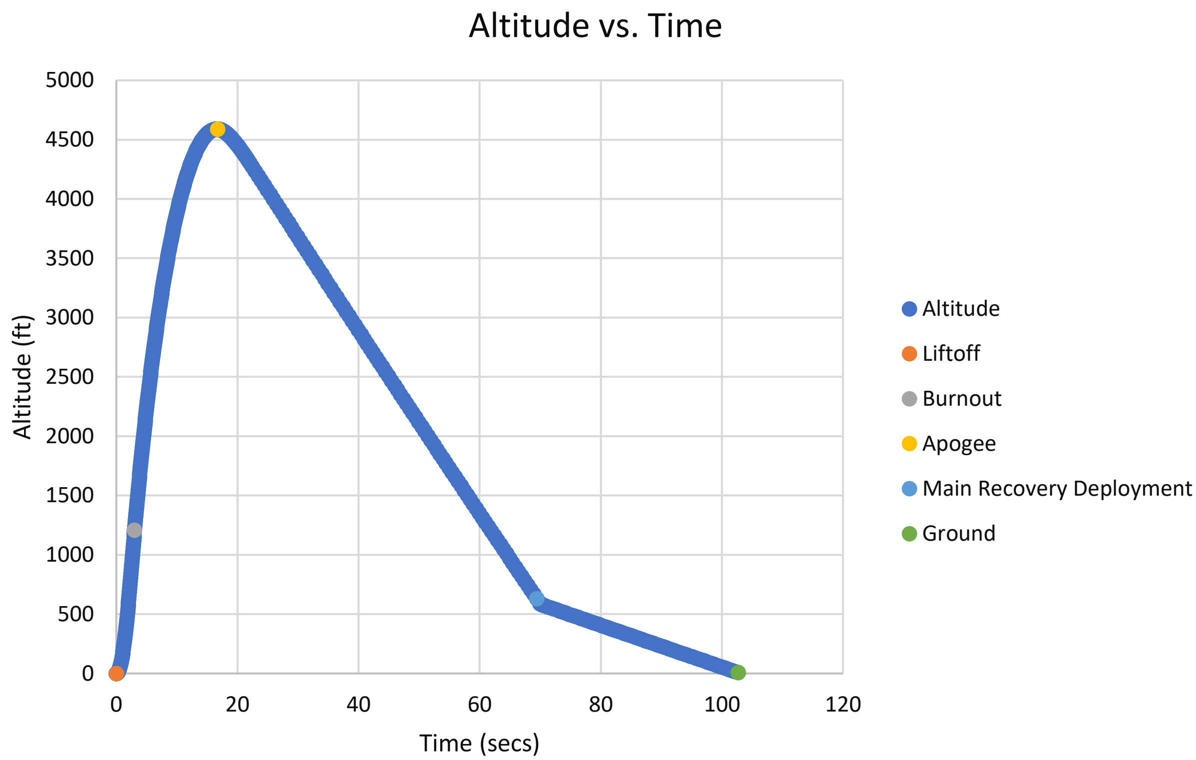

Figure 28: Altitude vs. time plot.

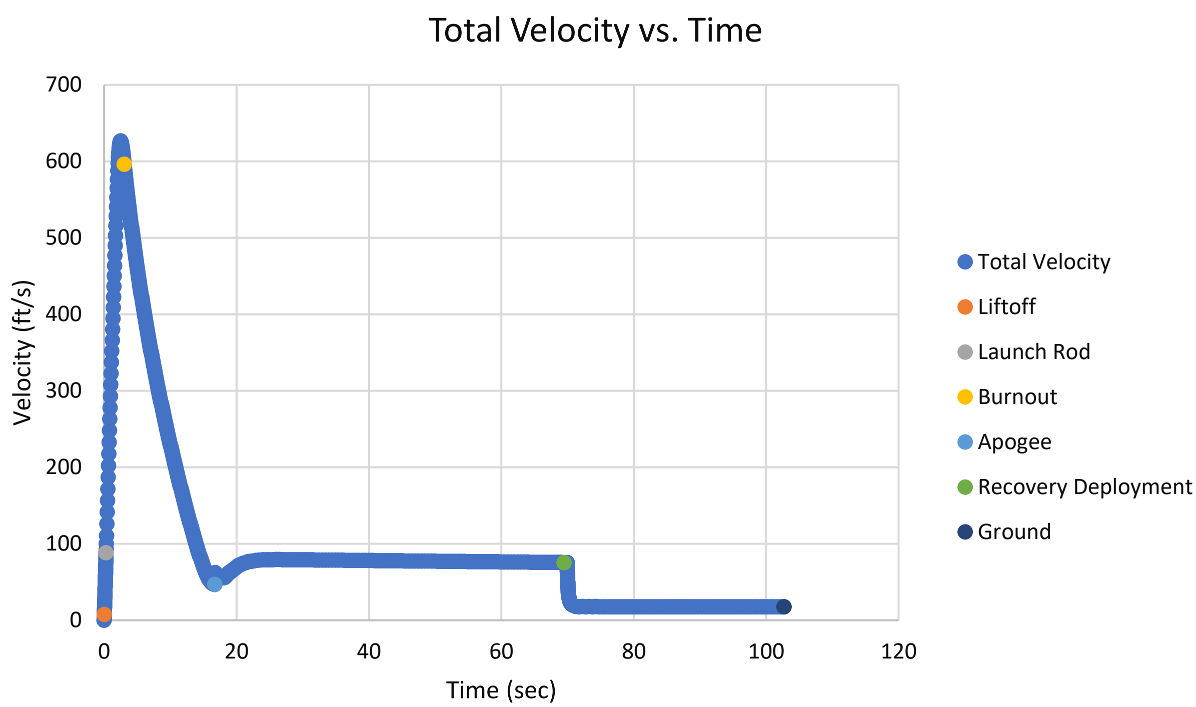

Figure 29: Total velocity vs. time plot.

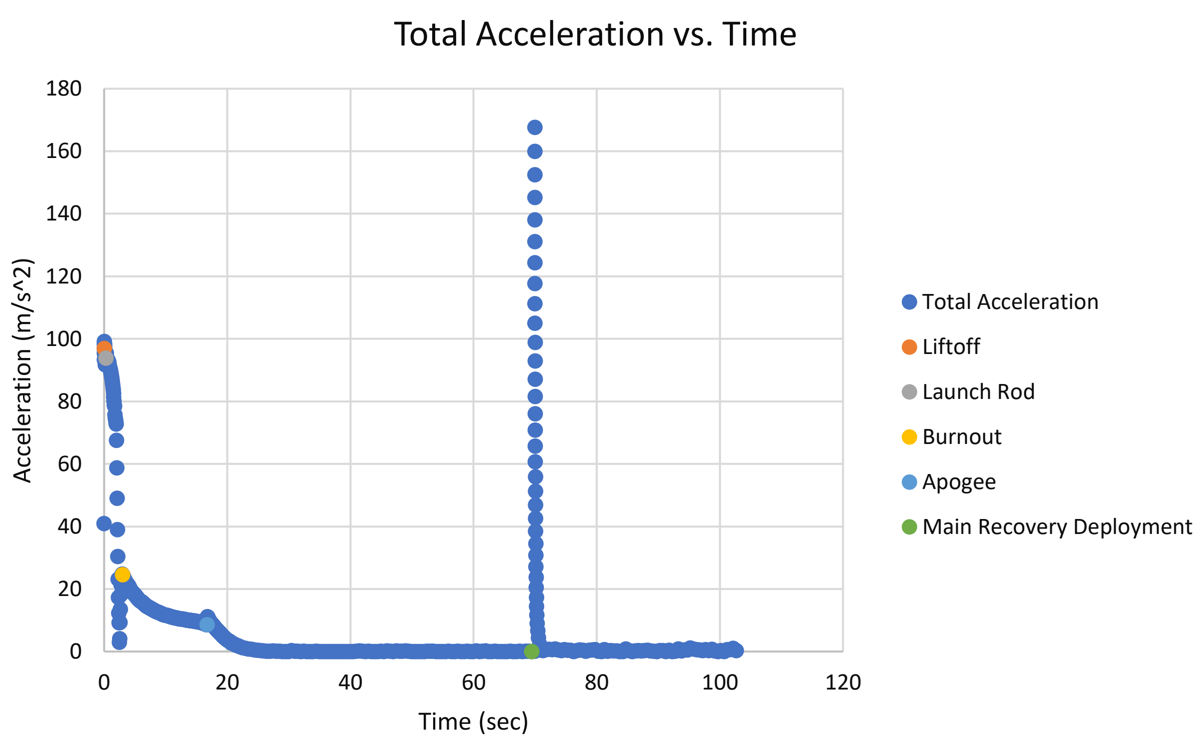

Figure 30: Total acceleration vs. time plot.

3.3.2.2 Motor Thrust Curve

The selected motor is the Aerotech L1090W motor. It was chosen to prioritize the launch vehicle's safety and to reach the target altitude. The motor choices were restricted to being 58 mm in diameter and a maximum 25 in. in length. The alternative motor options were the Cesaroni L1030 motor, and the Cesaroni L640 motor. Aerotech was chosen over the alternative motors as it best achieves the team's priority of safety and is most accessible for launches.

The Aerotech L1090W has a total impulse of 2736 N-s, and a maximum thrust of 1334 N. The maximum thrust occurs at the launch rod to propel the launch vehicle at 88.4 fps. The motor uses 1400 grams of propellant to produce a burn time of 3 seconds (Figure 31). The total weight of the launch vehicle is 428 oz, and the thrust-to-weight ratio is 9.17, fulfilling the competition's requirement of a minimum thrust-to-weight ratio of 5.

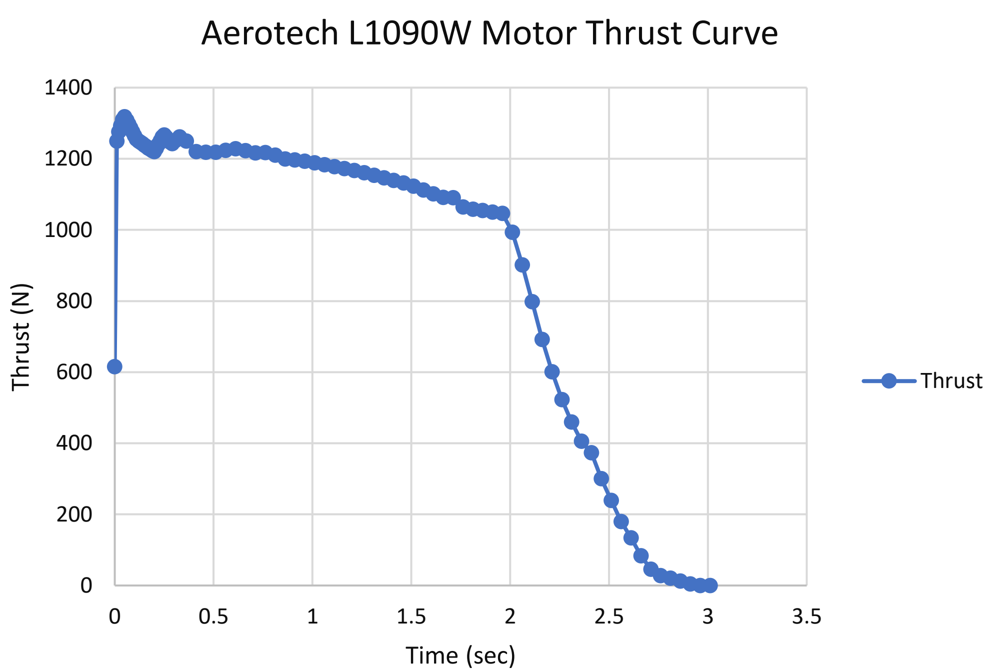

Figure 31: Motor thrust curve.

3.3.2.3 Static Stability Margin

The launch vehicle is statically stable when the center of pressure is located at least 1 body caliber behind the center of gravity. The center of gravity of the motor is located 78.1 in. from the tip of the rocket. The center of pressure of the motor is located 91.3 in. from the tip of the nosecone. The static stability of the launch vehicle when it is clearing the launch rod is 2.1 calibers, fulfilling the competition's requirement of 2 calibers off the launch rod. During the flight, the stability gradually increases to 3.9 calibers, due to the reduction of mass in the motor. However, the stability reaches a maximum of 4.2 calibers, at burnout, due to the increase in velocity and a minimum of 2.1 due to the decrease in velocity as it reaches apogee (Figure 32). The oscillations, seen in the figure, are an indication of the simulated wind gusts on the launch vehicle.

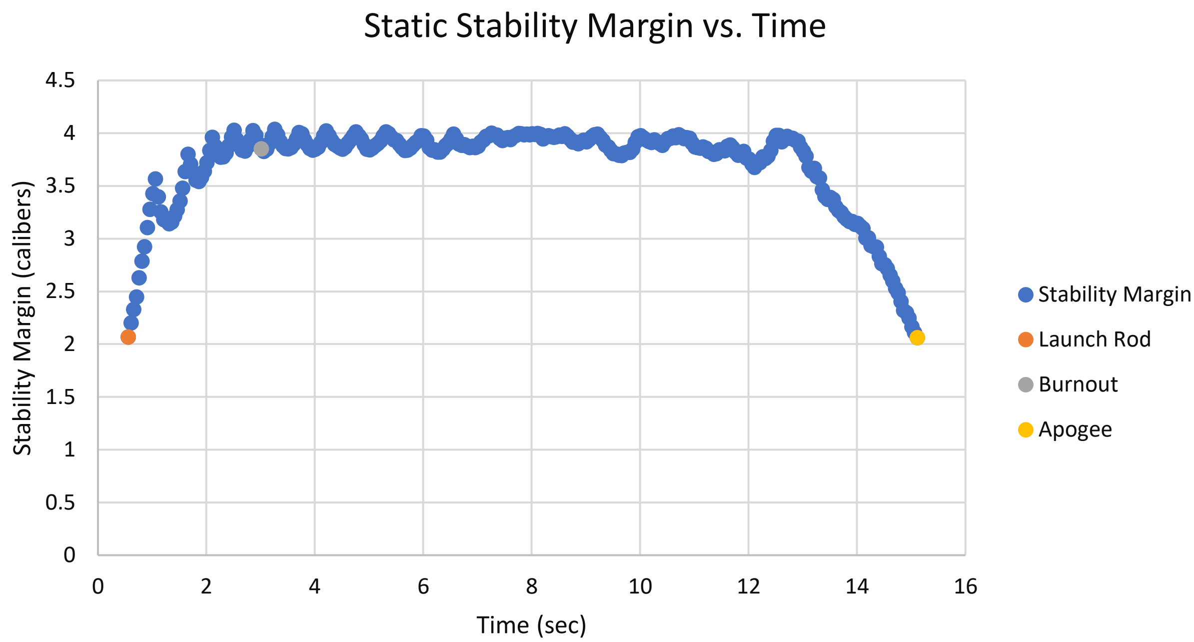

Figure 32: Static stability margin vs. time plot.

3.3.2.4 Drift

Drift calculations were made assuming constant wind speed and that apogee is reached directly above the launch pad (Table 17). The descent rate for the drogue parachute was held constant at the terminal velocity for the drogue parachute of 78.7 ft/s, and it was assumed that it descended at that rate once it was deployed at apogee. The main parachute descent rate was held constant at the terminal velocity for the main parachute of 17.7 ft/s, and it was assumed that the launch vehicle descends at this rate once the main parachute was deployed at 600 ft above ground level. The velocities were kept constant to simplify the calculations. Apogee was kept constant at 4578 ft. for all drift calculations done on the spreadsheet because it is the target altitude (3.3.1).

Drift Calculations Calculated with Spreadsheet				
Wind Speed	5 mph	10 mph	15 mph	20 mph
Drogue Drift (ft)	386	772	1158	1543
Main Drift (ft)	250	500	750	1000
Total Drift (ft)	**636**	**1272**	**1908**	**2543**

Table 17: Drift calculations from spreadsheet.

The second method used to calculate drift was through the OpenRocket simulation (Table 18). The standard deviation of the wind was set to 0, and the angle of the launch rod was set to 0 degrees to try and simulate the launch vehicle reaching apogee above the pad. This was not successful, as the simulation accurately depicted the rocket correcting into the wind during flight. It would then reached apogee up wind of where it would eventually drift to. To find total drift from the simulation, the distance traveled upwind was added to the final lateral distance from the launch pad. The simulation is more accurate in calculating the descent rate of the launch vehicle as the launch vehicle does not instantly reach terminal velocity when a parachute deploys but takes time to accelerate to terminal velocity. This should provide a more accurate drift calculation as well because the descent rate varies with time and air density as it should. This also accounts for the increasing difference in value between the two calculation methods as the wind speed increases. The spreadsheet calculations suggest the launch vehicle would not stay within the launch field, but because the simulation is more accurate to real world conditions, the launch vehicle should easily stay within the launch field as it is currently designed.

Drift Calculations Calculated with OpenRocket				
Wind Speed	5 mph	10 mph	15 mph	20 mph
Total Drift (ft)	**605**	**1215**	**1825**	**2350**

Table 18: Drift calculations from OpenRocket.

3.3.2.5 Decent Time

Descent time calculations were made assuming constant wind speed and that apogee is reached directly above the launch pad (Table 19). The descent rate for the drogue parachute was held constant at the terminal velocity for the drogue parachute of 78.7 ft/s, and it was assumed that it descended at that rate once it was deployed at apogee. The main parachute descent rate was held constant at the terminal velocity for the main parachute of 17.7 ft/s, and it was assumed that the launch vehicle descends at this rate once the main parachute was deployed at 600 ft above ground level. The velocities were kept constant to simplify the calculations. Apogee was kept constant at 4578 ft for all descent time calculations.

Descent Time Calculated with Spreadsheet	
Drogue Descent Time (s)	52.6
Main Descent Time (s)	34.1
Total Descent Time (s)	86.7

Table 19: Descent time calculations from spreadsheet.

The second method used to calculate descent time was OpenRocket (Table 20). OpenRocket was able to represent the acceleration of the launch vehicle more accurately to terminal velocity during parachute deployments. The wind speed of the simulation was held constant at 0 mph. The launch rail was also kept at 0 degrees to match the total drift simulation. The apogee did vary slightly with each run of the simulation, but it was consistently within 5 ft of the target altitude. Similar to the drift calculations, the OpenRocket calculations are more accurate due to the accurate simulation of the launch vehicle accelerating to its terminal velocity over time.

Descent Time Calculated with OpenRocket	
Time to Apogee (s)	16.6
Total Flight Time (s)	103
Total Descent Time (s)	**86.4**

Table 20: Descent time calculations from OpenRocket.

3.3.2.6 Kinetic Energy

Kinetic energy is calculated for each separated section at landing (Table 21). It will be assumed that all sections of the launch vehicle descend at the main parachute's terminal velocity from the OpenRocket at ground hit. The mass of each section is taken from the mass table (Table 1).

Kinetic Energy at Ground Hit Calculated with Spreadsheet	
Nosecone (ft-lbs)	6.9
Forward Section (ft-lbs)	39.5

Aft Section (ft-lbs)	61.7

Table 21: Kinetic energy at ground hit calculations from spreadsheet.

4. Payload Criteria

4.1 Selection, Design, and Rationale of Payload

4.1.1 Payload Objectives and Success Criteria

The payload's objective is to identify the vehicle's landing location and transmit this location to the team's ground station. To be considered successful, the payload must be able to capture, store, and process images of the launch field. The payload must continuously collect and later process IMU data and must be able to determine the vehicle's final landing location from this information. The payload must be able to transmit this determination to a ground station, where the result can be displayed and stored.

4.1.2 System Level Design Alternatives

The team considered three camera-based system alternatives: a forward camera system, a hanging camera system, and a rear-facing camera system. Each system was evaluated on its reliability, image capturing altitude window, and orthogonality of captured images to the launch field.

The vehicle's stability during each stage of flight was evaluated and considered for each system alternative. To determine the stability of each section during each stage of flight, the team reviewed video recordings of launches. The vehicle's orientation is stable during ascent and is approximately vertical during most of ascent. During drogue descent, the vehicle becomes unstable, and thus any cameras fixed to the airframe are unlikely to directly face the launch field. The vehicle becomes stable during main descent; however, the vehicle's altitude is limited to the main deployment altitude of 600 ft. The low altitude during main descent limits the portion of the launch field that is viewable without significant camera distortion.

4.1.2.1 Forward Camera System

The forward camera system alternative utilizes a camera in the nosecone to capture images of the launch field during descent (Figure 33). This system's image capturing window includes drogue and main descent. This system was not selected due to the volatile movement of the nosecone during drogue descent, which greatly reduces the likelihood of capturing images that are directly perpendicular to the launch field in this configuration.

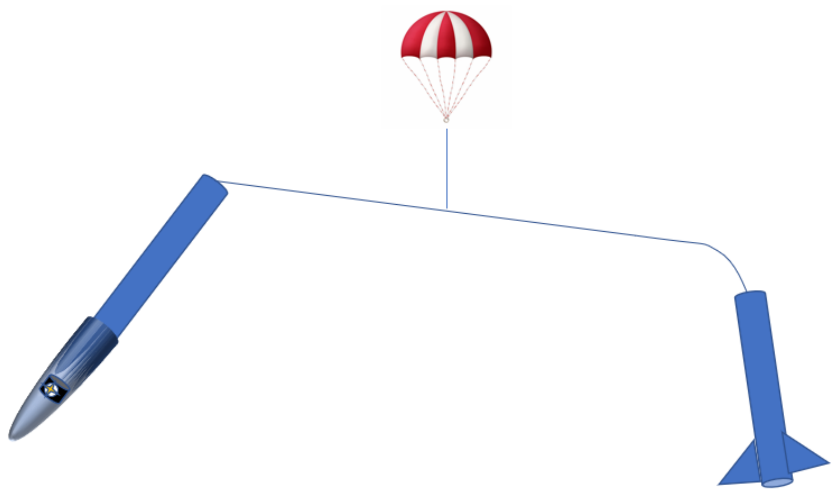

Figure 33: Forward camera design alternative.

4.1.2.2 Hanging Camera System

The hanging camera system alternative places the camera on a capsule that is tethered to the launch vehicle's drogue parachute via a harness (Figure 34). This capsule would be deployed with the drogue and would hang beneath the vehicle during descent, with a camera facing downward to capture images of the terrain. This option allows the payload to capture images of the terrain below without being obscured by the launch vehicle. However, this system was not selected due to the possibility of tangling between the payload capsule harness and drogue parachute recovery harness during descent.

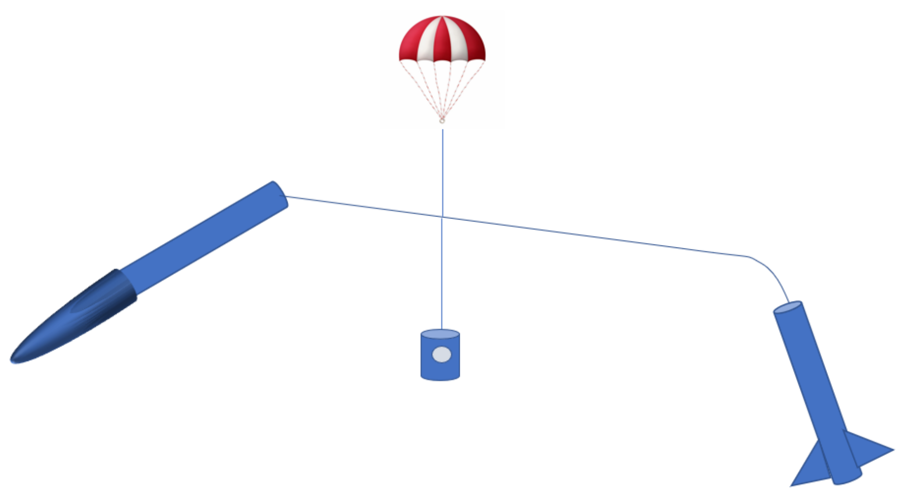

Figure 34: Hanging camera design alternative.

4.1.3 Leading Payload Design

A rear-facing camera system alternative places two external cameras on the aft airframe of the launch vehicle (Figure 35). This alternative differs from the others in that its images are captured primarily during ascent, when the launch vehicle is stable and near orthogonal to the launch field. During ascent, the rocket is at its most stable orientation and has the greatest degree of orthogonality with respect to the ground. The images taken during ascent provide the most useful data for determining the location of the rocket on the launch field and will thus be used to determine the location of the rocket as it reaches apogee. During drogue descent, the aft section of the rocket experiences volatile rotations and translations, drastically decreasing the possibility of obtaining an accurate image of the launch field. During main descent, the aft section's motion is less violent, providing a possibility of obtaining a clear image of the launch field. However, main descent occurs at a low altitude, reducing the field of view of the image and any identifiable portions of the launch field. Due to these image capturing windows, location analysis of the rocket will primarily occur during ascent, with any descent image analysis being conducted as a redundancy.

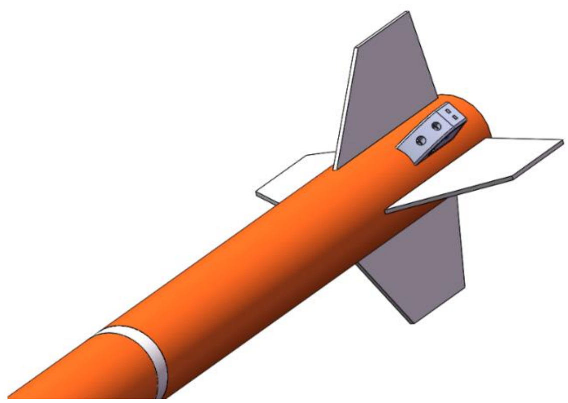

Figure 35: Leading payload design.

The payload continuously captures images and IMU data during flight. Upon landing, the payload begins scoring images based on multiple criteria including its timestamp, state, altitude, angle of image and number of keypoints. Keypoints are points in the image that help define how it stands out. The highest scoring image is analyzed to determine the rocket's location at the time of image capture. Because the rocket is still in motion when the image is captured, the payload must be able to determine its displacement from the determined location. To determine the rocket's displacement over time, the payload continuously measures its acceleration with an Inertial Measurement Unit (IMU). The payload processes the IMU data and finalizes the location of the rocket on the provided grid box.

4.1.3.1 Software Design

4.1.3.1.1 Payload Onboard Software

The software design of the payload refers to the program uploaded on the Raspberry Pi. The software will be performing image comparison using a Scale-Invariant Feature Transform (SIFT) algorithm in OpenCV. Image comparison will occur by pulling pictures from the camera, storing them in an SD card, and then analyzing them against a pre-uploaded image of the launch field. The image taken by the rocket will be compared against the image of the launch field using the SIFT algorithm. This then helps create bounding boxes around the reference point, which can be used to find the distance of the rocket from the point.

This helps identify the position of the rocket. This location will then be used as the initial position of the rocket, and the IMU data will be used to track the displacement of the rocket over time up until the rocket lands. The entire processing of the image and IMU data for the payload will be done post flight.

4.1.3.1.1.1 Image Analysis

The SIFT algorithm helps compare keypoints and on a positive match helps create bounding boxes around a reference object. The analysis will be done by calculating the distance from the principal point of the camera to the bounding box of the reference object. The altimeter will then be used to get the altitude at the time of the image being taken and the distance will be scaled accordingly. The known location of the reference object on the gridded map will be used to estimate the location of the rocket on the gridded map. Images taken at a tilted angle will use the IMU to account for the tilt and calculate the position accordingly.

4.1.3.1.1.2 Image and IMU Data Storage

The images will be stored and have multiple descriptors including - Timestamp, State, Altitude, Angle of image and Number of Keypoints.

The images captured will be defined into 4 capture states (Table 22).

State	Criteria
Best	2500ft – 4000ft
Good	1000ft – 2500ft
Fair	<1000ft
Poor	Over cloud cover

Table 22: Image capture states' definitions.

After landing the images will be put through the SIFT algorithm and stored in a matrix with the number of keypoints they have. The SIFT algorithm will also tell us if we are over cloud cover.

The IMU data will be stored with their timestamps. The angle of the image will be obtained from the IMU by comparing the image and IMU data timestamp.

The IMU will have 3-axis acceleration, 3-axis orientation, and 3-axis magnetometer reading. This data will be stored in a multidimensional array in the code.

4.1.3.1.1.3 Image Processing

The processing phase will begin once all the data is collected. All the images taken during descent under 1000 ft will be considered; however, the images may not contain enough keypoints because it is too close to the ground to capture enough terrain. Next, the images are analyzed in the order of when they were taken. If a good enough percentage match is found, location data is stored in a matrix with the details of the image (keypoints, timestamp, state) and continue. The images taken above cloud cover are eliminated and image processing stops. Location data will then be compared for inconsistencies.

If the location is not able to be detected, we begin processing images taken during descent starting from 1000ft to the time we hit cloud cover.

Priority will be assigned to the image depending on:

1. Time Stamp: Most recent has higher priority
2. Keypoints: Image with more keypoints will be assigned higher priority
3. Percentage match: Location data from how many images; higher percentage match is better

4.1.3.1.1.4 Location calculation

For the location to be found, the distance between the principal point and the reference point will be measured. To do this, the vertical tilt must be accounted for. The vertical tilt is defined as the angle between the ground and the vertical axis of the launch vehicle. Vertical tilt will be corrected by using measures to correct tilt errors in photogrammetry. Trigonometry will be employed and the angles will be used to calculate the deviation.

To determine the size of the image, the real width of the image will be calculated using (1) where FoV_{lens} is the field of view of the camera lens. The real width is defined as the distance from one end of the image to the other.

$$Real\ Width = Altitude \times (\tan\left[\left(\frac{FoV_{lens}}{2}\right) + tilt_{camera}\right] + \tan\left[\left(\frac{FoV_{lens}}{2}\right) - tilt_{camera}\right]) \tag{1}$$

This real width will then be used to scale the distance between the principal point and the reference point on the map to get the real distance.

We find the final location by calculating the deviation from the location in the image to the final location by using the data from the IMU.

4.1.3.1.1.5 Algorithm Comparison Matrix

The software design was chosen after comparing multiple alternatives (Table 23).

	Algorithm 1	Algorithm 2
Name	Modified Convoluted Neural Network (CNN)	SIFT
Computational Complexity (Lower is better)	Higher computational complexity because of highly adaptive trainable features	Lower computational complexity because of usage of only low-level features
Time Complexity (Lower is better)	Higher time complexity	Lower time complexity
Power Usage (Lower is better)	Higher	Lower
Accuracy of detection (Higher is better)	Higher	Lower

Table 23: Software design comparisons.

CNN with satellite imaging datasets was considered in place of SIFT. However, the computational power required would exceed the capabilities of any embedded system put on board at a reasonable cost. Therefore, SIFT was chosen as the algorithm for image comparison for location detection.

4.1.3.1.1.6 Software Program Flow

On the launch pad, the Raspberry Pi is in an idling state. The IMU is turned on pre-flight. The Raspberry detects flight utilizing the IMU and turns on. It then starts collecting and storing images. After landing, the images are all stored along with their timestamp, state, altitude, angle of image and number of Keypoints. After this, analysis is begun. Upon identifying the location, the grid location is transmitted to a ground station (Figure 36).

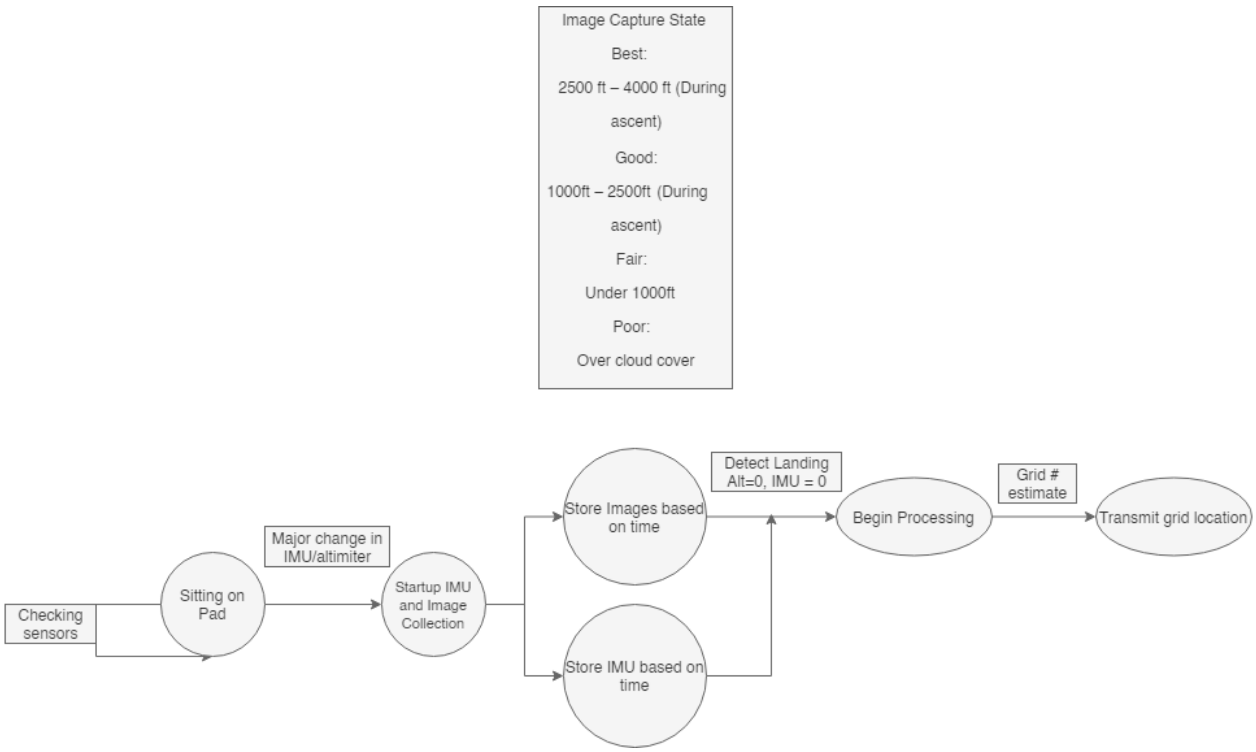

Figure 36: Software flow chart.

4.1.3.2 Electrical Design

4.1.3.2.1 Electrical Schematics

The payload contains a processor, inertial measurement unit, barometer, and two cameras. The interconnection between each electrical component is shown in Figure 37. Power supplied by the 7.4V lithium-ion batteries is passed through a 3.3V and a 5V linear voltage regulator. The 3.3V linear voltage regulator output supplies power to each of the two cameras, IMU, and XBee transceiver. The 5V linear voltage regulator supplies power to the Raspberry Pi 4. A 10 µF ceramic capacitor, and 220 µF electrolytic capacitor are placed on the input and output terminals respectively of each linear voltage regulator. These capacitors are used to reduce power ripple on each supply line, thereby reducing noise on each sensor’s output.

The Raspberry Pi 4 communicates with the IMU and cameras via the Serial Peripheral Interface (SPI). This interface, consisting of CLK, MOSI, MISO, and CS lines, permits the highest data rate for these sensors out of the available communication protocols. The Inter-Integrated Circuit (I2C) protocol is used for communication between the Raspberry Pi 4 and BMP388 because this is the only protocol supported by the BMP388. The Raspberry Pi 4 is connected to the XBee transceiver via the Universal Asynchronous Receiver-Transmitter (UART) pins, RxD and TxD, because this protocol only requires a two-wire interface, and a high data rate is not needed.

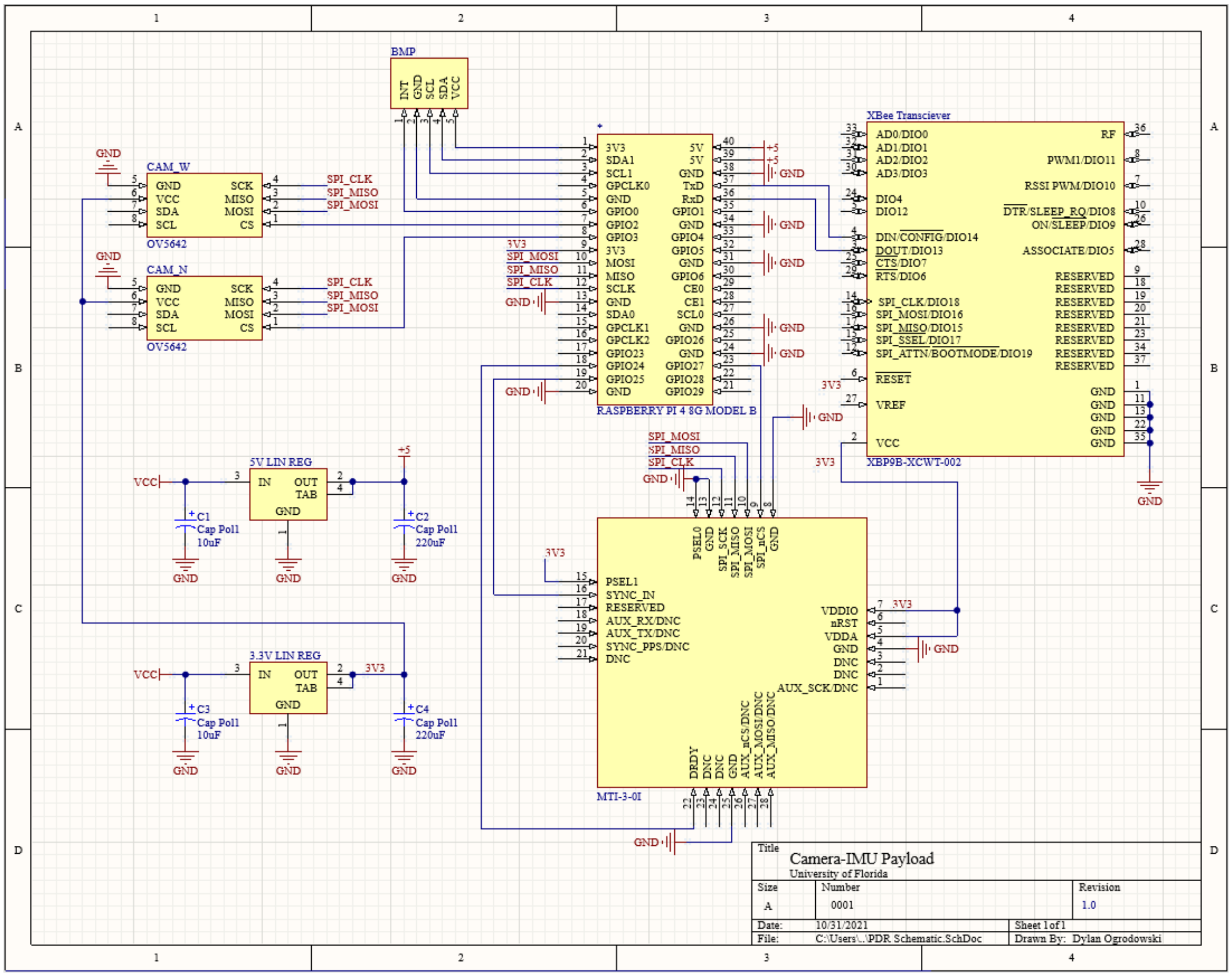

Figure 37: Payload electrical schematic.

The interconnection between each ground station component is shown in Figure 38. The ATmega328P is connected to the XBee transceiver and SD card via SPI interface and is connected to the LCD output panel using I^{2}C.

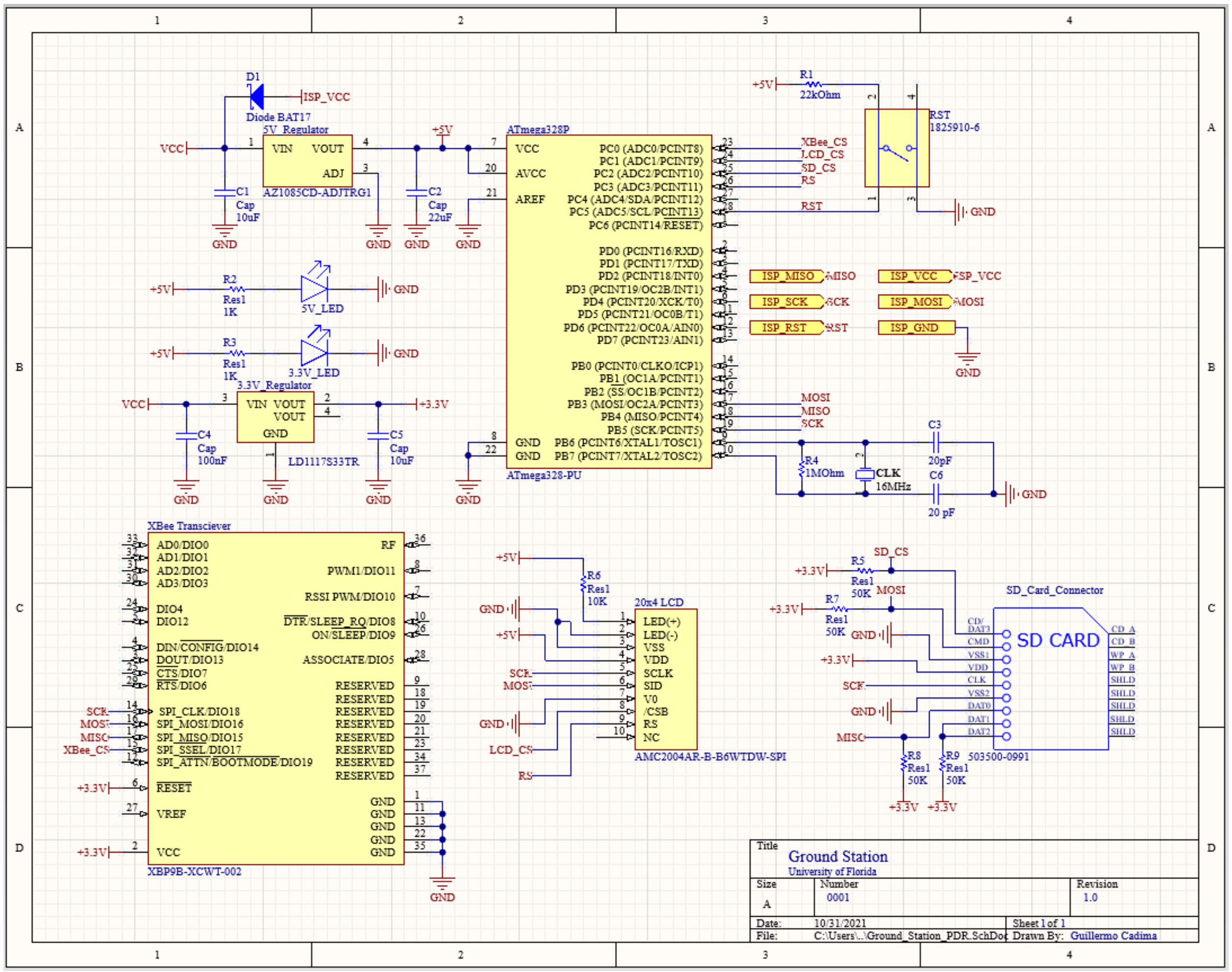

Figure 38: Payload ground station schematic.

4.1.3.2.2 Processor Selection

The payload computer is responsible for processing all images taken during the flight. The device must support OpenCV and be compatible with Linux operating system (4.1.3.1). Additionally, the processor must be low power, because of battery and thermal constraints. To meet these requirements, all considered processors use ARM architecture. All considered processors also support UART, SPI, and I^{2}C protocols to allow for the processors to communicate with external sensors. Qualitative objectives were scored according to (Table 2).

A decision matrix was used to evaluate the different options for the payload computer (Table 24).

4.1.3.2.2.1 Objective Definitions and Weighting Factors

Payload Computer			Raspberry Pi 4 Model B			TI TMDXSK437X		
Objective	Weighting Factor	Parameter	Mag.	Score	Value	Mag.	Score	Value
Cost	0.1	USD	149.99	8.50	0.85	249.00	5.12	0.51
CPU Performance	0.4	DMIPS	28200	5.17	2.07	2500	0.46	0.18
Board Size	0.2	in^2	7.38	10.00	2.00	14.7	5.00	1.00
Maximum Power Draw	0.1	W	12.50	10.00	1.00	12.50	10.00	1.00
User Friendliness	0.2	Experience	Great	10	2.00	Good	8	1.60
Overall Value					**7.92**			**4.29**
Payload Computer			**BeagleBone AI**			**TI SK-TDA4VM**		
Objective	Weighting Factor	Parameter	Mag.	Score	Value	Mag.	Score	Value
Cost	0.1	USD	127.43	10.00	1.00	199.00	6.40	0.64
CPU Performance	0.4	DMIPS	22857	4.19	1.68	54520	10.00	4.00
Board Size	0.2	in^2	7.45	9.90	1.98	20.3	3.63	0.73
Maximum Power Draw	0.1	W	15.00	8.33	0.83	15.00	8.33	0.83
User Friendliness	0.2	Experience	Okay	6	1.20	Okay	6	1.20
Overall Value					**6.69**			**7.40**

Table 24: Payload computer decision matrix.

The scores were calculated using linear scoring. The best device was assigned a score of 10 out of 10 points. A device with a magnitude of half or double the best design is assigned a score of 5 out of 10. This linear assignment continues in both directions.

Cost is the current-day price (USD) of the device from available suppliers (regardless of the product's nominal price). Cost is only weighted at 10% because the processor is one of the most critical components of the payload. The board with the lowest cost scores 10 out of 10 points.

CPU Performance is an estimation of the computational speed of each device's processor. The Dhrystone integer benchmark is used to compare performance in terms of millions of instructions per second (MIPS). The single-core Dhrystone MIPS/MHz is multiplied by the processor's maximum frequency. Since OpenCV can use multiple threads, this figure is also multiplied by the core count of the processor. Chips with digital signal processors (DSPs) have their base DMIPS multiplied by the estimated speedup when using DSP cores. This estimation is based on Texas Instruments' publications comparing OpenCV performance on ARM and DSP cores. The speedup from other hardware accelerators (embedded vision engines, vision processing accelerators) are not considered. This objective is weighted at 40% because more processing power allows for the payload to perform more complex vision processing. The fastest processor scores 10 out of 10 points.

Board Size is the area (in^2) of the printed circuit board (PCB). The payload compartment's limited size means that larger boards leave less space for other devices and cause the compartment to be harder to assemble. Consequently, the board size is weighted at 20%. The smallest board scores 10 out of 10 points.

Maximum Power Draw is based on the minimum power supply (W) requirements of each device, calculated by multiplying the supply voltage by the maximum current draw. Maximum power draw dictates the required capacity and maximum current output of the batteries and is weighted at 10%. The board with the lowest power draw scores 10 out of 10 points.

User Friendliness is a qualitative assessment of the ease at which the platform can be learned. Devices with more thorough documentation score higher. Guides from third parties are considered but are valued less than documentation from the original designer. User Friendliness is weighted at 20% because of its significant impact on software development time. The most user-friendly devices score 10 out of 10 points.

4.1.3.2.2.2 Scoring Justifications

The scores were calculated using linear scoring. The best device was assigned a score of 10 out of 10 points.

Cost

The Raspberry Pi 4 Model B with 8GB RAM is currently available for $149.99 in the United States. Since the cheapest device has a cost equal to 85.0% this device's cost, the Raspberry Pi 4 Model B receives a score of 8.50 out of 10.00.

The TI TMDXSK437X costs $249.00. Since the cheapest device has a cost equal to 51.2% of this device's cost, the TI TMDXSK437X receives a score of 5.12 out of 10.00

The BeagleBone AI costs $127.32, the cheapest of all devices considered. Therefore, it receives a score of 10.00 out of 10.00.

The TI SK-TDA4VM costs $199.00. Since the cheapest device has a cost equal to 64.0% of this device's cost, the TI SK- TDA4VM receives a score of 6.40 out of 10.00

CPU Performance

The Raspberry Pi 4 Model uses a quad-core ARM Cortex-A72 processor at 1.5 GHz. The ARM Cortex-A72 executes 4.7 DMIPS/MHz per core. Four cores at 1.5 GHz are capable of executing 28200 DMIPS. Since this device's performance is equal to 51.7% of the fastest device, the Raspberry Pi 4 Model receives a score of 5.17 out of 10.

The TI TMDXSK437X uses a single-core ARM Cortex-A9 processor at 1.0 GHz. The ARM Cortex-A9 executes 2.5 DMIPS/MHz per core. One core at 1.0 GHz is capable of executing 2500 DMIPS. Since this device's performance is equal to 4.6% of the fastest device, the TI TMDXSK437X receives a score of 0.46 out of 10.00.

The BeagleBone AI uses a dual-core ARM Cortex-A15 at 1.5 GHz along with two C66x DSPs. The ARM Cortex-A15 executes 4.01 DMIPS/MHz per core. Two ARM Cortex-A15 cores at 1.5 GHz are capable of executing 12030 DMIPS. The speedup from moving code from ARM cores to the two C66x DSPs is estimated to be 1.9x based on OpenCV gaussian blur benchmarks from Texas Instruments. The adjusted speed is 22857 DMIPS. Since this device's performance is equal to 41.9% of the fastest device, the BeagleBone AI receives a score of 4.19 out of 10.00.

The TI SK-TDA4VM uses a dual-core ARM Cortex-A72 at 2.0 GHz along with a single C7x DSP and two C66x DSPs. The ARM Cortex-A72 executes 4.7 DMIPS/MHz per core. Two ARM Cortex-A72 cores at 2.0 GHz are capable of executing 18800 DMIPS. The speedup from moving code from ARM to the C7x DSP and two

C66x DSPs is estimated to be 2.9x based on OpenCV gaussian blur benchmarks from Texas Instruments. The adjusted speed is 54520 DMIPS. Since this is the highest performance of all devices, the TI SK-TDA4VM receives a score of 10.00 out of 10.00.

Board Size

The Raspberry Pi 4 Model B uses a 85 mm x 56 mm PCB for an area of 4760 mm^2, the smallest of all devices considered. Therefore, it receives a score of 10.00 out of 10.00.

The TI TMDXSK437X uses a 134 mm x 71 mm PCB for an area of 9514 mm^2. Since the smallest device has an area equal to 50.0% of this device's area, the TMDXSK437X receives a score of 5.00 out of 10.00.

The BeagleBone AI uses an 89 mm x 54 mm PCB for an area of 4806 mm^2. Since the smallest device has an area equal to 99.0% of this device's area, the BeagleBone AI receives a score of 9.90 out of 10.00.

The TI SK-TDA4VM uses a 115 mm x 114 mm PCB for an area of 13110 mm^2. Since the smallest device has an area equal to 36.3% of this device's area, the TI SK- TDA4VM receives a score of 3.63 out of 10.00.

Maximum Power Draw

The Raspberry Pi 4 Model has a power supply requirement of 5.0 V at 2.5 A (12.5 W) when used without USB peripherals. This is tied for the lowest maximum power draw. Therefore, the Raspberry Pi 4 Model receives a score of 10.00 out of 10.00.

The TI TMDXSK437X has a power supply requirement of 5.0 V at 2.5 A (12.5 W). This is tied for the lowest maximum power draw. Therefore, the TI TMDXSK437X receives a score of 10.00 out of 10.00.

The BeagleBone AI has a power supply requirement of 5.0 V at 3.0 A (15.0 W). Since the lowest power device requires 83.3% of this device's power, the BeagleBone AI receives a score of 8.33 out of 10.00.

The TI SK-TDA4VM has a power supply requirement of 5.0 V at 3.0 A (15.0 W) when used without USB peripherals or expansion interfaces. Since the lowest power device requires 83.3% of this device's power, the TI SK-TDA4VM receives a score of 8.33 out of 10.00.

User Friendliness

The Raspberry Pi 4 Model B is well-documented. Additionally, it is very popular for educational and hobbyist use. This strong community provides additional guidance. Therefore, the Raspberry Pi 4 Model B receives a qualitative assessment of great and a score of 10.00 score of 10.00.

The TI TMDXSK437X is well-documented. It uses the Texas Instrument's AM437x series of processor. Therefore, the TI TMDXSK437X receives a qualitative assessment of good and a score of 8.00 of out of 10.00.

The BeagleBone AI uses Texas Instruments components which are thoroughly documented. The board itself has documentation available on GitHub, but is incomplete. Therefore, the BeagleBone AI receives a qualitative assessment of okay and a score of 6.00 out of 10.00.

The TI SK-TDA4VM is a relatively new product from Texas Instruments which uses components with less documentation than older alternatives from TI. Because the product is relatively new, there are fewer posts on this product on the TI E2E design support forums. Therefore, the TI SK-TDA4VM receives a qualitative assessment of okay and a score of 6.00 out of 10.00

4.1.3.2.3 Camera Selection

All cameras chosen have breakout pins and communicate with SPI, UART, or I2C. This limits the overall selection of cameras to ones that meet the hardware specifications. Two cameras with different FOV lenses are used to view the field. The camera with the wider FOV is used if the camera with the narrower FOV cannot find landmarks. The FOV of all camera lenses must be at least 60 degrees to capture the entire launch field at apogee.

4.1.3.2.3.1 Objective Definitions and Weighting Factors

A decision matrix was used to choose a camera for the payload (Table 25).

Camera			OV5642			MT9D111		
Objective	Weighting Factor	Parameter	Mag.	Score	Value	Mag.	Score	Value
Cost	0.1	USD	39.99	2.50	0.25	9.99	10.0	1.0
Size	0.2	mm^2	816	10.0	2.00	1600	5.10	1.02
Resolution at 30 fps	0.4	Columns x Rows	1920x1080	10.0	4.00	800x600	2.31	0.93
Power consumption	0.3	mW	1500	1.49	0.45	223	10.0	3.0
Overall value					**6.70**			5.95

Table 25: Camera decision matrix.

Cost

Cost is a factor, but not as important because these types of cameras have similar specifications. A budget of up to 50 USD is allowed for each camera. This accounts for up to 10% of the total score. While more expensive, the OV5642 offers better quality as discussed in another section. The module with the lowest price scores 10 out of 10.

Size

Size is considered in two dimensions, each in mm. These cameras protrude from the rocket and must be as small as possible to minimize interference with the flight path. The smallest scores 10.0 and other scores are based on the surface area relative to the smallest camera. This accounts for up to 20% of the total score.

Resolution at 30fps

Each camera supports different resolutions and capture speeds. Images need to be detailed at high altitudes to help identify landmarks. This being an important objective, is worth up to 40% of the overall score. 30 fps is used as a constant to properly evaluate the image quality. Measurements are in columns by rows of pixels. The highest resolution is scored as 10.0 and all others are scored on how many total pixels relative to the highest resolution.

Power consumption

It is important to consider how much power the camera uses during the flight so that less battery is consumed. Power consumption for each camera is assumed to be on normal settings in the conditions used to evaluate resolution (30 fps). The weight of the objective is up to 30% of the overall score. The MT9D111 power consumption was given in mW and the others were calculated using voltage and current values provided in the documentation. The lowest power is scored 10.0 and all others are scored on their power consumption relative to the lowest power consumption. Power consumption in low-powered mode for each is similar and not considered a significant objective.

4.1.3.2.3.2 Scoring Justifications

The scores were calculated using linear scoring. The best device was assigned a score of 10 out of 10 points. A device with a magnitude of half or double the best design is assigned a score of 5 out of 10. This linear assignment continues in both directions.

4.1.3.2.4 Inertial Measurement Unit Selection

All inertial measurement units (IMUs) chosen must have a range of at least 16 g due to the launch vehicle having a maximum acceleration of over 14 g. The required range heavily limits the selection of IMUs, with lower end IMUs having unsatisfactory bias values. IMUs with low bias values were rare, with not many fitting within the team's budget range. We must minimize values such as zero-g offset and other bias values to ensure accuracy of our data, since displacement values are derived by integrating acceleration twice, which leads to compound error.

4.1.3.2.4.1 Objective Definitions and Weighting Factors

A decision matrix was used to choose a inertial measurement unit (IMU) (Table 26).

Inertial Measurement Unit			**Adafruit LSM6DS33**			**MPU-6881**		
Objective	Weighting Factor	Parameter	Mag.	Score	Value	Mag.	Score	Value
Zero-g Offset	0.6	mg	40.00	0.50	0.30	80.00	0.25	0.15
DOF	0.3	axes	9.00	10.00	3.00	6.00	6.67	2.00
Price	0.1	USD	9.95	6.03	0.60	6.95	8.63	0.86
Overall Value					**3.90**			**3.01**
Inertial Measurement Unit			**BHI260AB**			**MTI-3-0I**		
Objective	Weighting Factor	Parameter	Mag.	Score	Value	Mag.	Score	Value
Zero-g Offset	0.6	mg	20.00	1.00	0.60	2.00	10.00	6.00
DOF	0.3	axes	6.00	6.67	2.00	9.00	10.00	3.00
Price	0.1	USD	15.30	3.92	0.39	283.66	0.21	0.02
Overall Value					**2.99**			**9.02**

Table 26: IMU decision matrix.

Zero-G Offset is the measurement's deviation from zero when the IMU is not accelerating. This factor contributes to the total positional error produced during the inertial navigation. This error comes from the fact that displacement is calculated by double integrating the acceleration, which causes constant error to compound quadratically. Therefore, Zero-G Offset is weighted at 60%. The unit with the lowest zero-g offset scores 10 out of 10 points.

Degrees of Freedom is the number of independent axis measurable by the unit. Each unit with nine degrees of freedom includes a 3-axis accelerometer, a 3-axis gyroscope, and a 3-axis magnetometer, while each unit with six degrees of freedom includes only a 3-axis accelerometer and a 3-axis gyroscope. Degrees of Freedom is weighted at 30% due to the ease of use presented by a 9-axis IMU. Without a built-in magnetometer a separate one would be required.

Price is the cost of an IMU in USD. This value wants to be minimized although it is only weighed at 10% since other parameters take precedence.

4.1.3.2.4.2 Scoring Justifications

The scores were calculated using linear scoring. The best device was assigned a score of 10 out of 10 points. A device with a magnitude of half or double the best design is assigned a score of 5 out of 10. This linear assignment continues in both directions.

4.1.3.2.5 Barometer Selection

All selected barometers can communicate using I^2C or SPI.

4.1.3.2.5.1 Objective Definitions and Weighting Factors

A decision matrix was used to choose a barometer (Table 27).

Barometer			Grove 101020068			Grove 101020812		
Objective	Weighting Factor	Parameter	Mag.	Score	Value	Mag.	Score	Value
Cost	0.1	USD	21.90	2.97	0.30	6.50	10.00	1.00
Range	0.45	mbar	300-1200	9.00	4.05	300-1200	9.00	4.05
Accuracy	0.45	mbar	0.01	10.00	4.50	0.06	1.67	0.75
Overall Value					**8.85**			**5.80**
Barometer			**MIKROE-2665**			**SEN0226**		
Objective	Weighting Factor	Parameter	Mag.	Score	Value	Mag.	Score	Value
Cost	0.1	USD	15.00	4.33	0.43	8.80	7.39	0.74
Range	0.45	mbar	260-1260	10.00	4.50	300-1100	8.00	3.60
Accuracy	0.45	mbar	0.10	1.00	0.45	0.12	0.83	0.37
Overall Value					**5.38**			**4.71**

Table 27: Barometer decision matrix.

Cost is the price (USD) of each barometer. The cost is a consideration that should be minimized but is not of utmost importance since all the parts are less than $40, therefore the weighting factor is 10%.

Range represents the maximum and minimum pressure values (mbar) that the barometer can record. This spread should be maximized to allow wider collection of data, and its importance is why it has a weighting factor of 45%.

Accuracy is the base offset (mbar) the data has. The higher the value, the more inaccurate the reading is. This parameter must be minimized to allow for accurate data, and its severity is why it has a weighting factor of 45%.

4.1.3.2.6 Ground Station Electronics

The ground station receives, outputs, and stores the payload's final landing location determination. The ground station consists of a microcontroller, an XBee radio transceiver, an LCD screen, and an SD card module. From the selection of microcontrollers considered, all can communicate with peripherals using SPI and UART. The ground station received power via a 7.4 V lithium ion battery.

4.1.3.2.6.1 Objective Definitions and Weighting Factors

A decision matrix was used to choose a microcontroller (Table 28).

Microcontroller			**ATmega168**			**ATmega328P**		
Objective	Weighting Factor	Parameter	Value	Score	Weighted Score	Value	Score	Weighted Score
Cost	0.20	USD	3.49	8.48	1.69	2.96	10.00	2.00
Pin count	0.40	# of pins	23.00	6.57	2.63	23.00	6.57	2.63
Memory	0.40	KB	16.00	5.00	2.00	32.00	10.00	4.00
Overall value					6.32			8.63
Microcontroller			**ATmega162**			**ATmega8515**		
Objective	Weighting Factor	Parameter	Value	Score	Weighted Score	Value	Score	Weighted Score
Cost	0.20	USD	6.04	4.90	0.98	3.46	8.55	1.71
Pin count	0.40	# of pins	35.00	10.00	4.00	35.00	10.00	4.00
Memory	0.40	KB	16.00	5.00	2.00	8.00	2.50	1.00
Overall Value					6.98			6.71

Table 28: Microcontroller decision matrix.

Cost is the price (USD) of each microcontroller. The cost is a factor and considered among the selections chosen, as the individual price of a microcontroller is inexpensive. Cost is weighted at 20% and the cheapest microcontroller will receive 10 points out of 10.

Pin Count is considered as any parallel component (some LCDs considered could not communicate with any serial standard) added could occupy a significant portion of the microcontroller's I/O and/or functionality. The number of usable pins is critical as it determines what peripherals can be used. Pin count is weighted at 40% and the microcontroller with the most pins available will receive 10 points out of 10.

Memory is the amount of data (KB) the microcontroller can store. An SD card reader is incorporated into the design to store relevant data received from the payload. In the event the SD card inserted fails, the on-board memory of the microcontroller can be written at the same time the SD card is written to and then re-written onto a properly function card. For this purpose, internal memory capacity available is vital and is weighted at 30%, the microcontroller with the greatest internal capacity will receive 10 points out of 10.

4.1.3.2.6.2 Scoring Justifications

The scores were calculated using linear scoring. The best device was assigned a score of 10 out of 10 points.

Cost

The ATmega 168 has a cost of $3.49/chip. As it cost 15.2% more than the ATmega 328P, it receives a score of 8.48 points out of 10.

The ATmega 328P has a cost of $2.96/chip, making it the most inexpensive microcontroller and receiving a score of 10 points out of 10.

The ATmega 162 has a cost of $6.04/chip. As it cost 39.6% more than the ATmega 328P, it receives a score of 6.57 points out of 10.

The ATmega 8515 has a cost of $3.46/chip. As it cost 14.5% more than the ATmega 328P, it receives a score of 8.55 points out of 10.

Pin Count

The ATmega 168 has 23 pins available for use. As it has 34.3% fewer pins than both the ATmega 162 and ATmega 8515, it receives a score of 6.57 points out of 10.

The ATmega 328P has 23 pins available for use. As it has 34.3% fewer pins than both the ATmega 162 and ATmega 8515, it receives a score of 6.57 points out of 10.

The ATmega 162 has 35 pins available for use, making it one of the two microprocessors selected with the greatest pin count. As such, both receive a score of 10 points out of 10.

The ATmega 8515 has 35 pins available for use, making it one of the two microprocessors selected with the greatest pin count. As such, both receive a score of 10 points out of 10.

Memory

The ATmega 168 has 16 KB of memory available. It has 50% of the capacity of the microcontroller with the greatest amount of memory, giving it a score of 5 points out of 10.

The ATmega 328P has 32 KB of memory available, the greatest capacity of the microprocessors selected. It receives a score of 10 points out of 10.

The ATmega 162 has 16 KB of memory available. It has 50% of the capacity of the microcontroller with the greatest amount of memory, giving it a score of 5 points out of 10.

The ATmega 8515 has 8 KB of memory available. It has 25% of the capacity of the microcontroller with the greatest amount of memory, giving it a score of 2.50 points out of 10.

4.1.3.2.7 Electronics Mass

The mass of each electrical payload component is listed (Table 29). The payload electronics have a total mass of 10.19 oz.

Part/Assembly	Mass (oz)
Raspberry Pi 4	6.77
7.4 V Lithium-Ion Batteries	1.94
OV5642 Cameras	0.64
Printed Circuit Board	0.71
XBee Radio	0.32
Inertial Measurement Unit	0.07
Barometer	0.04
Wiring	0.35
Total	**10.19**

Table 29: Payload electronics mass table.

4.1.3.3 Mechanical Design

The mechanical design of the payload consists of the payload sled, the rail system, the battery compartment, the latch system, and the external camera mounts (Figure 39). The payload sled is responsible for housing the Raspberry Pi and all electronics related to the payload. The rail system is the component responsible for supporting the weight of the payload sled, preventing it from moving inside of the launch vehicles airframe. The camera mounts are the two structures that will mount the camera on the exterior of the launch vehicles aft section, enabling the images needed for the image processing software.

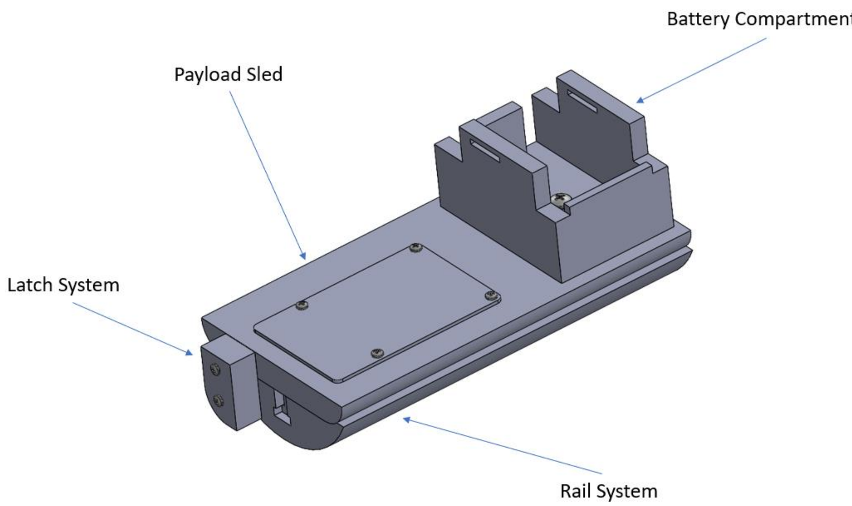

Figure 39: Mechanical structure of payload.

4.1.3.3.1 Payload Sled PCB Attachment Selection

The payload sled's main objective is to safely store the Raspberry Pi and all electronics inside of the aft airframe. To mount the payload, three different methods were considered: Embedded nuts, threaded inserts (heat-staking), and a rail slide. The rail slide was the initial design of the payload sled, where the PCB would slide into a rail cutout in the payload sled. The embedded nuts and threaded inserts take the approach of fastening the PCB to the sled using fasteners and an insert. The embedded nuts method utilizes a hex-nut inside of the sled, which will secure the PCB to the sled through screws. The threaded inserts method utilizes heat-staking inserts that are inside of the sled, enabling fasteners to be screwed in and out without risking the integrity of the sled's plastic (Table 30).

Sled PCB Attachment			Embedded Nuts			Threaded Inserts (Heat-Staking)		
Objective	Weighting Factor	Parameter	Mag.	Score	Value	Mag.	Score	Value
Material Cost	0.15	USD	7.5	10.0	1.5	9.0	8.3	1.2
Reliability	0.40	N	Good	8.0	3.2	Great	10.0	4.0
Manufacturability	0.15	hours	4.0	5.0	0.8	2.0	10.0	1.5
Modularity	0.30	fasteners	4.0	5.0	1.5	4.0	5.0	1.5
Overall Value					**7.0**			**8.2**

Sled PCB Attachment			Rail Slide		
Objective	Weighting Factor	Parameter	Mag.	Score	Value
Material Cost	0.15	USD	12.0	6.3	0.9
Reliability	0.40	N	Poor	2.0	0.8
Manufacturability	0.15	hours	4.0	5.0	0.8
Modularity	0.30	fasteners	2.0	10.0	3.0
Overall Value					**5.5**

Table 30: Sled PCB attachment decision matrix.

4.1.3.3.2 PCB Attachment Objective Definitions and Weighting Factor Justifications

Material Cost is the cost of the materials needed for each system of attachment for the PCB onto the sled. This cost includes the filament needed for the part, as well as any parts ordered for the fastening of the PCB. The weighting factor of material cost was set at 15% because the teams budget is very large in comparison to the prices of the components needed for PCB attachment. The design that had the cheapest material cost received a score of 10 out of 10 and the rest followed a linear scale.

Reliability of the design was determined by comparing the pull-out strengths of each fastening method. These were determined by the manufacturer's provided values on the strength of the fastening methods, as well as their implementation process. The weighting factor for reliability was set at 40% because the purpose of the attachment method is to safely secure the PCB onto the sled. Any failure in the attachment method would lead to overall system failure. The method with the greatest pull-out strength received a score of 10 out of 10 and the rest followed the provided scale for qualitative assessments.

Manufacturability of the design was determined by the 3D print time needed for the fastening method, as well as the time needed to utilize the different fasteners. The weighting factor for manufacturability was set at 15% because the variation in print time is not immense, as well as the time to install the fasteners. The design with the shortest manufacturing time received a score of 10 out of 10 and the rest followed a linear scale.

Modularity of the design was determined by the number of fasteners required to secure the PCB to the sled. This received a weighting factor of 30% because removing the PCB for any electronics changes is important to keep updating the payload system. The design with the fewest fasteners received a score of 10 out of 10 and the rest followed a linear scale.

4.1.3.3.3 PCB Attachment Scoring Assignments

Material Cost

Embedded Nuts cost $6.00 for a pack from Lowe's and the plastic needed to print the top portion of the payload sled cost about $1.50, making the total cost of the embedded nuts design $7.50. Following a linear score, embedded nuts received a score of 10.0.

Threaded inserts for plastic cost $7.50 for a pack from McMaster Carr, and the plastic needed to print the top portion of the payload sled cost about $1.50, making the total cost of the threaded inserts design $9.00. Following a linear scale, threaded inserts received a score of 8.3.

The rail slide increases the cost of the plastic needed to $4.00 and the rubber inserts cost $8.00 from amazon, making the total cost of the rail slide design $12.00. Following a linear scale, the rail slide received a score of 6.3.

Reliability

Embedded nuts have a strong pull-out strength but are secured using tight tolerances for 3D printing and an adhesive like super glue. The strength of the embedded nuts is similar to threaded inserts, but there is a possibility in slippage or error in manufacturing. The embedded nuts received a score of "Good," which correlates to an 8.0 using the qualitative scoring legend.

Threaded inserts for plastic are extremely strong and are the standard for attaching fasteners to 3D printed materials. Due to their excellent seal on the plastic and their internal threads, replacing fasteners is easy and does not damage the plastic's integrity, along with extreme ease in manufacturing. The threaded inserts received the highest score of "Great," which correlates to a 10.0 using the qualitative scoring legend.

The rail slide uses a friction fit from rubber seals to retain the PCB inside of the sled. The rubber seals provide support for counteracting the vibrations in the system, but they are very unreliable and could potentially let the PCB slide out of the sled. This would be catastrophic for the payload; thus, the rail sled received a score of "Poor," correlating to a 2.0 using the qualitative scoring legend.

Manufacturability

Embedded nuts require extreme precision in the 3D printing process to ensure the nut does not slip when using fasteners. Due to this, the 3D print time for the sled is roughly 4.0 hours to print the nuts profile into the PCB mounting holes. Following a linear scale, the embedded nuts design received a score of 5.0.
Threaded inserts for plastic only require a clearance hole of a specific diameter for the insert to be placed into, and then heated to expand and attach to the plastic. For this reason, the 3D printing process is shorter, where the holes can be made easily or even drilled in after printing. Following a linear scale, threaded inserts received a score of 10.0.

The rail slide must print the frame of the payload sled along with the side rails that have the cutout for the PCB. This extra section of the sled increases the printing time and requires more precision than clearance holes. Following a linear scale, the rail slide received a score of 5.0.

Modularity

Embedded nuts would require the use of four nuts and four fasteners to secure the PCB to the sled using the PCB's mounting holes. These four fasteners would be screwed in using a regular screwdriver. Following a linear scale, the embedded nuts received a score of 5.0.

Threaded inserts for plastic would require the use of four inserts and four fasteners to screw in the PCB to the sled as well. These four fasteners would be screwed in using a regular screwdriver. Following a linear scale, threaded inserts received a score of 5.0.

The rail slide would require two rubber insert cutouts to be placed on the ends of the rail slide. These rubber cutouts are a friction fit and can be removed by hand. Following a linear scale, the rail slide received a score of 10.0.

4.1.3.3.4 Payload Latch System Selection

The payload latch system consists of three design options: the flat face door, the sliding lock, and the pin lock. The flat face door is a rectangular 3D printed piece with two fasteners, providing a physical link between the payload sled and the rail system. The sliding lock is a 3D printed bracket with one fastener and a sliding metal section. This sliding metal section can be engaged at full position to prevent the sled from moving. The pin lock utilizes three fasteners, two for the square bracket and one for the pin. The pin runs through the length of the rail system and engages with the square bracket to prevent any motion (Table 31).

Latch/Retainment Method			**Flat Face Door**			**Sliding Lock**		
Objective	Weighting Factor	Parameter	Mag.	Score	Value	Mag.	Score	Value
Material Cost	0.20	USD	10.0	10.0	2.0	15.0	6.6	1.3
Surface Stress	0.40	in^2	Great	10.0	4.0	Great	10.0	4.0
Manufacturability	0.20	hours	2.0	10.0	2.0	4.0	5.0	1.0
Modularity	0.20	fasteners	2.0	5.0	1.0	1.0	10.0	2.0
Overall Value					**9.0**			**8.3**

Latch/Retainment Method			**Pin Lock**		
Objective	Weighting Factor	Parameter	Mag.	Score	Value
Material Cost	0.20	USD	19.0	5.0	1.0
Surface Stress	0.40	in^2	Fair	4.0	1.6
Manufacturability	0.20	hours	6.0	3.3	0.7
Modularity	0.20	fasteners	3.0	3.3	0.7
Overall Value					**4.0**

Table 31: Retainment method decision matrix.

4.1.3.3.5 Latch/Retainment Method Objective Definitions and Weighting Factor Justifications

Material Cost is the price (USD) of the materials needed for each design of the latch/retainment method. This cost includes the filament needed for the part, as well as any parts ordered for the fastening of the latch system onto the payload. The weighting factor of material cost was set at 15% because the designs did not have expensive components, barely affecting the team budget. The design that had the cheapest material cost received a score of 10 out of 10 and the rest followed a linear scale.

Surface Stress is the amount of area (in^2) the different designs were in contact with the payload sled and rail system. The design that has the most surface area in contact with the payload sled and rail system will be able to withstand the most stress during flight. The weighting factor of surface stress was set at 40% because failure in the retainment method would lead to potential failure in the payload's electronics. The design that had the most surface stress area received a score of 10 out of 10 and the rest followed a linear scale as defined by the qualitative scoring legend (Table 2).

Manufacturability of the design was determined by the 3D print time (hours) needed for the latch method, as well as the time needed to install and use the latch. The weighting factor for manufacturability was set at 15% because each method had either a short print time or simple installation procedures. The design with the shortest manufacturing time received a score of 10 out of 10 and the rest followed a linear scale.

Modularity of the design was determined by the number of fasteners required to secure the latch to the sled. This received a weighting factor of 30% because being able to remove the payload in a timely manner is needed for any electrical component changes or structural changes. The design with the fewest fasteners received a score of 10 out of 10 and the rest followed a linear scale.

4.1.3.3.6 Latch/Retainment Method Scoring Assignments

Material Cost

The flat face door consists of a rectangular 3D printed part, two threaded inserts and two fasteners with a total cost $10.00. Following a linear scale, the flat face door received a score of 10.0.

The sliding lock design consists of a square bracket, a sliding metal section, one threaded insert and one fastener with a total cost of $15.00. Following a linear scale, the sliding lock received a score of 6.6.

The pin lock design consists of a rectangular 3D printed part, an aluminum rod, one threaded insert and one fastener with a total cost of $19.00. Following a linear scale, the pin lock received a score of 5.0.

Manufacturability

The flat face door consists of one 3D printed part, with a print time of one hour total. Installation of the flat face door requires the use of two threaded inserts and two fasteners screwed in with a screwdriver. The total time for the flat face door is 2.0 hrs., following a linear scale this received a score of 10.0.

The sliding lock consists of one 3D printed square bracket with a print time of one hour and a sliding metal section with a manufacturing time of one hour. Installation of the sliding lock requires the use of one threaded insert and fastener. The total time for the sliding lock is 2.5 hrs., following a linear scale this received a score of 8.0.

The pin lock consists of a rectangular 3D printed part with a print time of one hr. and an aluminum rod with a manufacturing time of one hr. Installation of pin lock requires the use of one threaded insert and one fastener, along with placing the pin through the rail section of the payload. The total time for the pin lock is 3.0 hrs., following a linear scale this received a score of 6.7.

Surface Stress

The flat face door has a surface area of 0.9 in^2, with a rectangular shape and a circular fillet on one end. The surface area is defined as the area in contact with any part of the payload sled or rail. The surface area of the flat face door and the sliding lock had similar values, so a qualitative assessment was used. The flat face door received a “Great,” which correlated to a score of 10.0.

The sliding lock has a surface area of 0.95 in^2, with a rectangular shape. The surface area is defined as the area of the sliding metal section that is in contact with the payload sled or rail. The sliding lock received a “Great,” which correlated to a score of 10.0.

The pin lock has a surface area of 0.3 in^2, because the area of the square bracket had to be small to fit the pin in the system. The surface area is defined as the area of the bracket in contact with the payload sled or rail. The pin lock received a “Fair,” which correlated to a score of 4.0.

Modularity

The flat face door requires two threaded inserts and two fasteners in total. Following a linear scale, the flat face door received a score of 5.0.

The sliding lock requires one threaded insert and one fastener to secure the bracket to the payload sled. Following a linear scale, the sliding lock received a score of 10.0.

The pin lock requires one threaded insert and one fastener to secure the bracket to the rail system. Following a linear scale, the pin lock received a score of 10.0.

4.1.3.3.7 Payload Latch Leading Design

The payload latch system is a 3D printed rectangular piece that has one corner fillet (Figure 40). The two clearance holes are to allow two M2.5 fasteners to secure the latch to both the payload sled and the rail system. This connection prevents the payload sled from moving independent of the rail system that is epoxied to the vehicles airframe (Figure 41).

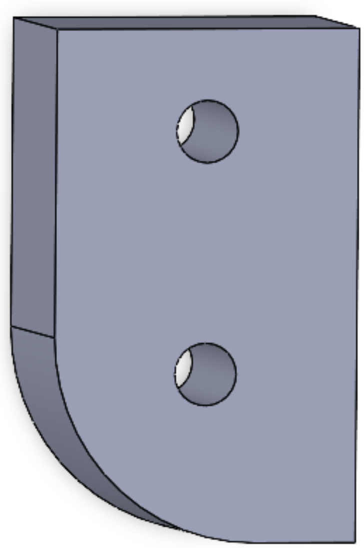

Figure 40: Latch 3D model.

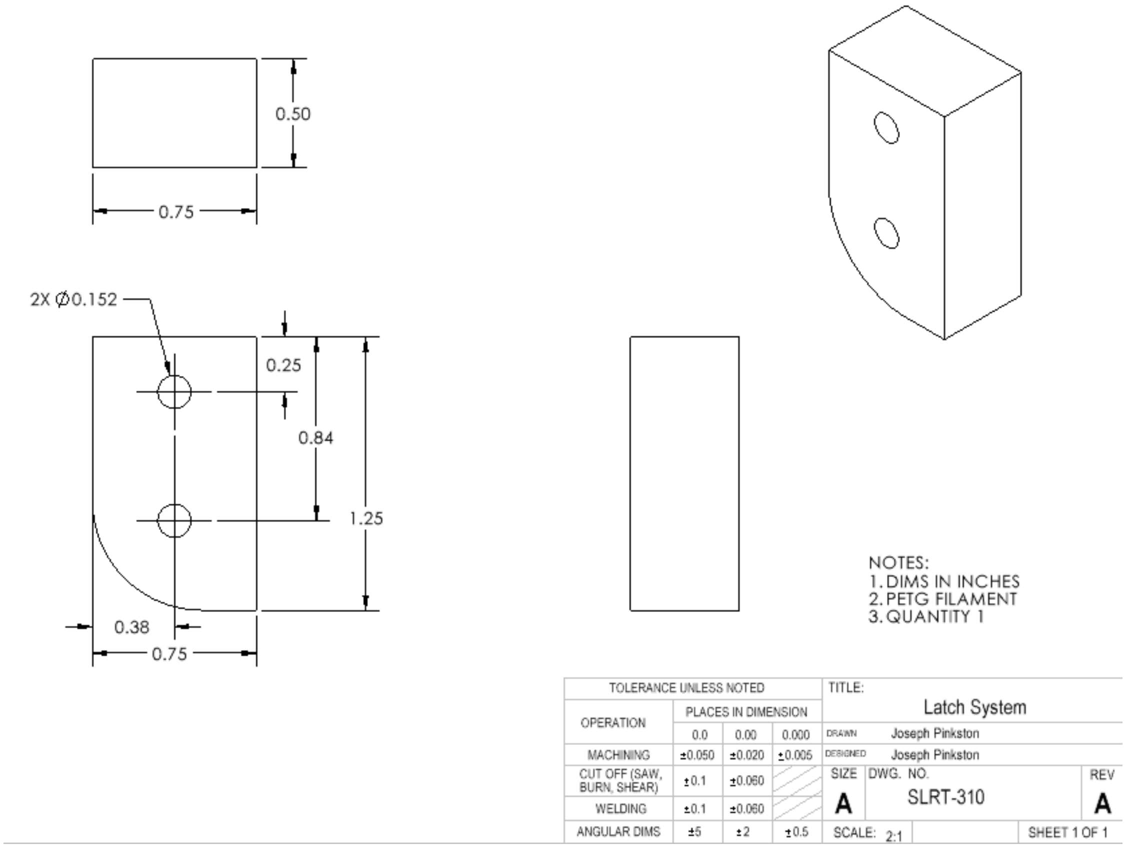

Figure 41: Latch drawing.

4.1.3.3.8 Payload Sled

The payload sled is a 3D printed structure made from PETG filament (Figure 42). The percent infill used on the beam section will be greater than other components due to the forces this part will be experiencing during flight. The sled will have clearance holes for the locations that require threaded inserts used for the fasteners. There is one clearance hole towards the rear of the sled that is for the battery compartment, four in the front of the sled for the Raspberry Pi board, and one on the front of the sled for the latch system to attach to. The mounting holes for the Raspberry Pi and the latch system are for the M2.5 threaded inserts, whereas the battery compartments mounting hole is a 10-24 threaded insert. The holes are set at the manufacture's recommended diameter for the specific threaded insert, to ensure a proper fit. The depth of the holes is slightly larger than the length of the threaded inserts, to allow extra room for the fasteners to screw in (Figure 43).

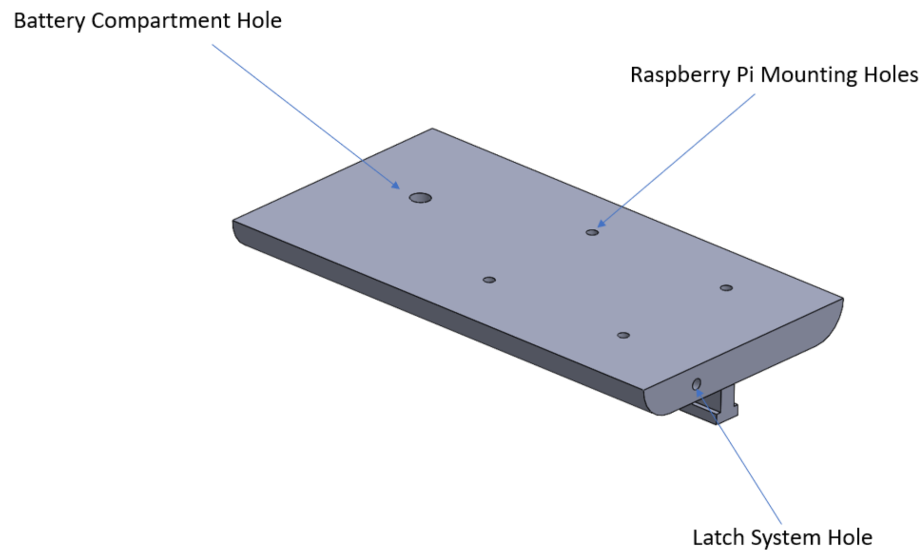

Figure 42: Payload sled 3D model.

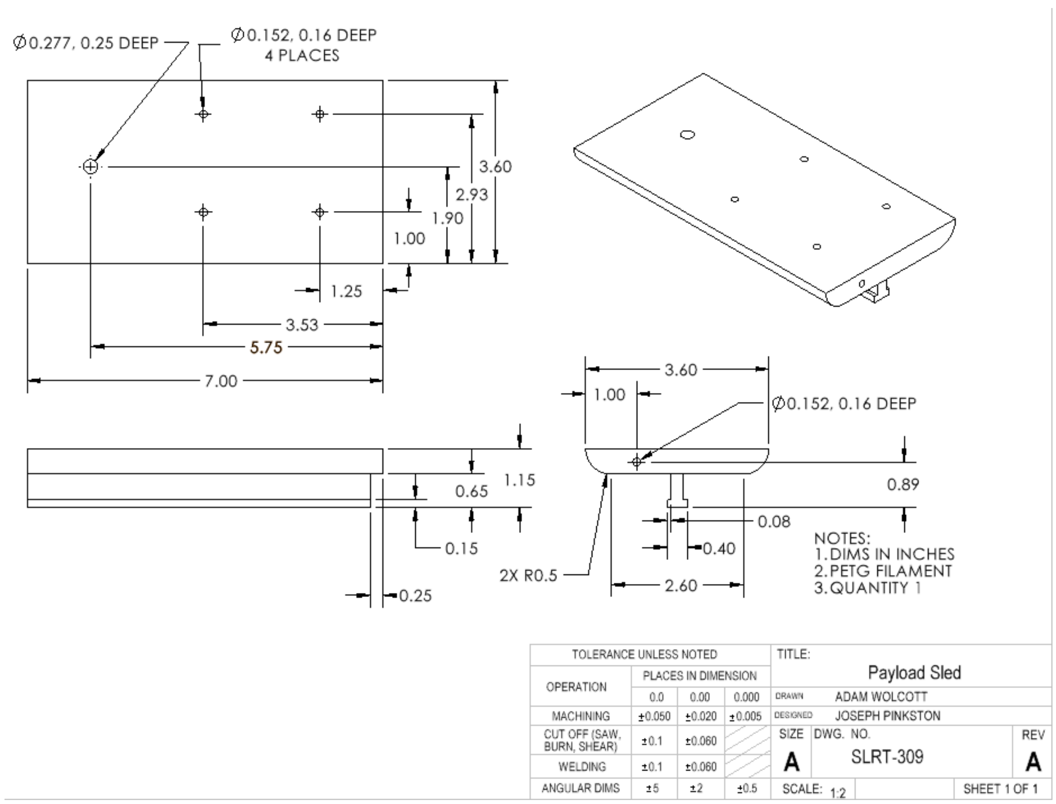

Figure 43: Payload sled drawing.

4.1.3.3.9 Payload Rail System

The payload rail system is the 3D printed structure that is permanently inside of the payload coupler section (Figure 44). The round bottom of the rail has a 4 in. diameter to match the launch vehicles airframe and is epoxied to the payload coupler. The beam cutout of the rail system matches the beam on the bottom of the payload sled, enabling a smooth connection between the two. The hole in the front end of the rail system is for the M2.5 threaded hole needed for the latch system (Figure 45).

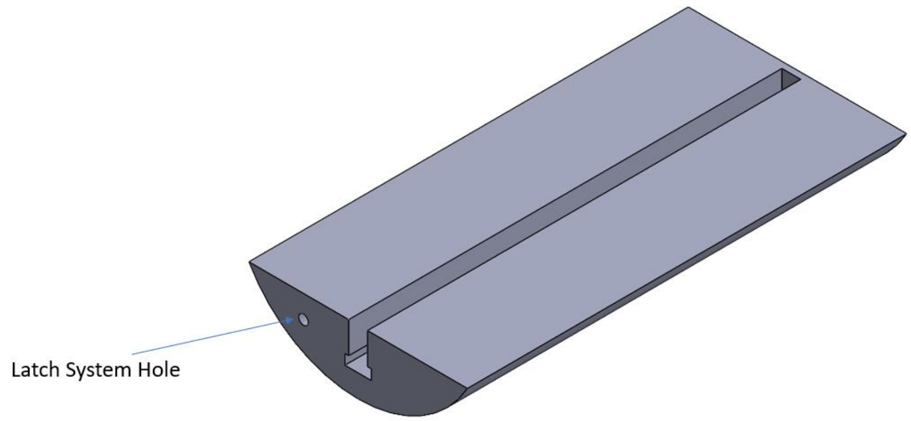

Figure 44: Payload rail system 3D model.

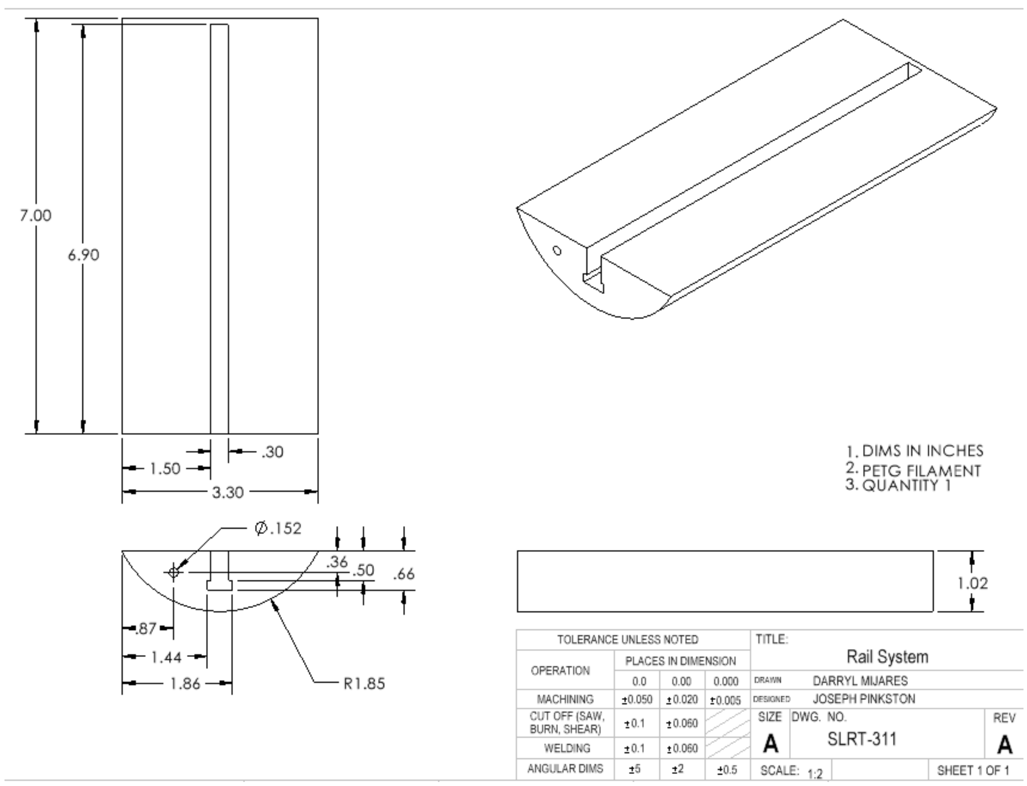

Figure 45: Payload rail system drawing.

4.1.3.3.10 Payload Battery Compartment

The battery compartment is a 3D printed case for the two lithium ion batteries needed to supply power to the Raspberry Pi (Figure 46). The battery compartment is 3D printed using PETG filament. The percent infill on the battery compartment will be greater than other compartments due to the thin walls used for this component. The case allows the batteries to be secured to the payload sled, while also being positioned convenient for connecting to the Raspberry Pi. The top slits in the battery compartment allows for a Velcro strap to pass around the batteries, to prevent any upward displacements. The clearance hole in the bottom of the battery compartment is fitted for a 10-24 fastener that is fastened into a 10-24 threaded insert on the payload sled (Figure 47).

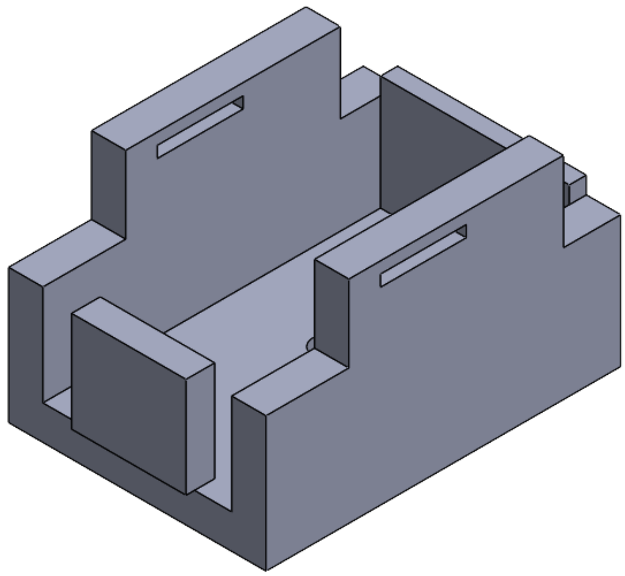

Figure 46: Payload battery compartment 3D model.

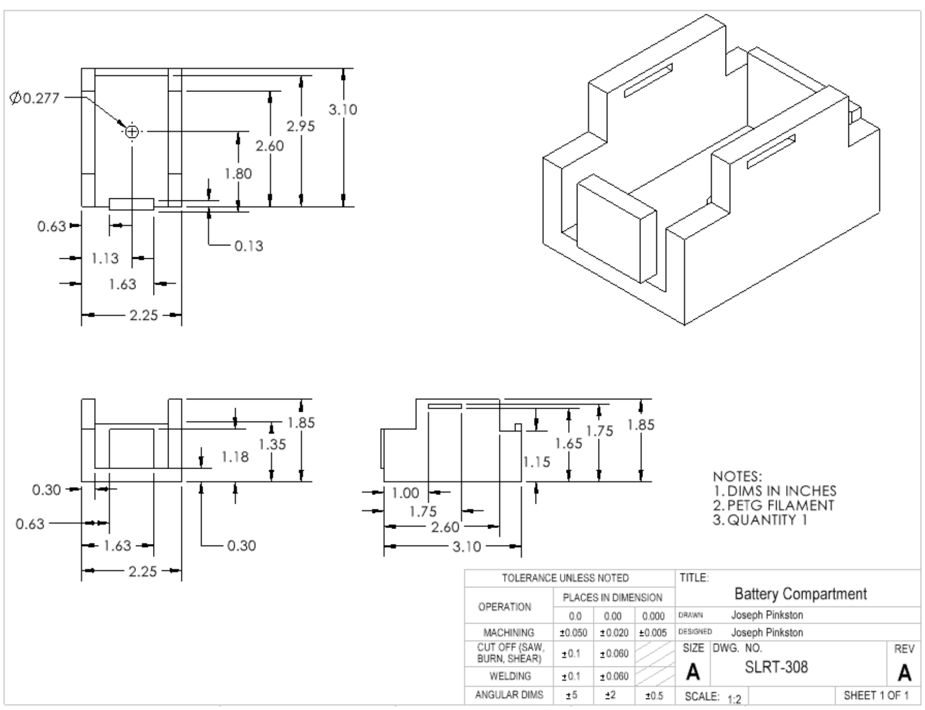

Figure 47: Payload battery compartment drawing.

4.1.3.3.11 Payload Assembly

The payload assembly consists of four main components: the payload sled, the battery compartment, the rail system, and the latch system (Figure 48, Figure 49). On the payload sled, the Raspberry Pi is attached along with the lithium ion batteries needed to power it. The battery compartment and the Raspberry Pi are attached using threaded inserts and screws. There are four M2.5 threaded fasteners and corresponding fasteners for the Raspberry Pi, two M2.5 threaded inserts and corresponding fasteners for the latch system, and one 10-24 threaded insert and corresponding fastener for the battery compartment (Figure 50).

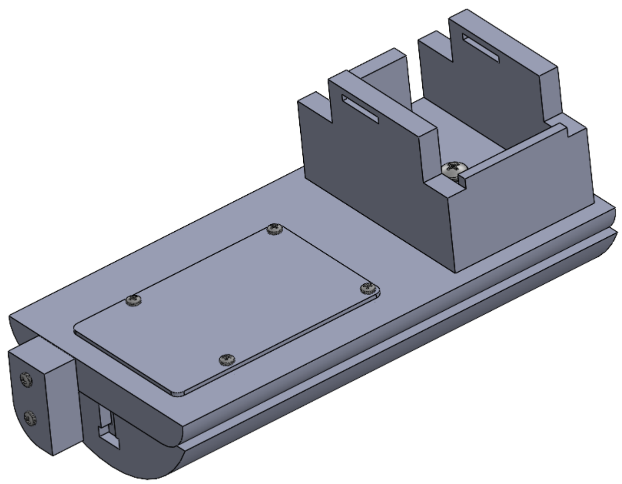

Figure 48: Payload mechanical assembly 3D model.

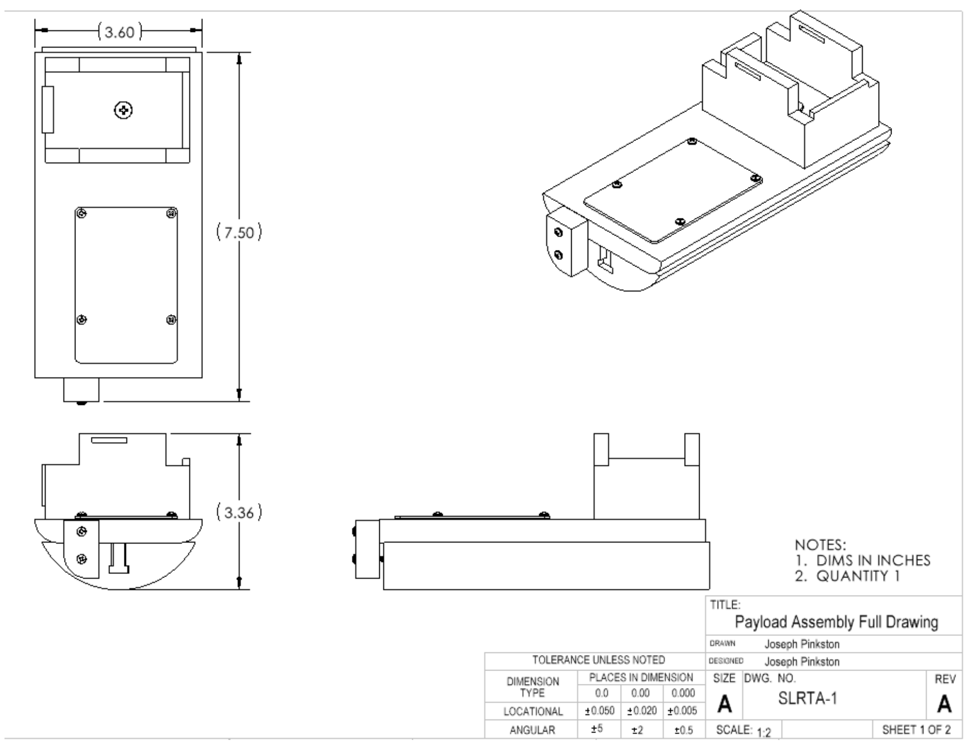

Figure 49: Payload mechanical assembly drawing.

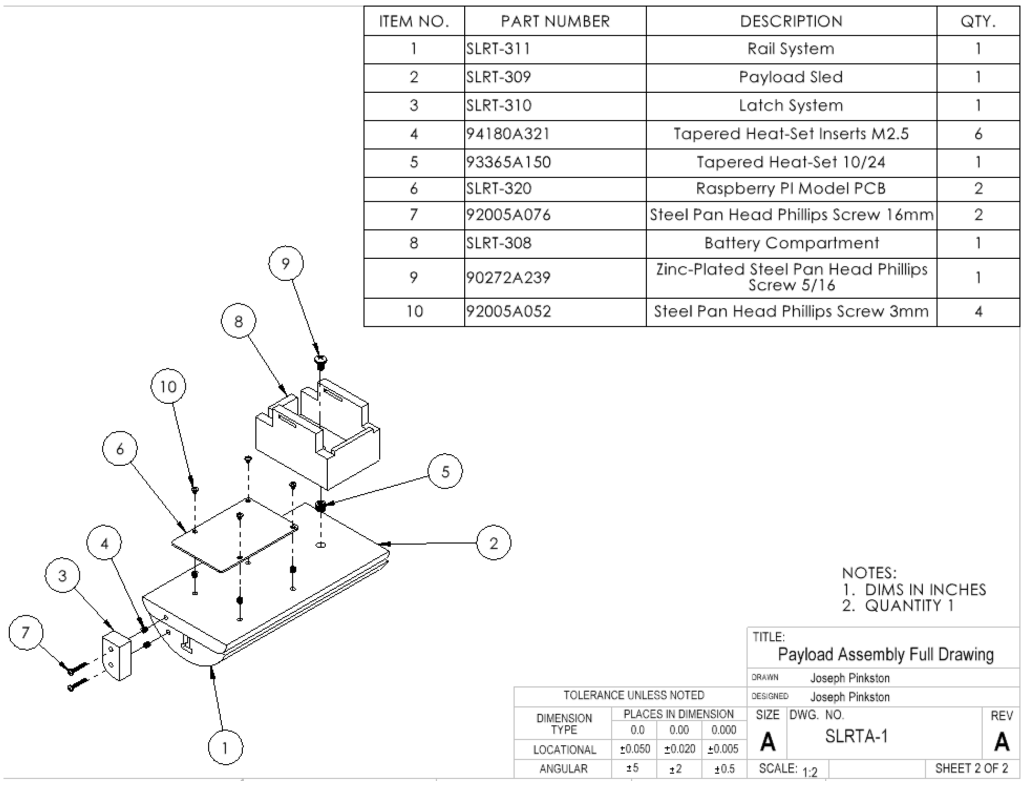

ITEM NO.	PART NUMBER	DESCRIPTION	QTY.
1	SLRT-311	Rail System	1
2	SLRT-309	Payload Sled	1
3	SLRT-310	Latch System	1
4	94180A321	Tapered Heat-Set Inserts M2.5	6
5	93365A150	Tapered Heat-Set 10/24	1
6	SLRT-320	Raspberry PI Model PCB	2
7	92005A076	Steel Pan Head Phillips Screw 16mm	2
8	SLRT-308	Battery Compartment	1
9	90272A239	Zinc-Plated Steel Pan Head Phillips Screw 5/16	1
10	92005A052	Steel Pan Head Phillips Screw 3mm	4

Figure 50: Payload mechanical assembly drawing exploded view.

Part/Assembly	Mass (oz)
Payload Sled	7.95
Rail System	9.72
Battery Compartment	3.5
Latch System	0.32
Fasteners and Threads	0.85
Full Payload Assembly	22.3

Table 32: Payload mechanical mass table.

4.1.3.3.12 Camera Mount and Cover Assembly

The camera mount consists of both the camera housing and the camera cover parts, and both are 3D printed (Figure 51). The camera housing is designed to be aerodynamic, as it will experience drag forces exhibited on the exterior of the launch vehicle airframe. The camera in use has two M2.5 mounting holes, a lens, and pins to connect wires from the payload. There is also a hole in the camera bay to allow the wires from the payload to pass through into the camera bay. The two mounting holes on the top of the camera bay are for the 10-24 well nuts that attach to the launch vehicles airframe. Well nuts were chosen for great reusability a need for self-securing method. The two hex-nut cutouts are for securing the camera cover to the camera housing, using ¼-20 fasteners and hex nuts (Figure 52).

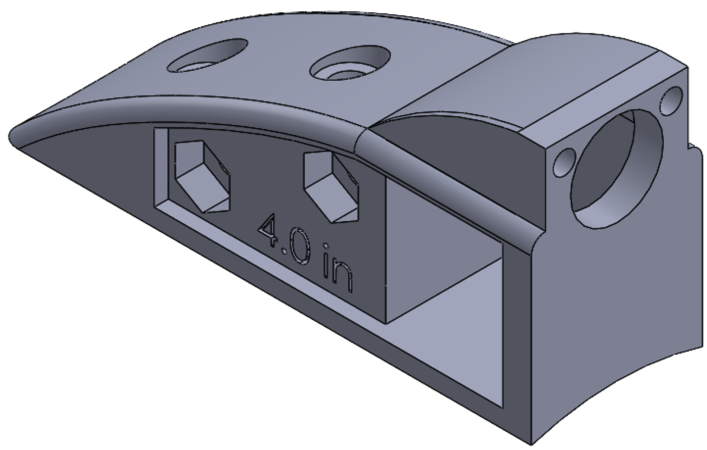

Figure 51: Payload camera housing assembly 3D model.

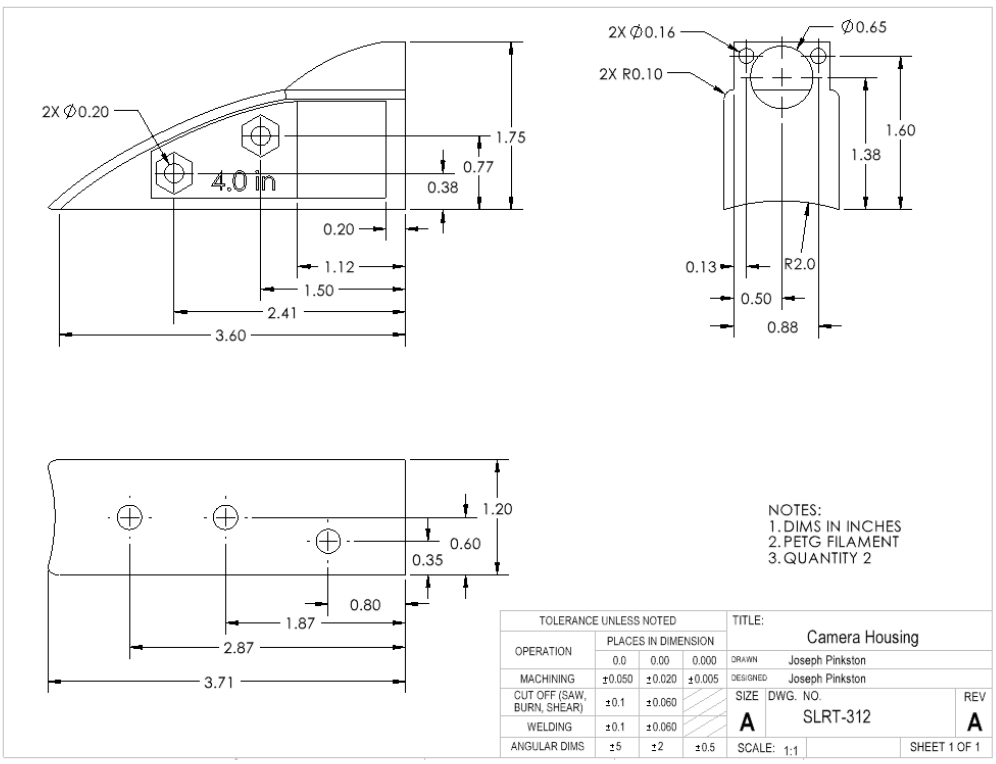

Figure 52: Payload camera housing assembly drawing.

The camera cover is needed to prevent damage to the camera bay (Figure 53). The cover prevents any wind or other external aerodynamic forces from damaging the camera or the camera's wiring. This part is 3D printed and is secured to the camera housing using the ¼-20 fastener holes. Having a removable cover was essential to be able to check the cameras wiring or remove the camera from the housing whenever needed. This allows the team to ensure the camera is properly wired to the payload prior to the launch (Figure 54).

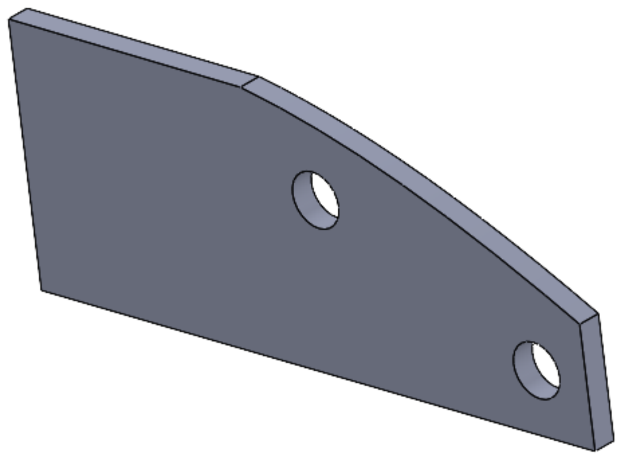

Figure 53: Payload camera cover 3D model.

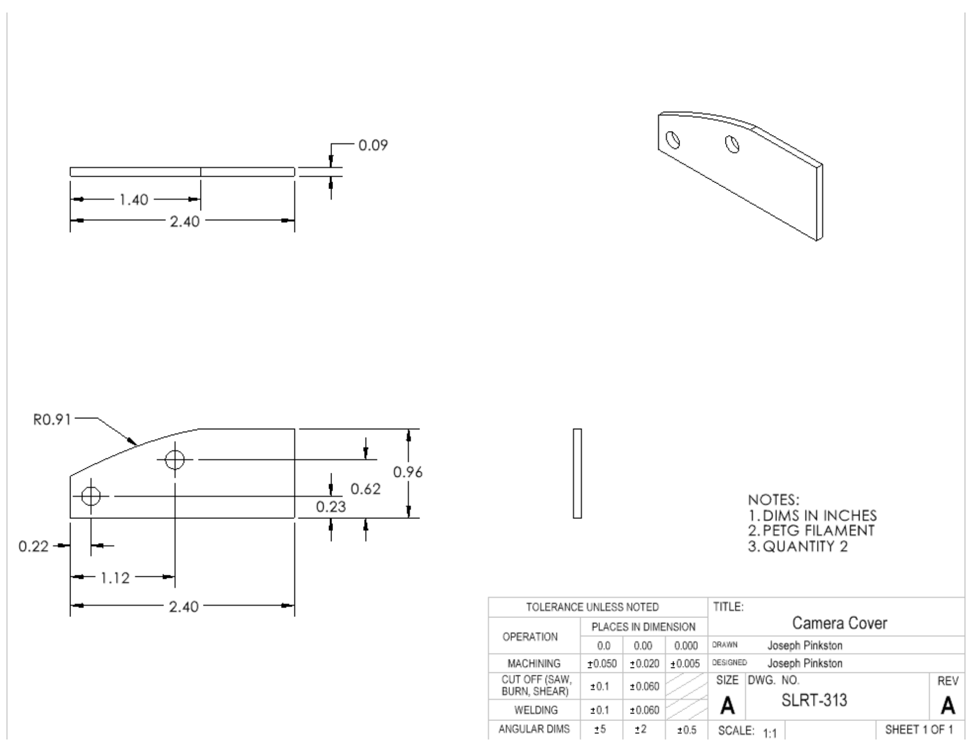

Figure 54: Payload camera cover drawing.

The camera mount assembly attaches the camera housing to the camera cover using ¼-20 fasteners. The mount is then attached to the vehicle's airframe using ¼-20 well nuts and their corresponding fasteners. The hex nuts are also ¼-20 and are epoxied into the camera housing before assembly is completed.

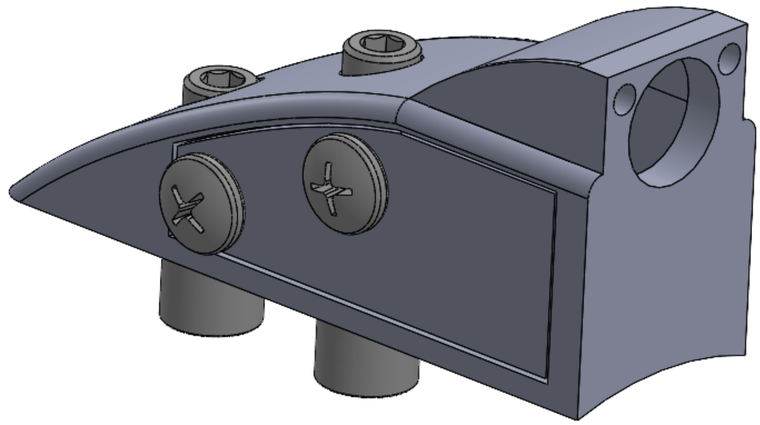

Figure 55: Payload camera mount assembly.

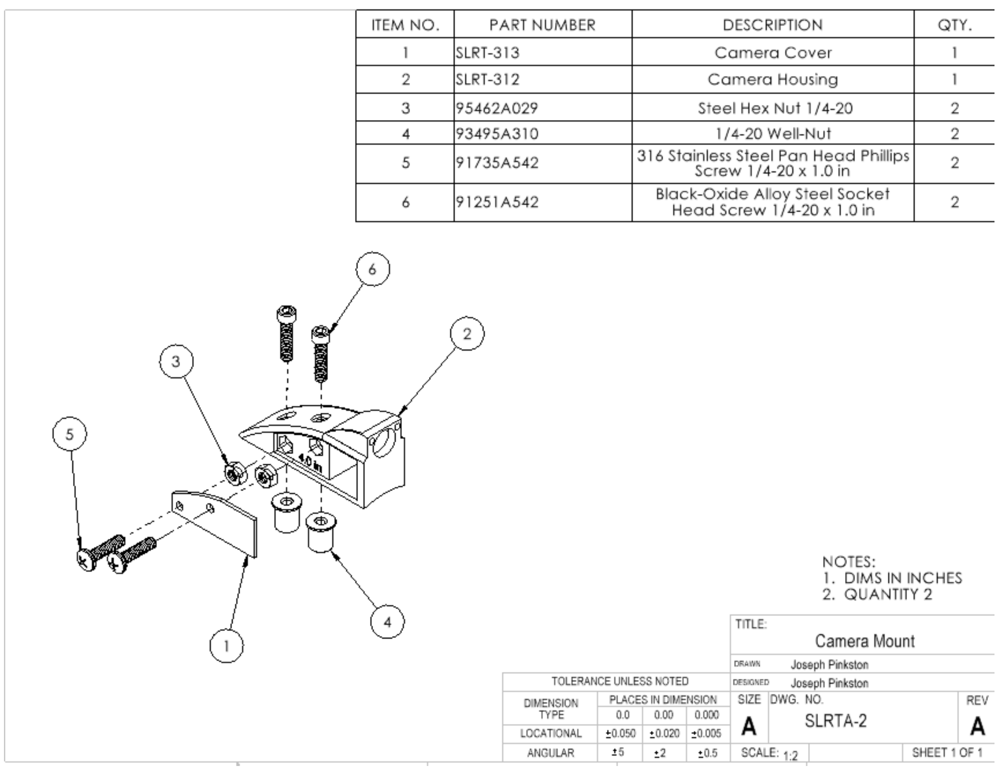

Figure 56: Payload camera mount assembly drawing exploded view.

Part/Assembly	Mass (oz)
Camera Housing	2.1
Camera Cover	0.16
Fasteners and Threads	0.31
Camera Mount Assembly	2.57

Table 33: Payload camera mount mass table.

4.1.4 Payload-Vehicle Interface

The interface between the payload and the launch vehicle is in the payload coupler section; the payload remains within the payload coupler section throughout the duration of the flight (Figure 57, Figure 58). The payload coupler section houses the payload electronics. The payload coupler section is in the aft section of the launch vehicle and is not exposed to any ejection charge gas. The payload is in the aft section of the launch vehicle to reduce the wiring needed to travel from the payload to the camera mounts. The camera mounts are on the aft section of the launch vehicle between the fins. The camera mounts are connected to the payload bay through a cardboard tube that houses the wires needed for the camera. This tube runs from the payload bay, through the aft centering rings and into the camera mount.

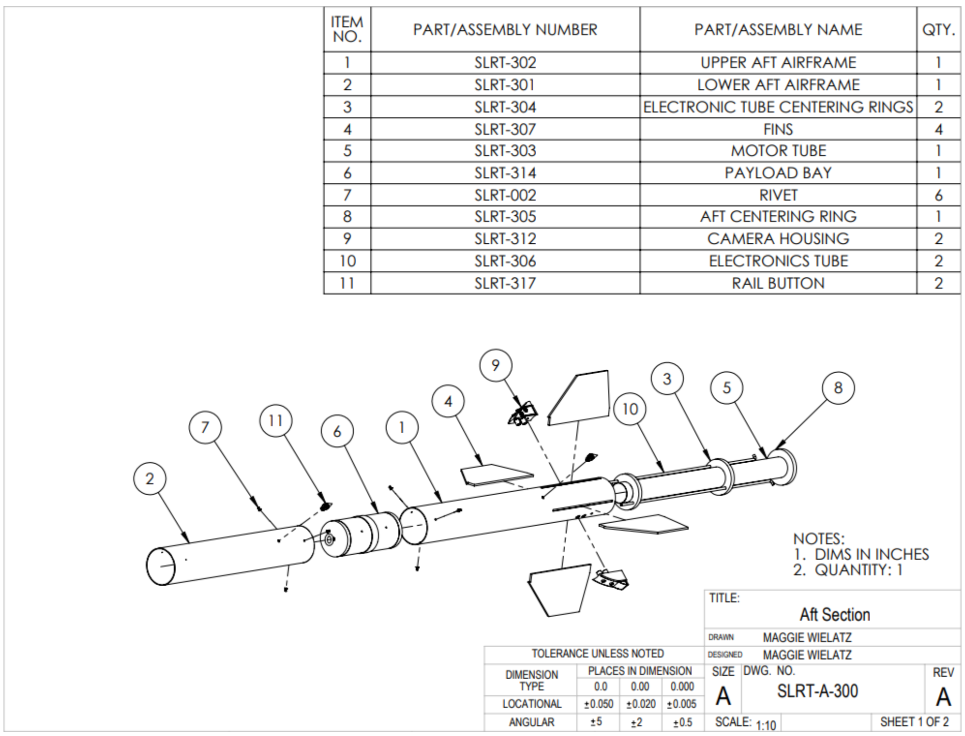

ITEM NO.	PART/ASSEMBLY NUMBER	PART/ASSEMBLY NAME	QTY.
1	SLRT-302	UPPER AFT AIRFRAME	1
2	SLRT-301	LOWER AFT AIRFRAME	1
3	SLRT-304	ELECTRONIC TUBE CENTERING RINGS	2
4	SLRT-307	FINS	4
5	SLRT-303	MOTOR TUBE	1
6	SLRT-314	PAYLOAD BAY	1
7	SLRT-002	RIVET	6
8	SLRT-305	AFT CENTERING RING	1
9	SLRT-312	CAMERA HOUSING	2
10	SLRT-306	ELECTRONICS TUBE	2
11	SLRT-317	RAIL BUTTON	2

Figure 57: Aft section assembly drawing exploded view.

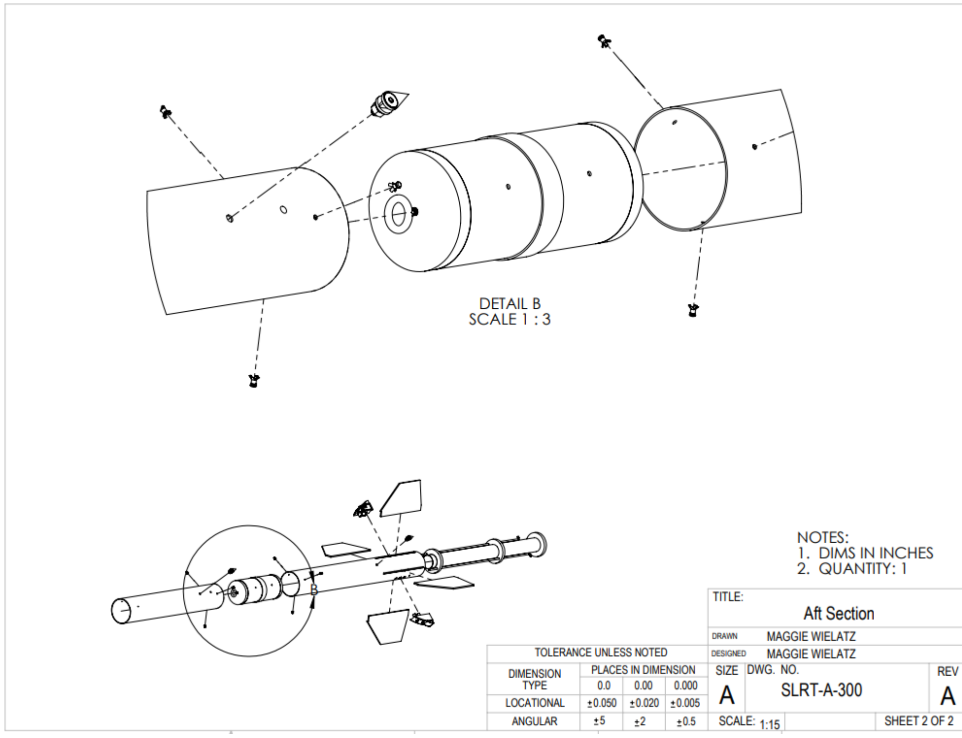

Figure 58: Payload bay retention drawing exploded view.

4.1.5 Retention System Design

The retention system is a two-part system involving both the stationary rail system and the latch system. Removal of the payload was determined to be essential to check all the wiring and implement any electrical components changes needed. The removal of the payload was made possible using a rail system, designed to slide the payload sled in and out, allowing access to any electronics onboard. The rail system has a circular base that is concentric with the couplers' inner diameter, and a flat top that helps support the weight of the payload sled. The latch system was implemented to prevent the payload sled from moving out of the rail system during launch. The latch system consists of a 3D printed rectangular bracket that has two clearance holes for fasteners. These holes are mated to their corresponding locations on the payload sled and the rail system. Since the latch system is connected to both the rail system and the payload sled, the sled and rail system must move together. While the latch system is secured, the payload sled cannot move due to the rail system being epoxied to the payload coupler. To remove the payload sled from the coupler bay, the latch system is unfastened, and the payload sled slides off the rail system (Figure 59).

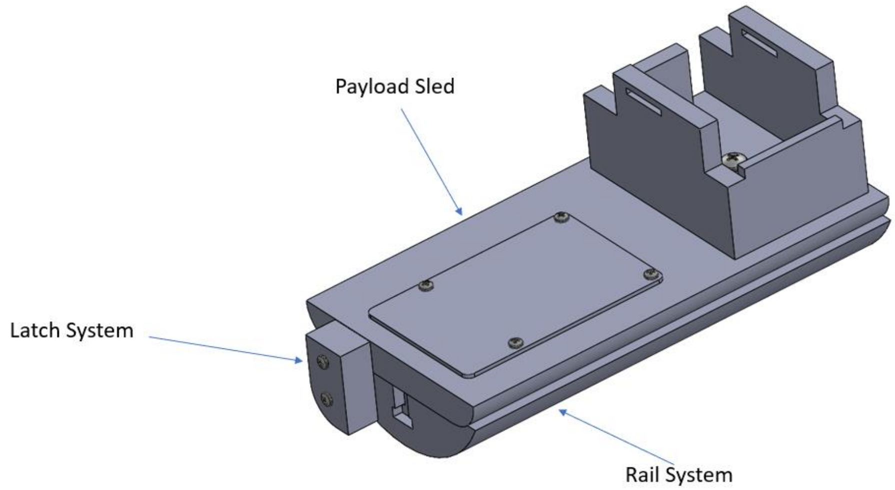

Figure 59: Payload mechanical assembly 3D model.

5. Safety

The team will prioritize safety throughout the competition. There are inherent risks due to the nature of this project. The team has put in place measures to ensure that every team member takes an active part in mitigating risk and is aware of potential hazards.

A safety plan has been developed that covers all aspects of project activities, including design, assembly and manufacturing, testing, and launch attempts. The safety plan also outlines the responsibilities of the Safety Officers and Safety Stewards. The entire team has been briefed on the current safety plan through meetings hosted by the Leads. Any updates to the safety plan will be communicated via the team Slack channel and through additional meetings hosted by the Leads or the Safety Officers.

5.1 Safety Team Responsibilities

The safety team is led by a primary Safety Officer Jason Rosenblum and secondary Safety Officer Raymond Pace. The primary Safety Officer has final say over any disagreement between Safety Officers. It also includes Safety Stewards certified by the University of Florida Mechanical and Aerospace Engineering (MAE) department.

5.1.1 Safety Officer Responsibilities

The Safety Officers will be responsible for ensuring the safety of the team from all project hazards. A list of the Safety Officer's specific duties outlines the plan for how they will use the role to fulfill this responsibility. The Safety Officers have been identified in team General Body Meetings, and team members have been informed of all available methods of contact. These include email, phone, and direct message through the team Slack channel.

1. The Safety Officers will monitor team activities to emphasize safe practices and hazard mitigation.
    a. Safety-related feedback on launch vehicle and payload design choices
    b. Supervision of manufacturing activities
        i. Enforce adherence to machine and tool standard operating procedures
    c. Supervision of launch vehicle and payload assembly
        i. Enforce proper launch-day assembly procedure
    d. Supervision of ground testing
        i. NAR/TRA mentor shall also supervise ground tests
    e. Supervision of subscale launch testing
        i. Enforce adherence to launch preparation procedure
        ii. Ensure all checks are carried out and redundancies are in place
    f. Supervision of full-scale launch testing
        i. Enforce adherence to launch preparation procedure
        ii. Ensure all checks are carried out and redundancies are in place
        iii. NAR/TRA mentor shall also supervise launch day procedure
    g. Supervision of team activities on Launch Day
        i. Hazard recognition around team launch vehicle and vehicles of others
        ii. Compliance with NAR/TRA policies
        iii. NAR/TRA mentor shall also supervise launch day procedure
    h. Supervision of recovery activities after launch attempt
        i. Close observation of launch vehicle descent and landing
        ii. Enforcement of caution around launch vehicle debris
    i. Verification of hazard mitigation strategies in place for STEM engagement

i. Supervision if active hazard mitigation is required

2. The Safety Officers shall verify the team has developed procedures for actively mitigating potential hazards. The Officers shall also enforce the implementation of the procedures.
3. The Safety Officers shall manage and maintain current revisions of the team's safety documentation.
    a. Personal Hazard Analysis
    b. Failure Mode Effect Analysis
    c. Environmental Hazard Analysis
    d. Material Safety Data Sheets
    e. Standard Operating Procedures
4. The Safety Officers shall assist in the writing and development of the team's new safety documentation.
    a. Revisions or updates to hazard analyses
    b. Failure mode analyses for the updated payload and launch vehicle designs
    c. Launch procedures for the updated payload and launch vehicle designs
    d. Updated material safety data sheets for new materials

5.1.1.1 NAR High Power Rocket Safety Code

The following safety code will be enforced by the Safety Officers during launch preparation and launch to ensure the safety of all team members and spectators.

1. The team will have a member with a Level 2 or higher high power rocket certification perform handling and installation of the launch vehicle motor.
2. The team will only use lightweight materials for the construction of the rocket.
3. The team will only use certified, commercially made rocket motors, and will not tamper with these motors or use them for any purposes except those recommended by the manufacturer. No smoking, open flames, or other heat sources will be allowed within 25 ft. of these motors.
4. The launch vehicle will use an electrical launch system which will only be installed after the rocket is on the launch pad or designated preparation area. The launch system will have a safety interlock in series with the launch switch. The launch switch will not be installed until the vehicle is ready for launch and it will return to the "off" position when released. The motor and ejection charges will be inhibited until the vehicle is in firing position.
5. If the rocket does not launch when the launch system is activated, the safety interlock or battery will be disconnected. No one will approach the pad for 60 s. after that last launch attempt.
6. A 5 s. countdown will be used before launch. Only required team members will be present on the pad when arming the vehicle's firing circuits and altimeters. The stability of the vehicle will be verified before flight, and it will not fly if it is not stable.
7. The vehicle will be launched from a launch stand that provides rigid guidance until the vehicle attains a speed that ensures stable flight. The launch stand will be within 20 deg. of vertical. If winds exceed 5 mph, a launcher length long enough to ensure a safe velocity will be used. Blast deflectors will be used on the pad to prevent motor exhaust from hitting the ground. All dry grass will be cleared within 75 ft. of the launch stand.
8. The launch vehicle will not contain any combination of motors that exceeds a total impulse of 40,960 N-s. The vehicle at liftoff will not weigh more than one-third of the certified average thrust of the motor used for launch.
9. The launch vehicle will not be launched at any targets, clouds, airplanes, overhead of spectators, or beyond the boundaries of the launch site. The team will not use any flammable or explosive payload. The vehicle will not be launched if wind speeds exceed 20 mph, and all Federal Aviation Administration airspace regulations will be following when flying.

10. The launch vehicle will be launched outdoor in an open area where trees, power lines, occupied buildings, and persons do not present a launch hazard.
11. The launch vehicle will not launch within 1500 ft. of any occupied building or public highway where traffic exceeds 10 vehicles/hr. The launch will not occur within 200 ft. of any boundary of the launch site.
12. The team will use a recovery system on the launch vehicle so that all parts of the rocket return safely, undamaged, and can be flown again. The team will only use flame-resistant or fireproof recovery system wadding in the vehicle.
13. The team will not attempt to recover the rocket from power lines, tall trees, and other dangerous places, fly it in conditions where the vehicle is likely to land in spectator areas or outside the launch site boundaries, or attempt to catch the vehicle as it descends.

5.1.2 Safety Steward Responsibilities

Safety Stewards will assist the Safety Officers with the supervision of team members during work in the Student Design Center. This will ensure hazard mitigation strategies are being followed. A certified and experienced Safety Steward is qualified to supervise a team manufacturing process without the presence of a Safety Officer, but at least two Safety Officers or Safety Stewards will always perform supervision together. Additionally, the Safety Stewards will have multiple methods of quick communication with the Safety Officers, such as phone or Slack direct message. The official responsibilities of the Safety Stewards have been provided by the MAE Facilities Operations Specialist, Daniel Preston.

1. Safety Stewards shall enforce all protocols outlined in the SDC's Rules for Facility Use document. This includes policies for personal safety; equipment uses; facility cleanliness, organization, and respect; proper language; use of the Material & Tool List and Broken / Lost Tooling List; and all other miscellaneous policies.
2. Safety Stewards must have a strong understanding of each machine at the SDC.
3. Safety Stewards shall train students on machines, administer knowledge quizzes, and sign authorization sheets to allow future supervised equipment use.
4. Safety Stewards shall verify students are trained and authorized on each machine they use.
5. Safety Stewards shall set up each approved equipment each time a user works on a new part.
6. Safety Stewards shall keep watch of powered machinery as it is being used.
7. Safety Stewards shall manage access to common-use tools via the Material & Tool Use List.
8. Safety Stewards shall ensure students clean machines after each use and accept responsibility for stations not up to SDC cleaning standards.
9. Safety Stewards shall ensure students keep the team's bay neat and clean.

5.2 Personnel Hazards Analysis

Personnel hazards were quantified using a total score given by the product between the severity and likelihood of each hazard (Table 34).

<table>
<tr><th></th><th>Severity (S)</th><th>Likelihood (L)</th></tr>
<tr><td>1</td><td>No injury obtained</td><td>Extremely Unlikely</td></tr>
<tr><td>2</td><td rowspan="2">Very minor injury</td><td rowspan="3">Unlikely/low probability</td></tr>
<tr><td>3</td></tr>
<tr><td>4</td><td rowspan="2">Minor injury</td></tr>
<tr><td>5</td><td>Likely</td></tr>
</table>

6	Moderate injury	
7		Highly likely/high probability
8		
9	Severe injury or death of personnel	
10		Extremely likely/almost certain

Table 34: Personnel risk assessment chart.

A hazard with a low severity and likelihood will receive a lower score than a hazard with a large difference between severity and likelihood. Furthermore, a hazard with a high severity and likelihood will receive a higher score than hazards with inconsistent severity and likelihood scores. Thus, quantifying scores using this method accurately shows the significance of the hazards present while completing the project. The scores have been color coded to visually represent the importance of each hazard (Table 35).

		Likelihood									
Severity		1	2	3	4	5	6	7	8	9	10
	1	1	2	3	4	5	6	7	8	9	10
	2	2	4	6	8	10	12	14	16	18	20
	3	3	6	9	12	15	18	21	24	27	30
	4	4	8	12	16	20	24	28	32	36	40
	5	5	10	15	20	25	30	35	40	45	50
	6	6	12	18	24	30	36	42	48	54	60
	7	7	14	21	28	35	42	49	56	63	70
	8	8	16	24	32	40	48	56	64	72	80
	9	9	18	27	36	45	54	63	72	81	90
	10	10	20	30	40	50	60	70	80	90	100

Table 35: Risk assessment score chart.

5.2.1 Chemical Hazards

Chemical hazards are those posed by the team's chemical inventory. The personal protective equipment (PPE) and storage requirements for mitigating each hazard were identified using the material safety data sheets (MSDS) of each chemical (Table 36).

Hazard	Cause	Effect	S	L	Score	Mitigation Strategy
Irritant contacts skin	Working with epoxy resin	Skin redness, itching, other moderate irritation	4	6	24	Use alternative adhesive if materials allow. Wear liquid-proof, chemical resistant gloves and full-body covering clothing when handling.

Irritant contacts eyes	Working with epoxy resin	Eye redness, moderate irritation	6	3	18	Use alternative adhesive if materials allow. Wear chemical goggles when applying epoxy.
Exposure to noxious fumes	Working with epoxy resin	Headache, nausea, dizziness, respiratory irritation	6	4	24	Use alternative adhesive if materials allow. Use in well ventilated area. Limit use of curing agents which cause additional vapors due to heat. When process produces heat or heat is applied, wear respirator.
Uncontrolled detonation of black powder	Heat, or flame ignites black powder	Severe burns	8	2	16	Store black powder in cool, dry conditions until use. Wear metal-free and non-static producing clothes when handling. Release static buildup prior to beginning work.
Spray paint can explodes	Heat or flame causes can to explode, can is pierced	Severe burns, shrapnel injuries	8	2	16	Store in a cool, well-ventilated area away from sunlight.
Spray paint aerosol combusts	Heat, sparks, flames, or other ignition sources ignite aerosol	Severe burns	6	3	18	Use away from any heat sources, flames, sparks, and other ignition sources.
Spray paint aerosol contacts skin	Working with spray paint	Skin irritation, allergic reaction	4	7	28	Wear protective gloves and clothing when handling. Work outdoors or in a well-ventilated area. Wash hands and other exposed areas after handling.
Spray paint aerosol contacts eyes	Working with spray paint	Serious eye irritation	6	4	24	Wear eye or face protection when handling.
Spray paint aerosol is inhaled	Working with spray paint	Respiratory irritation, drowsiness, dizziness	7	3	21	Work outdoors or in a well-ventilated area. Wear face protection and respirator when handling.

Table 36: Chemical hazards chart.

5.2.2 Manufacturing Hazards

Manufacturing hazards are those posed by team activities during the manufacturing process. The hazards and mitigations were identified using the operator's manuals of each machine (Table 37).

Hazard	Cause	Effect	S	L	Score	Mitigation Strategy
Bandsaw blade contacts hand	Hand in path of blade	Severe skin lacerations	8	3	24	Keep hand out of the path of the blade. Use a sacrificial handle when workpiece is too small to hold.
Spinning tool or workpiece contacts person	Hand pulled into work area	Severe skin laceration, physical trauma	8	3	24	Keep hands at least six inches away from cutting area. Do not wear gloves while operating powered tools. Do not wear jewelry or loose articles of clothing and tie up long hair when machining.
Flying workpiece or tool hits person	Improper clamping of tool or workpiece	Skin laceration, physical trauma	6	3	18	Ensure proper clamping of workpiece and tool in machine. At least two clamps used when clamping any workpiece for machining. When using a vise, tighten vise jaws with proper force.
Sharp tooling cuts skin	Handling sharp tools with bare hands	Skin lacerations	3	5	15	Cover sharp edges with a rag when handling.
Sharp edges on workpiece cuts skin	Handling workpieces with burrs recklessly	Skin lacerations	2	5	10	Carry newly machined parts with a rag. Deburr workpiece as soon as machining is finished.
Pressurized water contacts person	Leak in waterjet system, hand too close to jet stream when cutting	Severe skin laceration	8	2	16	Stand a safe distance from the pressurization system when active. Do not put any body parts near cutting zone while waterjet is running.
Extended duration loud processes	Unprotected hearing while operating loud machinery	Hearing loss	6	5	30	Wear hearing protection when operating loud machinery.
Sudden loud sound	Person startled by sudden noise while operating machinery	Skin lacerations, physical trauma	6	4	24	Verbally warn any nearby people before making any sudden loud noises.
Small particles in air from manufacturing	Machining crates small chips and debris in air	Respiratory irritation, eye irritation	4	7	28	Work in a well-ventilated area. Wear respirators when machining certain materials.

Burn from soldering iron	Person touches heated portion of soldering iron	Burn	5	2	10	Handle soldering iron properly.
Fumes from soldering	Inhalation of soldering iron fumes	Respiratory irritation, eye irritation	3	6	18	Working outdoors or in a well-ventilated area. Wear face and eye protection.

Table 37: Manufacturing hazards chart.

5.2.3 Launch Hazards

Launch hazards are those posed by team activities throughout launch preparation, launch, and vehicle retrieval (Table 38).

Hazard	Cause	Effect	S	L	Score	Mitigation Strategy
Falling debris	Shock cord fails Motor retainer fails	Falling debris hits person	9	1	9	Properly fold parachute and check shock cord and motor retainer connections.
	Parachute fails to deploy	Ballistic vehicle hits person	10	2	20	Complete ejection charge testing to verify number of rivets. Fold parachute properly and verify it will not get stuck inside airframe.
Burns from motor ignition	Ignition while loading motor	Severe Burns, hearing loss	10	2	20	No one may stand in line of motor during loading and transit to pad. No smoking, open flames, or other heat sources are allowed within 25 ft. of the motor.
	Person too close to launch pad during ignition					No person may be within 200 ft. of the launch pad. If rocket misfires, the battery will be disconnected from the launch system and no one will approach the rocket for 60 s after the misfire.
Uncontrolled detonation of black powder	Heat, or flame ignites black powder	Severe burns	8	2	16	Wear metal-free and non-static producing clothes when handling. Release static buildup prior to beginning work.
Vehicle lands in unsafe area	Vehicle drifts from wind	Injuries from environment during recovery	4	3	12	Monitor wind on launch day and only launch in acceptable wind speeds. Angle the launch rail into the wind.
Heat	High heat at launch site	Heat exhaustion	7	3	21	Bring water to launch site. Give all team members water and check their well-being throughout the day.

						Bring pop-up canopy for shade.

Table 38: Launch hazards chart.

5.3 Failure Mode and Effects Analysis

Failure mode and effects analysis (FMEA) evaluates the impact of component failure on the launch vehicle and its ability to complete the mission. The FMEAs include Structures, Payloads, Avionics and Recovery, and Flight Dynamics. Three ratings are given to each failure mode to quantify the significance of the failure: severity, occurrence, and detection. Severity is rated from 1 to 10 where a rating of 1 means that the failure has no effect while a rating of 10 is a catastrophic failure. Occurrence is rated from 1 to 10 where a rating of 1 means that the failure has little to no chance of occurring while a 10 indicated it is incredibly likely to occur. Detection is rated from 1 to 10 where a 1 is a failure that has a high likelihood of detection while a 10 is a failure that has an extremely low likelihood of detection. A risk priority number (RPN) is calculated as the product of the ratings and will be used to inform the team where mitigation strategies are needed.

5.3.1 Structures

Component	Function	Failure Mode	Failure Cause	Failure Effects			S	O	D	RPN	Corrective Actions
				Local Effects	Next Higher Level	System Effects					
Airframe and coupler	Contains the payload and vehicle hardware	Breaks	Manufacturing defect or poor transportation	Fails to contain payload and other internal components	Launch vehicle assembly fails	Launch vehicle is unrecoverable	10	3	3	90	Inspect launch vehicle before and after each launch
Fin Fillets	Epoxy keeps the fins attached to the aft airframe and motor tube assembly	Epoxy fails	Improper application	Launch vehicle loses stability	Uncontrolled flight	Launch vehicle drifts or moves uncontrollably, posing a hazard	8	2	4	64	Follow proper procedures for applying epoxy to fins
Centering ring	Keeps the motor centered within the airframe	Epoxy fails	Improper application	Launch vehicle loses stability	Uncontrolled flight	Launch vehicle drifts or moves uncontrollably	10	2	5	100	Inspect launch vehicle before and after each launch
Centering ring	Keeps the motor centered within the airframe	Breaks	Manufacturing defects	Launch vehicle loses stability	Uncontrolled flight	Launch vehicle drifts or moves uncontrollably	10	2	3	60	Inspect component for defects immediately after manufacturing
Bulkhead	Seals the ends of the couplers and protects internal components	Epoxy fails	Improper application	Fails to maintain sufficient seal	Ejection charges fail to separate vehicle	Parachutes not deployed properly, or internal components are damaged	8	2	2	32	Inspect component for defects immediately after manufacturing
Bulkhead	Seals the ends of the couplers and protects internal components	Breaks	Manufacturing defects	Fails to maintain sufficient seal	Ejection charges fail to separate vehicle	Parachutes are not deployed properly, or internal components are damaged	8	2	2	32	Inspect launch vehicle before and after each launch

Shear pins	Keeps components connected before separation events	Early shearing	Excessive pressure from other events or excessive force from poor packing	Airframe and couplers separate	Premature parachute deployment	Reduced altitude, failure to complete payload mission	8	3	8	192	Test ejection charges and ensure that design adequately houses internal components, so shear pins do not break prematurely (Tests 11, 12)
Shear pins	Keeps components connected before separation events	Do not shear	Insufficient ejection charge during separation event	Parachutes do not deploy	Rapid descent of launch vehicle	Launch vehicle impacts ground with high velocity	8	4	8	256	Test ejection charges to find sufficient amount of black powder for separation (Test 15)

Table 39: Structures FMEA

5.3.2 Payloads

5.3.2.1 Payload Mechanical

Component	**Function**	**Failure Mode**	**Failure Cause**	**Failure Effects**			**S**	**O**	**D**	**RPN**	**Corrective Actions**
				Local Effects	Next Higher Level	System Effects					
3D Printed Sled	Protect and hold all electronics on the payload	Fracture	Stresses and vibrations	Cracking/breaking of plastic	Damaged electronics on payload	Loss of payload functionality	7	2	4	56	Extensive vibrations and stress tests to ensure structural integrity (Test 16)
Rail System	Secure payload in rocket	Fracture	Stresses and shearing	Cracking or shearing from payload	Payload comes loose during flight	Extensive damage to payload	8	3	2	48	Test for payload compatibility and flight performance (Test 16)
Latch System	Retain payload sled in rail system	Fracture	Stresses and shearing/fastener stripping	Latch system breaks or strips off payload sled	Damaged payload sled and/or electronics	Loss of payload functionality	7	2	2	28	Perform testing on latch system to determine maximum force it can withstand (Test 35)
Battery Compartment	Secure batteries on payload sled	Fracture	Stresses and shearing/fastener stripping	Battery compartment breaks or strips off payload sled	Batteries lose connection to electronics on payload	Loss of electronics functionality	1	1	2	2	Ensure fastener and plastic can withstand predicted forces during flight and landing (Test 36)
Camera Mount	House the cameras	Fracture	Stresses and vibrations	Camera mount is damaged	Camera cannot obtain accurate photographs	Inaccurate readings of rocket's current location	2	3	5	30	Test the strength of the camera mount and fly test subjects on subscale launch (Test 37)

Table 40: Payload mechanical FMEA.

5.3.2.2 Payload Electronics

Component	Function	Failure Mode	Failure Cause	Failure Effects			S	O	D	RPN	Corrective Actions
				Local Effects	Next Higher Level	System Effects					
Lithium Battery	Provides power to electronic payload components.	Short circuit	Unintended connection between the positive and negative battery terminals.	High current flow within the battery, generating excessive heat.	Fire within the launch vehicle.	Loss of the payload and vehicle.	9	2	2	36	Ensure no loose or exposed metallic objects are present in the payload bay. Ensure power terminals are fully insulated.
Radio Transceiver	Provides communication between the payload and ground station.	Radio interference	Two or more transmitters transmitting on the same frequency simultaneously.	Data received by the ground station is altered.	The ground station is unable to correctly receive the vehicle's landing location.	The ground station is unable to display the vehicle's landing location.	5	1	1	5	Report all radio frequencies used to NASA officials to avoid overlap with other teams.
Payload Computer	Controls payload peripherals and calculates vehicle's grid location.	Momentary power loss	Poor connection between the battery terminals and control board and/or vehicle vibrations.	The payload computer reboots and the program reinitiates.	The payload is momentarily unable to capture or process images.	The payload's positional estimates become less accurate or the payload is unable to produce an estimate.	5	2	6	60	Use power connectors with strong mechanical latches and include software power-loss recovery mechanisms.

Table 41: Payload electronics FMEA.

5.3.2.3 Payload Software

Component	Function	Failure Mode	Failure Cause	Failure Effects			S	O	D	RPN	Corrective Actions
				Local Effects	Next Higher Level	System Effects					
Microprocessor	Controls payload peripherals and calculates vehicle's grid location.	Software debug error	Unaccounted edge case in software, causing system to crash	The microprocessor reboots. Data may be lost/overwritten	Information regarding the vehicle's flight state and position is lost.	The payload is unable to determine its current grid location.	5	2	5	50	Run testcases preflight, by simulating effect at different altitude/terrain

Table 42: Payload software FMEA.

5.3.3 Avionics and Recovery

Component	Function	Failure Mode	Failure Cause	Failure Effects			S	O	D	RPN	Corrective Actions
				Local Effects	Next Higher Level	System Effects					
Altimeter	Track and record the altitude of the rocket in order to accurately set off	Instant detonation of ejection	Polarity of battery reversed due	Ejection charges detonating on the launch pad	Hot gases and heavy rocket components moving near	Unable to launch, potential for burns and	10	3	1	30	Test wiring of altimeters before placing in rocket and attaching

	ejection charges to cause separation and parachute deployment for both main and drogue parachutes.	charges when powered on	to improper installation.		team member responsible for arming altimeter	other injuries					ejection charges. (Test 9).
Altimeter	Track and record the altitude of the rocket in order to accurately set off ejection charges to cause separation and parachute deployment for both main and drogue parachutes.	Sudden power loss	Disconnection of battery due to inflight motion	Tracking and recording of altitude halts	Ejection charges do not go off, separation does not occur, and parachutes are not deployed.	The launch vehicle goes ballistic and descends uncontrolled	10	1	5	50	Altimeters and their power sources will be secured in the avionics bay. The secondary altimeter will have its own power source.
Altimeter	Track and record the altitude of the rocket in order to accurately set off ejection charges to cause separation and parachute deployment for both main and drogue parachutes.	Reverse wiring of ejection charges, (main ejection plugged into drogue terminal)	Mislabeling of terminals or improper programing of altimeter	Detonation of main parachute ejection charges	Main parachute is deployed at apogee	Launch vehicle drifts out of launch field, potential for launch vehicle to be lost	6	2	4	48	Proper labeling of ejection charges and altimeter terminals.
Recovery Harness	The recovery harness tethers the separated sections of the launch vehicle together during descent.	Tearing of recovery harness	Melting of the harness due to ejection charge gases, insufficient strength of recovery harness	The launch vehicle becomes two or more untethered sections	Sections disconnected from the parachutes will descend significantly faster than intended	Partial damage to the launch vehicle	6	1	5	30	Protect the recovery harness from ejection gasses using the parachute protector, ensure the recovery harness is strong enough for the mission during design and testing.
Parachute Protector	Protects the parachute and recovery harness from hot ejection charge gases during separation	Holes or tears in the parachute protector	Excessive use and age	Ejection gases burn the parachute	Holes form or parts of the parachute are melted together	Faster than anticipa ted descent rate leading to damage to the launch vehicle	7	2	1	14	Inspection of the parachute protector before use
Main parachute	Slows the launch vehicle to an acceptable landing velocity	Tangled lines	Improper storage or packing of the parachute	Parachute does not fully inflate on descent	Faster than anticipated descent rate	Minimal to mild damage to the launch vehicle or payload	4	5	1	20	Inspection of parachute pre-packing and safety officer or avionics recovery lead pack the parachute for launch.
Main parachute	Slows the launch vehicle to an acceptable landing velocity	Holes or tears in parachute	Parachute protector failure or	Holes or tears could increase in size and reduce	Faster than anticipated descent rate	Damage to the launch vehicle or payload	6	2	1	12	Inspection of parachute before selecting it for use. Perform regular

			exposure to sharp edges	the effectiveness of the parachute							maintenance on parachutes
Drogue Parachute	Deploys at apogee to slow the initial descent of the launch vehicle	Failure of the drogue parachute to deploy and slow the initial descent	Holes in drogue, failure to deploy due to insufficient ejection charges, failed altimeter, torn recovery harness	Launch vehicle descends much faster initially until deployment of main parachute	Launch vehicle zippers or other components are damaged during main parachute deployment	Damage to the launch vehicle or payload	6	1	4	24	Properly pack the drogue parachute and follow mitigation strategies for other potential causes of failure

Table 43: Avionics and recovery FMEA

5.3.4 Flight Dynamics

Component	**Function**	**Failure Mode**	**Failure Cause**	**Failure Effects**			**S**	**O**	**D**	**RPN**	**Corrective Actions**
				Local Effects	Next Higher Level	System Effects					
Propellant	Generate appropriate thrust to propel the rocket.	Propellant Failure	Improper storage of motor.	Improper propellant burnout or incomplete propellant ignition.	Changes the propellant burn distribution creating abrupt changes in thrust.	Overpressure risks, unpredictable trajectory/flight, or rocket does not take off.	9	3	4	108	Ensure the structural integrity of the propellant by visually ensuring defects, or moisture is not present. Motors need to be contained in a Climate Regulated room, and ensure they are handled carefully.
Nozzle	Controls the mass flow rate of the propellant	Nozzle Deformation	Structural failure of nozzle.	Nozzle exit area, nozzle exhaust pressure, propellant flow rate change.	Abrupt changes in the thrust vector.	Altered trajectory of the rocket creating potential danger to bystanders.	9	3	5	135	Always handle nozzle carefully, and visually inspect ensuring defects are not present.
Motor Case (including forward and aft closures)	Enclose solid propellant to protect the body from ignited propellant.	Case Defect	Defect or structural failure of the motor case including the forward and aft enclosures.	Propellant burns through motor case interacting with the rocket body.	Motor assembly gets damaged.	Structural integrity of motor tube and body tube are compromised.	7	2	8	112	Always handle motor case carefully, and visually inspect ensuring defects are not present. Always have a protective cover over the casing until launch.
Motor Tube	Encloses the motor assembly in the correct position.	Motor Tube Fails or Dislodges	Defect or structural failure of the motor tube	Motor case is not held in correct position.	Improperly aligned thrust vector	Altered flight trajectory and potential damage to	6	3	6	108	Always handle motor tube carefully, and visually inspect ensuring

						other components.					defects are not present.
Motor Mount	Retains the motor inside the rocket	Motor Mount Fails	Structural failure of mount or screws improperly fastened	Motor case moves forward in the rocket	Damage to forward rocket components	Rocket integrity is compromised, and function is lost.	7	4	7	196	Visually inspect ensuring defects are not present and tighten screws.
Thrust Plate	Transfers thrust from centering rings to airframe	Thrust Plate Fails	Structural failure of thrust plate or screws improperly fastened	Structural integrity of centering ring becomes compromised	Improperly aligned thrust vector	Altered flight trajectory and potential damage to other components.	5	4	7	140	Visually inspect ensuring defects are not present and tighten screws.

Table 44: Flight dynamics FMEA

5.4 Environmental Concerns

Environmental concerns are any hazards that the vehicle poses on the environment, or the environment poses on the vehicle. These concerns are quantified by assigning severity and likelihood values to each hazard (Table 45). This method yields a score from 1-100 in the same manner as personnel hazards (Table 35).

	Severity (S)	Likelihood (L)
1	No effect on environment or launch vehicle	Extremely Unlikely
2	Minimal effect on environment or launch vehicle	Unlikely/low probability
3		
4	Moderate but resolvable harm to environment or launch vehicle	
5		Likely
6	Moderate harm to environment or launch vehicle with lasting impact	
7		Highly likely/high probability
8		
9	Serious environmental harm requiring immediate and drastic response/Launch vehicle suffers extensive damage	
10	Catastrophic impact on launch environment, difficult to resolve with lasting damage/Total loss of launch vehicle	Extremely likely/almost certain

Table 45: Environmental concerns score chart.

5.4.1 Effect of Vehicle on Environment

The effects of the vehicle on the environment include any hazards posed by the vehicle during testing, launch preparation, and launch (Table 46).

Hazard	Cause	Effect	S	L	Score	Mitigation Strategy
Falling debris	Shock cord fails Parachute fails to deploy Motor retainer fails	Debris pollutes land around launch site	5	2	10	Properly fold parachute and check shock cord and motor retainer connections.

Environment around vehicle ignites	Sparks from ejection charge testing Motor exhaust	Uncontrolled fire	8	2	16	Follow range safety officer instructions on properly conducting ejection charge testing. Only test and launch in approved areas cleared of flammable debris.
Chemical leaks	Battery leaks	Ground around vehicle is polluted	6	2	12	Check battery for damage before loading it on the vehicle. Isolate battery from components with the potential to pierce the battery casing.
Noise pollution	Rocket motor emits sound when firing	Disturbing wildlife	3	10	30	Only launch at designated NAR/TRA launch sites

Table 46: Effect of vehicle on environment chart.

5.4.2 Effect of Environment on Vehicle

The effects of the environment on the vehicle include any hazards present during testing, launch preparation, and launch (Table 47).

Hazard	Cause	Effect	S	L	Score	Mitigation Strategy
Vehicle exposed to moisture	Humidity Precipitation soaks vehicle	Warping of plywood centering rings	3	3	9	Store vehicle in a cool, dry, well-ventilated area. Check for changes in weather while vehicle is exposed to the environment.
	Vehicle lands in water	Electronics are ruined	9	3	27	
Clouds obscure camera	Cloudy skies on launch day	Landmarks for mission objective cannot be identified	7	4	28	Only launch when skies are clear. Monitor weather in launch area as launch day approaches to explore alternatives.
Vehicle drifts off course	Wind during vehicle flight	Vehicle lands in unsafe area	8	5	40	Monitor wind and weather conditions at the launch site. Only launch when wind is within acceptable ranges. Angle the launch rail into the direction of the wind.
		Vehicle drifts far from launch site	5	7	35	
		Vehicle lands outside of grid	6	6	36	
Vehicle lost in sky	Fog at launch site Clouds at flight altitudes	Vehicle descends into unknown area	7	3	21	Monitor weather conditions at the launch site. Only launch when there is high visibility around the launch site and sky.

Heat	Heat from the weather	Electronics overheat and fail	7	5	35	Keep vehicle shaded and cool prior to loading onto launch stand.

Table 47: Effect of environment on vehicle chart.

5.5 Project Risks

Project risks are hazards associated with the resources, budget, and scope of the project (Table 49). These concerns are quantified by assigning severity and likelihood values to each hazard (Table 48). This method yields a score from 1-100 in the same manner as personnel hazards (Table 35).

	Severity (S)	Likelihood (L)
1	No effect on flight/no risk of mission loss	Extremely Unlikely
2	Slight impact on flight or launch vehicle/mission obstructed	Unlikely/low probability
3		
4	Moderate impact on flight/significant effect on mission	
5		Likely
6	Severe flight impact/partial mission loss or entire mission at risk	
7		Highly likely/high probability
8		
9	Complete loss of vehicle/Complete inability to complete mission	
10		Extremely likely/almost certain

Table 48: Project risks score chart.

Risk	Cause	Effect	S	L	Score	Mitigation Strategy	Effects of Mitigation
Functionality of Payload	Team has never implemented image processing into a payload design	Inability to reliably locate vehicle	9	6	54	Recruitment of additional members from computer science backgrounds (already occurred)	Decreased likelihood of payload issues
Time	High lead times due to purchase approval and shipping times	Inability to manufacture and launch before team/ competition deadlines	10	5	50	Ensuring general use items purchased well before need arises (cordless drill, Dremel, gloves, etc.) Communicating team needs to Student Government Budget Committee	Lower likelihood of not meeting deadlines, increased risk in budget.

	Manufacturing delays	Vehicle or payload is not complete in time for scheduled launch	10	4	40	Scheduling machine access far in advance. Frequent team meetings to check subteam progress.	
Budget	Limited funding available from University/Department	Inability to secure parts necessary for a successful mission	6	5	30	Effective planning for budget requests Outreach to corporate sponsors	Lower likelihood of budget issues

Table 49: Project risks chart.

6. Project Plan

6.1 Requirements Verification

6.1.1 Team-Derived Requirements

The team has created requirements that are specific to the team's design. These team-derived requirements specify components of the design that go beyond the minimum competition requirements and are applied to ensure success of the team's design.

6.1.1.1 Vehicle Requirements

The team-derived requirements for the launch vehicle are defined (Table 50).

Requirement	Justification	Verification Method
1.1 The apogee of the launch vehicle must reach between 4100 and 4700 ft.	The final apogee of the launch vehicle must be within this apogee range to ensure that it does not fall below the absolute minimum set forth.	The Flight Dynamics Lead will perform various simulations using the subscale design to ensure that the launch vehicle will meet this requirement through all external conditions.
1.2 The motor centering rings' holes must be aligned sufficiently in order for electronics tubes to fit through the holes properly.	The electronics tubes cannot bend as this may compromise the wiring within and cause the payload to fail.	Marks will be made by the Structures Lead during manufacturing that indicate where the centering rings must align.

Table 50: Vehicle team derived requirements.

6.3.2 Recovery Requirements

The team-derived requirements for recovery are defined (Table 51).

Requirement	Justification	Verification Method
2.1 The drogue parachute will have a descent rate of 80 ft/s.	This descent rate ensures the vehicle is at a slow enough velocity once the main parachute must be deployed.	Test #7, Parachute Drag Test, will ensure the drag induced by the parachute is sufficient.
2.2 The main parachute will have a descent rate of 18 ft/s.	This descent rate ensures the launch vehicle will not be harmed during landing by landing at an appropriate velocity.	Test #7, Parachute Drag Test, will ensure the drag induced by the parachute is sufficient.
2.3 Each recovery harness will have a length of 2.5 times the total length of the vehicle.	This length is required to ensure the separate sections of the launch vehicle do not collide during descent. This length also prevents breakage of the recovery harness during	Visual verification of the length of the recovery harness will be performed by the Avionics and Recovery Lead and the Project Manager.

	separation, as a longer harness provides more slack.	
2.4 There will be a delay of the secondary aft ejection charge of 0.5 seconds after the ejection of the primary charge.	The delay ensures that the launch vehicle does not over-pressurize, a possible occurrence during ejection that may occur if multiple charges ignite at once.	Test#10, Barometer Functionality Test, will ensure that the barometer functions correctly and thus ignites the ejection charge at the appropriate time.
2.5 There will be a delay of the secondary forward ejection charge to eject at an altitude of 50 ft below the altitude of primary charge, thus ejecting at an altitude of about 550 ft.	The delay ensures that the launch vehicle does not over-pressurize, a possible occurrence during ejection that may occur if multiple charges ignite at once.	Test #10, Barometer Functionality Test, will ensure that the barometer functions correctly and thus ignites the ejection charge at the appropriate time.
2.6 The secondary ejection charges will be 25% larger in black powder weight than the primary charges.	The secondary charge must be larger than the primary in the event that the primary fails to separate the vehicle and thus the larger secondary charge can provide a greater force and result in successful separation.	The weight of the black powder will be verified by the Avionics and Recovery Lead and the Project Manager prior to launch.

Table 51: Avionics and recovery team derived requirements.

6.3.3 Payload Requirements

The team-derived requirements for the payload are defined (Table 52).

Requirement	**Justification**	**Verification Method**
3.1 The payload will be able to resume operation after a momentary power loss.	The payload must be able to continue operation without losing previously captured images or data.	Test #34, Power Loss Test, ensures that the payload will continue operation correctly in a circumstance of loss of power.
3.2 The payload IMU expected positional drift must not exceed 100 ft over 90 sec.	The payload must be able detect the correct grid space the launch vehicle is located in.	Test #50, IMU Drift Test, determines the expected drift and ensures it does not exceed 100 ft.
3.3 The payload must be able to detect launch.	Launch detection allows the payload to idle in a low-power state while on the launch pad, preserving battery life.	Test #47, Payload Launch Detection Test, ensures that the payload can detect the sudden acceleration that will occur during launch.
3.4 The payload transmitter must have a range of at least one mile.	The payload must be able to communicate its results successfully even in the event of	Test #49, Payload Transmission Range Test, ensures that the payload

	maximum drift as well as possible obstructions.	can transmit data over at least one mile.
3.5 The payload must be able to process at least 100 images within five minutes of landing.	The payload must be able to compile the data in the allowed amount of time in order to determine its grid location.	Test #48, Payload Data Compilation Test, ensures that the data can be compiled in the appropriate amount of time.

Table 52: Payload team derived requirements.

6.2 Testing Plan

The tests detailed in the testing tables are performed in order to verify that the requirements set forth in the student handbook as well as the team-derived requirements will be met.

6.2.1 Launch Vehicle Testing Plan

The testing plan for the launch vehicle are defined (Table 53).

Test Number	Test Name	Required Materials and Machinery	Test Procedure	Justification
1	Airframe Compression Test	Fiberglass airframe, Instron Machine	Place the airframe material in the Instron Machine to simulate compressive forces and record data. Compress airframe both laterally and axially.	Determine if the airframe is strong enough to withstand compressive forces that will occur when landing and ensure that it will not be damaged.
2	Airframe Resistance Drop Test	Fiberglass airframe, test parachute	Drop airframe material from height of at least 6 ft to simulate how launch vehicle would land after launch onto a similar landing terrain of grass. Assess resulting behavior of fiber glass.	Ensure that the airframe will not be damaged when landing. The height specified will result in expected airframe landing speed of 18 ft/s.
3	Bulkhead Resistance Test	PVC bulkhead, coupler, eyebolts, Instron Machine	Place coupler inside Instron Machine and pull on the eyebolts and bulkhead to simulate how bulkhead would behave during	Ensure that bulkheads will not be damaged when parachutes deploy.

			ejection and resulting shear forces.	
4	Rotation & Rolling Test	Ansys Simulation	Run a computer simulation and evaluate the resulting data concerning the rotation and rolling of the rocket.	Determine how severe the rotation (pitch and yaw moment) and rolling (axial motion) effects are during launch and stabilize the launch vehicle accordingly.
5	Nosecone Drag Test	Computational fluid dynamics (CFD) simulation software	Use CFD simulation to measure resulting drag from nosecone oriented at multiple angles.	Ensure drag is not too great on nosecone to affect flight and adjust nosecone accordingly.
6	Body Tube Drag Test	Computational fluid dynamics (CFD) simulation software	Use CFD simulation to measure resulting drag from body tube oriented at multiple angles.	Ensure drag is not too great on body tube to affect flight and adjust body tube accordingly.
7	Parachute Drag Test	Testing parachutes, weights, video camera	Attach weight to parachute and drop from a height of about 82 ft. Analyze the time versus height found in the recorded video and use data to calculate coefficient of drag for each parachute.	Establish which parachutes to utilize by determining which provides the appropriate drag to slow the launch vehicle during descent.
8	Fin Drag Test	Computational fluid dynamics (CFD) simulation software	Use CFD simulation to measure resulting drag from fin configuration oriented at multiple angles.	Ensure drag is not too great on fins to affect flight and adjust fins accordingly.
9	Recovery Altimeter Resolution Test	Entacore AIM Altimeter, Stratologger Altimeter	Place the altimeter at multiple heights.	Ensure both altimeters are detecting the correct altitude.

10	Barometer Functionality Test	Barometer, plastic straw	Place plastic straw over barometer, seal edges, and provide suction on the straw.	Ensure it reads change in pressure.
11	Main Parachute Ejection Test	Launch vehicle, main parachute, black powder, electric match, copper wires, test stand, altimeter, remote igniter	Fire ejection charge when launch vehicle is configured for ejection.	Ensure that main parachute will successfully deploy when the launch vehicle separates.
12	Drogue Parachute Ejection Test	Launch vehicle, drogue parachute, black powder, electric match, copper wires, test stand, altimeter, remote igniter	Fire ejection charge when launch vehicle is configured for ejection.	Ensure that drogue parachute will successfully deploy when the launch vehicle separates.
13	Recovery Harness Strength Test	Recovery harness, accelerometer	Induce an instantaneous force on the recovery harness. Determine yield strength of recovery harness. Compare strength value to calculated force estimate using accelerometer data and ensure yield strength exceeds expected force.	Determine if recovery harness is strong enough to withstand forces occurring during separation.
14	Zippering Test	Fiberglass, recovery harness	Induce an instantaneous force to simulate deployment.	Ensure there is no damage to the launch vehicle structure.
15	Black Powder Test	Launch vehicle, black powder, electric match, copper wires, test stand, altimeter, remote igniter	Ignite charges to commence ejection. Perform test for main parachute and drogue parachute.	Establish amount of black powder necessary for full separation of airframe and deployment of parachutes.
16	Vibrational	Launch vehicle	Simulate vibrational forces, similar to those expected	Ensure launch vehicle will not be damaged during launch due to

	Resistance Test		during launch, on payload.	vibrational movement.
17	RocketPoxy Weight Test	RocketPoxy epoxy, fiberglass	Weigh two pieces of fiberglass, epoxy pieces together with RocketPoxy and weigh once more.	Determine weight of epoxy per inch.
18	JBWeld Weight Test	JBWeld epoxy, fiberglass	Weigh two pieces of fiberglass, epoxy pieces together with JBWeld and weigh once more.	Determine weight of epoxy per inch.
19	Epoxy Heat Test	Epoxy, fiber glass	Create epoxy fillet between two pieces of fiberglass and place in sunlight for a minimum of two hours.	Verify that epoxy will not overheat and soften.
20	Epoxy Strength Test	Epoxy, fiber glass, Instron Machine	Create epoxy fillet between two pieces of fiberglass and place in the Instron Machine. Record any resulting separation between fiberglass bonding surfaces and compare to calculated expected landing forces.	Determine if epoxy will uphold during large compressive forces during landing and ensure it will not allow fins to separate from launch vehicle.
21	Parachute Packing Test	Main and drogue parachute, parachute cover, airframe, insulation, recovery harness, eyebolts, swivels	Fold parachute in an appropriate manner and place in airframe.	Ensure that parachute fits in airframe and will deploy smoothly.
22	Parachute Opening Test	Main and drogue parachute, recovery harness, airframe	Drop airframe from height of at least 20 ft.	Ensure that parachute opens correctly and does not get tangled. The drop height was set to give parachute

				ample time to open during descent.
23	Subscale Demonstration Launch	Subscale model in full configuration	Launch the subscale model.	Ensure all components of the subscale perform successfully.
24	Vehicle Demonstration Launch	Launch vehicle in full configuration	Launch the launch vehicle in its final configuration.	Ensure all components of the launch vehicle perform successfully.
25	Launch Rehearsal	Launch vehicle and payload in full configuration	Fully assemble launch vehicle (without the motor) and payload in appropriate amount of time.	Determine required amount of time to assemble launch vehicle in order to prepare for final launch day and ensure preparation can be completed in less than 2 hours.

Table 53: Launch vehicle testing plan.

6.2.2 Payload Testing Plan

The testing plan for the payload are defined (Table 54).

Test Number	Test Name	Required Materials and Machinery	Test Procedure	Justification
26	Drone Camera Landmark Test	OV5642 camera, testing drone	Place payload camera on a testing drone and fly it to predicted altitude, then fly back to the ground. Allow camera to take photos during ascent and descent. Perform test for both the cameras.	Ensure camera can capture sufficient keypoints during ascent and descent time.
27	Drone Camera Quality Test	OV5642 camera, testing drone	Place payload camera on a testing drone and fly it to predicted altitude, then fly back to the ground. Allow	Ensure the quality of the images captured is high enough to detect

			camera to take photos during ascent and descent. Perform test for both the cameras.	sufficient keypoints.
28	Field-of-View Test	OV5642 camera, testing drone	Place payload camera on a testing drone and measure the distance the camera can see. Confirm observations with calculations of field-of-view. Perform test for both the cameras.	Determine the field-of-view of the cameras.
29	Drone Offset Test	OV5642 camera, gyroscope, testing drone	Place payload camera on a testing drone and fly it to predicted altitude. Fly drone at multiple angles and observe angle of offset. Apply offset calculations to code.	Determine angle of offset of camera to ensure camera can adjust its angles.
30	Battery Life Test	Battery, payload	Allow battery to run for a minimum of 2 hours.	Ensure that the battery can maintain a charge so that the launch vehicle can be launch-ready for at least 2 hours.
31	Accelerometer Accuracy Test	Accelerometer, recovery harness, eyebolt	Simulate launch movement by attaching accelerometer to recovery harness and spinning it. Move the spinning accelerometer a straight measured distance.	Ensure it is reporting the appropriate displacement.

32	Heat Resistance Test	Payload, fiberglass airframe, thermometer	Place payload inside airframe and allow it to run software while leaving it outside in sunlight for a minimum of 2 hours. Measure temperature using thermometer and assess possible resulting damage from heat.	Ensure that the payload will not overheat so that the launch vehicle can be launch-ready for at least 2 hours.
33	Ejection Resistance Test	Payload, black powder, copper wire, electric match, test stand, remote igniter, launch vehicle	Perform a separation ejection test with payload inside launch vehicle.	Ensure payload will not be damaged from ejection charges.
34	Power Loss Test	Launch vehicle in launch configuration, payload	Momentarily disconnect power when the launch vehicle is configured for launch. Assess if the system's redundancies allow it to recover and continue operation.	Ensure payload will continue operation correctly in a circumstance of loss of power.
35	Vibrational Resistance Test	Payload	Simulate vibrational forces similar to those expected during launch on the payload.	Ensure payload will not be damaged during launch due to vibrational movement.
36	Payload Drop Test	Payload, airframe, test parachute	Drop payload in airframe from height of at least 6 ft. to simulate how payload would land after launch.	Ensure payload will not be damaged when landing. The height specified will result in expected launch vehicle landing speed of 18 ft/s.

37	Strength of Camera Mount Test	Computational fluid dynamics (CFD) simulation software	Use CFD simulation to determine forces on camera and camera mount during launch.	Ensure payload will remain attached securely to the airframe during launch.
38	Static Firing Test	Motor, motor retention system, test stand, fiberglass airframe, payload	Test stand will be designed and built by the Structures Lead. Configure payload and motor inside airframe, place on test stand, and fire the motor.	Ensure that payload cameras and wiring do not overheat as the motor fires.
39	Software Implementation Test	OpenCV software, payload	Run code utilized for payload completely through.	Evaluate if software is properly implemented with hardware and debug code if necessary.
40	Raspberry Pi Functionality Test	Raspberry Pi, starter kit software	Plug Raspberry Pi into laptop and run starter kit software.	Ensure Raspberry Pi is functioning correctly and determine if there are any bugs in the system.
41	Inertial Measurement Unit (IMU) Functionality Test	IMU, testing kit software, Raspberry Pi	Plug IMU into laptop, orient it in a certain configuration, and collect acceleration and orientation data. Compare collected data to measurements made of the current orientation.	Ensure IMU is measuring correctly and determine if there are any bugs in the system.
42	XBee Radio Functionality Test	XBee radio, serial converter, X-CTU software, Raspberry Pi	Plug the XBee transmitter and XBee receiver into separate laptops and	Ensure the XBee radios are able to

			send data packets through X-TCU.	establish a connection.
43	Microprocessor Functionality Test	Microprocessor, computer	Plug microprocessor into computer and upload an example program.	Ensure microprocessor is functioning correctly.
44	SD Card Functionality Test	SD card, computer	Write data to the SD card through the Raspberry Pi. Read back data and confirm that it matches the originally written data.	Ensure SD card is functioning correctly.
45	Payload Altimeter Functionality Test	Payload Altimeter	Place the altimeter at multiple heights.	Ensure altimeter is detecting the correct altitude.
46	Wire Tube Test	Electronics tubes, centering rings, airframe	Configure wire tube set-up and determine if tube interferes with centering rings and if tube fits in airframe.	Ensure that wire tube is large enough to protect wires without compromising motor position.
47	Payload Launch Detection Test	Raspberry Pi, barometer, IMU	Induce a sudden movement on the payload from rest.	Ensure that the payload can detect sudden acceleration and thus detect launch initiation.
48	Payload Data Compilation Test	Fully configured payload	Run the software in completion and determine the amount of time required for the payload to compile the received data.	Ensure that the payload can compile at least 100 images in the given time of five minutes.

49	Payload Transmission Range Test	Xbee radio, Raspberry Pi	Test the transmission ability of the payload.	Ensure it has a transmission range of at least one mile.
50	IMU Drift Test	Payload MTI-3-0I IMU	Measure the offset error produced by the IMU while at rest. Evaluate this data over 90 s. to determine the expected drift.	Ensure the expected drift does not exceed 100 ft. in the allotted time frame of 90 s.
51	Payload Demonstration Flight	Launch vehicle and payload in full configuration	Launch fully constructed payload in launch vehicle.	Ensure payload captures sufficient keypoints and defines location.

Table 54: Payload testing plan.

6.2.3 Testing Safety by Reference Number

The necessary safety precautions that must be taken when performing the listed tests are detailed. The table refers to each test by its number and includes a description of the safety steps that will be taken (Table 55).

Test Number	Safety Precautions
1	The Instron Machine will only be operated by permitted personnel while other team members will maintain a safe distance from the machine when in use.
2	The airframe will be dropped at a safe distance away from team members or pedestrians.
3	The bulkhead will be dropped at a safe distance away from team members or pedestrians.
4	Not applicable, negligible risk.
5	Not applicable, negligible risk.
6	Not applicable, negligible risk.
7	The parachutes will be dropped at a safe distance away from team members or pedestrians.
8	Not applicable, negligible risk.
9	Not applicable, negligible risk.
10	Not applicable, negligible risk.
11	Team members will maintain a safe distance of 25 ft. from the launch vehicle during ejection.
12	Team members will maintain a safe distance of 25 ft. from the launch vehicle during ejection.

13	Team members will maintain a safe distance of 25 ft. from the launch vehicle during induced force.
14	Team members will maintain a safe distance of 25 ft. from the launch vehicle during induced force.
15	Team members will maintain a safe distance of 25 ft. from the launch vehicle during ejection.
16	Team members will maintain a safe distance of 25 ft. from the launch vehicle during vibrational simulation.
17	Not applicable, negligible risk.
18	Not applicable, negligible risk.
19	Not applicable, negligible risk.
20	The Instron Machine will only be operated by permitted personnel and other team members will maintain a safe distance from the machine when in use.
21	Not applicable, negligible risk.
22	The airframe will be dropped at a safe distance away from team members or pedestrians.
23	Team members will follow safety regulations set by the NAR/Tripoli Range Safety Officer.
24	Team members will follow safety regulations set by the NAR/Tripoli Range Safety Officer.
25	Not applicable, negligible risk.
26	Team members will maintain a safe distance from the drone during takeoff and landing.
27	Team members will maintain a safe distance from the drone during takeoff and landing.
28	Team members will maintain a safe distance from the drone during takeoff and landing.
29	Team members will maintain a safe distance from the drone during takeoff and landing.
30	Not applicable, negligible risk.
31	Team members will maintain a safe distance from accelerometer when spinning it.
32	Not applicable, negligible risk.
33	Team members will maintain a safe distance of 25 ft. from the launch vehicle during ejection.
34	Not applicable, negligible risk.
35	Team members will maintain a safe distance from the launch vehicle during vibrational simulation.
36	The payload will be dropped at a safe distance away from team members or pedestrians.
37	Not applicable, negligible risk.

38	Team members will maintain a safe distance from the launch vehicle during firing and fire extinguishers will be provided in case of emergency.
39	Not applicable, negligible risk.
40	Not applicable, negligible risk.
41	Not applicable, negligible risk.
42	Not applicable, negligible risk.
43	Not applicable, negligible risk.
44	Not applicable, negligible risk.
45	Not applicable, negligible risk.
46	Not applicable, negligible risk.
47	Team members will maintain a safe distance from the launch vehicle during acceleration simulation.
48	Not applicable, negligible risk.
49	Not applicable, negligible risk.
50	Not applicable, negligible risk.
51	Team members will follow safety regulations set by the NAR/Tripoli Range Safety Officer.

Table 55: Testing safety

6.3 Completed Tests

Test #17, RocketPoxy Weight Test, was conducted.

6.3.1 Test #17 – RocketPoxy Weight Test

This test was conducted to determine the total weight of RocketPoxy epoxy implemented in the design. Two pieces of fiberglass were weighed and then epoxied together with RocketPoxy using a fillet technique. The epoxy was mixed with equal parts resin and hardener and the epoxied pieces were left to harden for 30 mins. The fillet technique was achieved by applying epoxy to the corner where the two fiberglass pieces met, and the epoxy was smoothed out with a 1-in. wooden popsicle stick to create a fillet.

The calculation performed to determine the total weight of RocketPoxy required for the launch vehicle was performed. A 5 in. fiberglass piece weighs 1 oz., a 6 in. fiberglass piece weighs 3.2 oz., and the total weight of the epoxied fiberglass pieces is 4.6 oz. Therefore, the epoxy weight is 0.4 oz. This weight is divided by the 5 in. to find that the epoxy has a density of 0.08 oz/in. The fins implemented in the launch vehicle design are 10 in. long, and therefore required 0.8 oz. of epoxy per side of each fin. The fins are epoxied on both sides to the outside of the airframe so therefore, this weight was multiplied by 2 to account for both sides of the fin. There are 4 fins implemented on the launch vehicle, so the total weight of the external epoxy required for the fins is 6.4 oz. The fiberglass pieces that were epoxied for this test are shown (Figure 60).

Figure 60: Fin fillet epoxy test

6.4 Budgeting and Timeline

6.4.1 Funding

6.4.1.1 Funding Plan

This project will be primarily funded by the University of Florida's Student Government during the Fall 2021 semester. The team will also be seeking funding from the University of Florida's Mechanical and Aerospace Engineering Department. The request approval will determine how much funding is allotted to travel and the full-scale rocket build in the Spring 2021 semester. The team sponsor is Aerojet Rocketdyne. The team is actively seeking more corporate sponsorships by having weekly meetings specifically dedicated to reaching out to potential sponsors. The sponsorships range from $250 to $1,000, with additional donations made optional. Funding will first be received by our advisors, Dr. Lind and Dr. Niemi, and will then be allocated to our group. The team has also started an alumni program to stay in touch with dedicated members who have graduated, encouraging them to stay involved and support the future of the group.

6.4.1.2 Funding Contingency Plan

Since the team's funding comes primarily out of the University's Student Government, unforeseen budget cuts should be accounted for by a mitigation plan. Although the team was allotted funding with margins for additional purchases in the Fall 2021 term, a contingency plan is important since the campus has returned to in-person activity, and it is suspected that the University has had to make budget cuts as well. Team component purchases have been made in bulk using the Fall 2021 term funding. The purchase included the components needed for the current project, as well as components to increase stock of components to account for required activities. If the team's funding is reduced below what the design has accounted for, the team will adjust their designs as necessary.

6.4.2 Budgeting

The team's expected budget for the 2021-2022 season is $5,600.00 (Figure 61), (Table 56). This budget is based off a total of all estimated component and travel costs, including components needed for the full-scale rocket design and the subscale rocket build. It also accounts for changes that may occur from any necessary changes and testing or unexpected damages. The components are broken down by rocket subgroup (Table 57) and listed out (Table 58, Table 59, Table 60, Table 61, Table 62). Travel costs are also included in the budget accounting for road travel and hotel stays for the competition and launches.

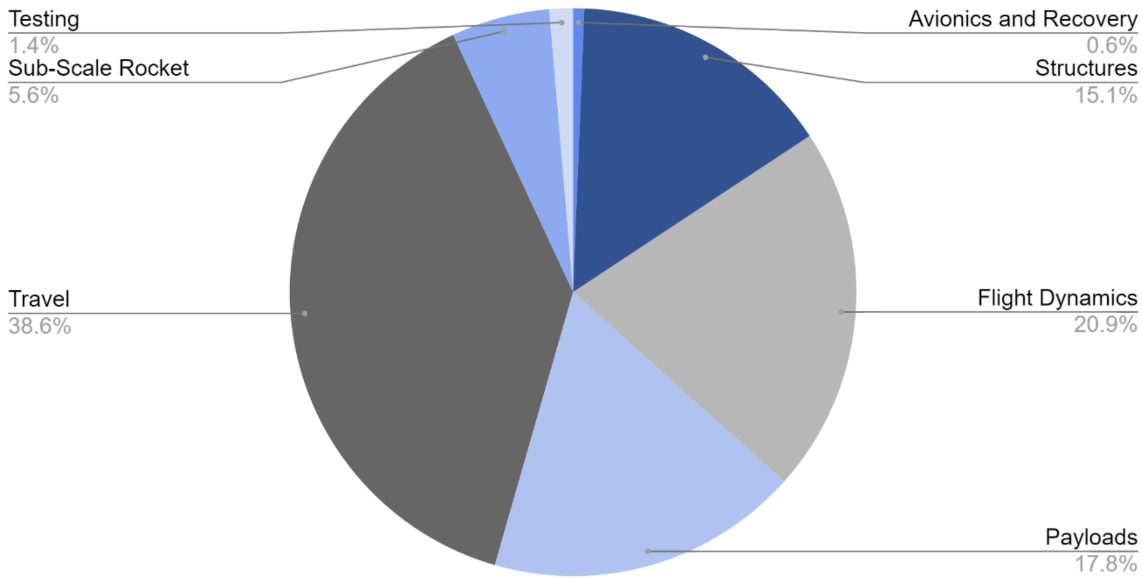

Figure 61: Budget pie chart.

Category	Total Cost ($)
Full-Scale Rocket	3,225.00
Travel	2000.00
Subscale	291.23
Testing	70.00
Total:	5586.23

Table 56: Project costs by category.

Subgroup	Total Cost ($)
Structures	782.31
Avionics and Recovery	33.13
Flight Dynamics	1082.34
Payloads	925.34
Total:	3225.00

Table 57: Full-scale rocket costs by subgroup.

Component	Quantity	Unit Cost ($)	Total Cost ($)
4" 5:1 fiberglass Ogive nosecone w/ metal tip	1	79.95	79.95
4" diameter fiberglass airframe (5 ft)	2	116.75	233.50
2.1" fiberglass motor tube (3 ft)	1	43.20	43.20
3/16" thick, 24" x 24" G10 fiberglass sheets (fins)	2	51.30	102.60
1/2" thick, 24" x 24" plywood (bulkheads, centering rings)	2	17.60	35.20

Jewel (10 oz)	4	14.27	57.08
RocketPoxy (2 qt)	2	85.31	170.62
Shear Pins	4	3.52	14.08
Rivets	4	7.41	29.64
Rail buttons	2	8.22	16.44
Sandpaper	N/A	N/A	Inventory
Total:			782.31

Table 58: Structure's costs by component.

Category	Quantity	Unit Cost ($)	Total Cost ($)
9 V Battery	2	8.00	16.00
Eyebolt	4	4.28	17.12
Main Parachute	1	N/A	Inventory
Drogue Parachute	1	N/A	Inventory
Recovery Harness	2	N/A	Inventory
Swivel	2	N/A	Inventory
Quick Link	6	N/A	Inventory
Altimeter	2	N/A	Inventory
Terminal block	4	N/A	Inventory
Key lock switch	2	N/A	Inventory
Total:			33.13

Table 59: Avionics and recovery's costs by component.

Category	Quantity	Unit Cost ($)	Total Cost ($)
Motor Retainer	1	46.66	46.66
Motor Forward Closure	1	77.52	77.52
Motor Aft Closure	1	56.18	56.18
Motor Casing	1	203.92	203.92
Thrust Plate	1	44.87	44.87
Aerotech J1090W	3	217.73	653.19
Total:			1082.34

Table 60: Flight dynamics' costs by component.

Category	Quantity	Unit Cost ($)	Total Cost ($)
Digital Signal Processor	2	86.00	172.00
OV5640 Camera	4	24.99	99.96
XBee Transceiver	4	54.08	216.32
Lithium-Ion Batteries	4	14.50	58.00
IMU	4	59.78	239.12
Altimeter	2	12.98	25.96
Printed Circuit Board	5	12.00	60.00
Wiring	1	5.99	5.99
JST Connector Kit	1	23.99	23.99
1/4-20 Well Nuts	4	6.00	24.00
1/4-20 Fasteners	8	N/A	Inventory

1/4-20 Hex nuts	4	N/A	Inventory
Total:			925.34

Table 61: Payload's costs by component

Category	Quantity	Unit Cost ($)	Total Cost (includes shipping) ($)
3" diameter fiberglass nosecone	1	59.95	59.95
3" diameter fiberglass airframe	2	102.55	205.10
1.5" diameter motor tube (2 ft)	1	26.18	26.18
Total:			291.23

Table 62: Subscale structural costs

6.4.3 Schedule

To ensure that all deliverables for the project were completed in the required timeframes, an overall project schedule was developed. Additionally, the schedule was broken up into individual schedules that highlighted each subteam's responsibilities.

6.4.3.1 Overall Project Schedule

An overall project schedule was developed for the team to account for all project milestones and test flights, as well as allow time for the necessary preparations including manufacturing, purchase orders, and design revisions (Figure 62).

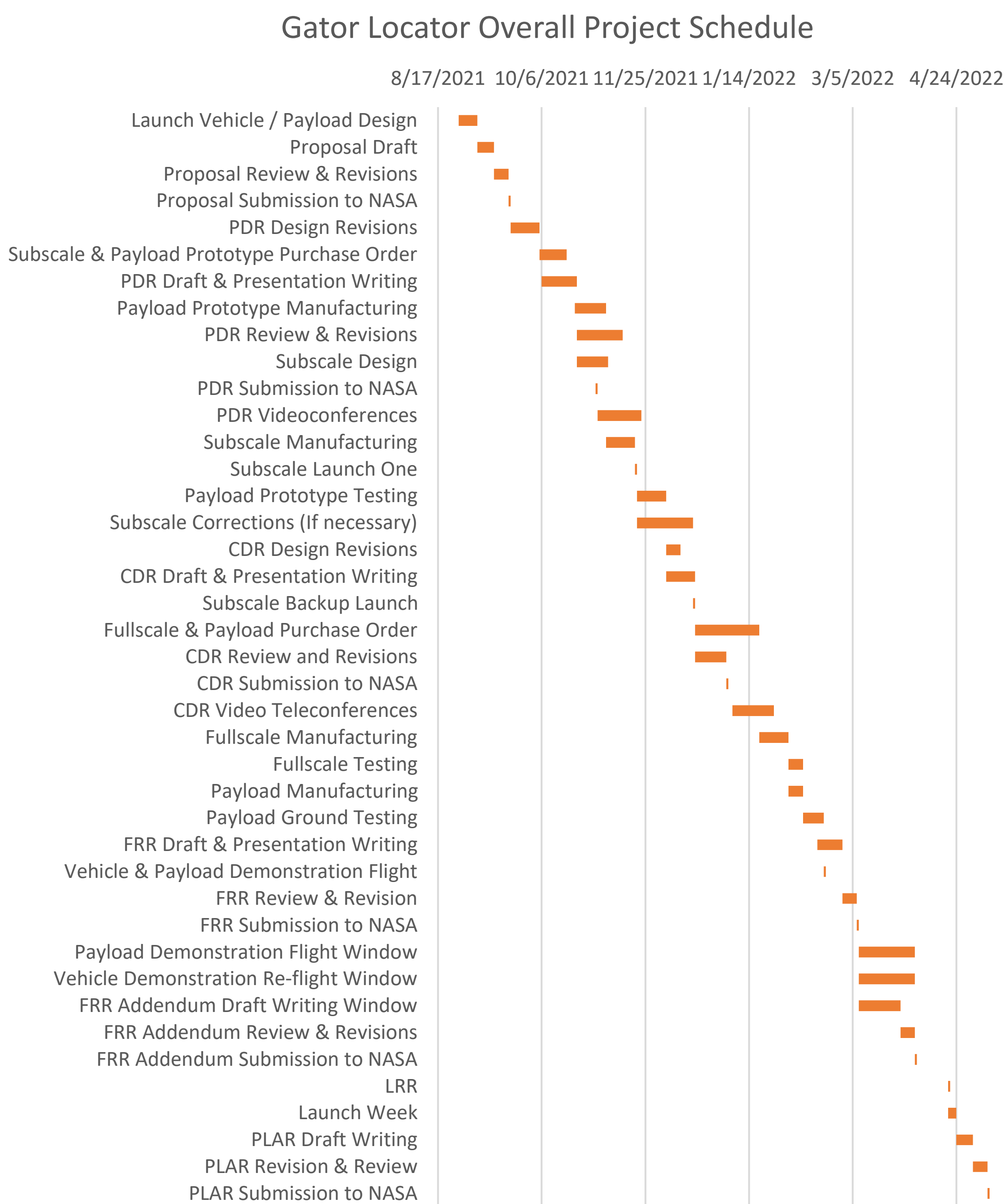

Figure 62: Gator Locator project schedule

6.4.3.2 Flight Dynamics and Simulation Schedule

A flight dynamics and simulation schedule was developed for the Flight Dynamics subteam to ensure all requirements were completed along with the associated milestones (Figure 63).

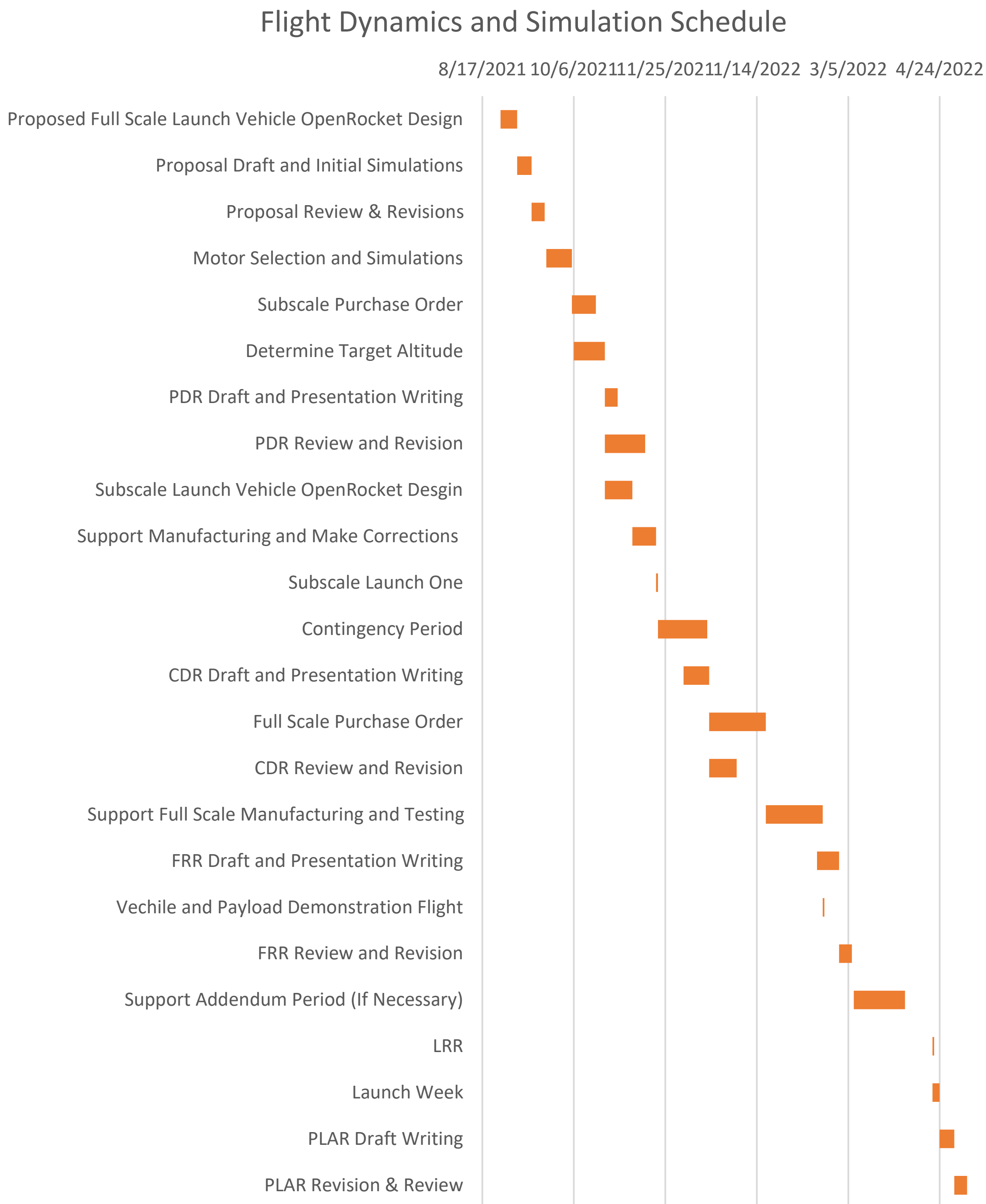

Figure 63: Flight dynamics and simulation schedule.

6.4.3.3 Structures and Manufacturing Schedule

A structures and manufacturing schedule was developed for the Structures and Avionics and Recovery subteams to ensure that all designs and manufacturing were completed in line with the milestone deadlines (Figure 64).

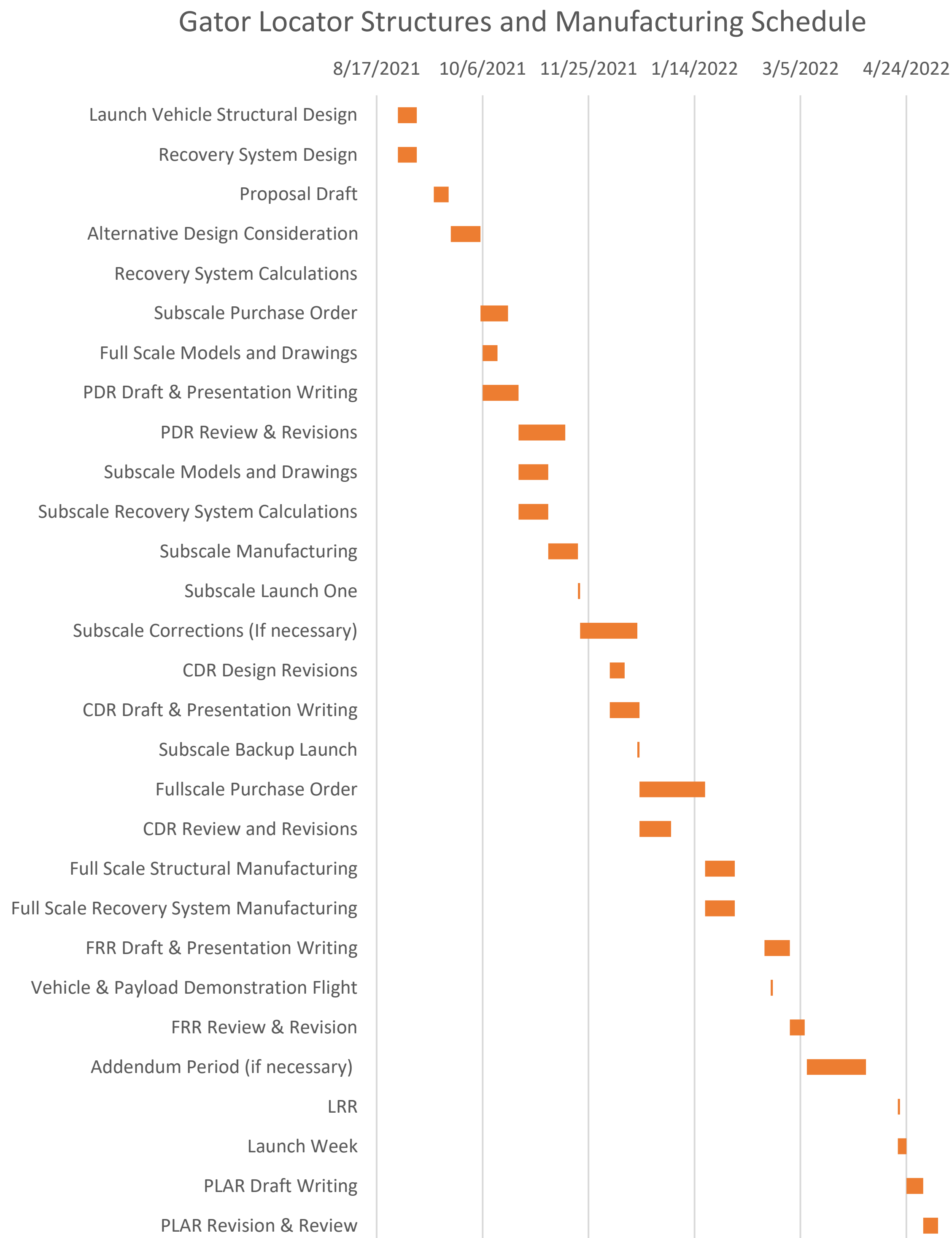

Figure 64: Gator Locator structures and manufacturing schedule.

6.4.3.4 Payload Development and Manufacturing Schedule

A payload development and manufacturing schedule was formulated to ensure the payload design would be prepared to successfully complete the mission for each given milestone (Figure 65).

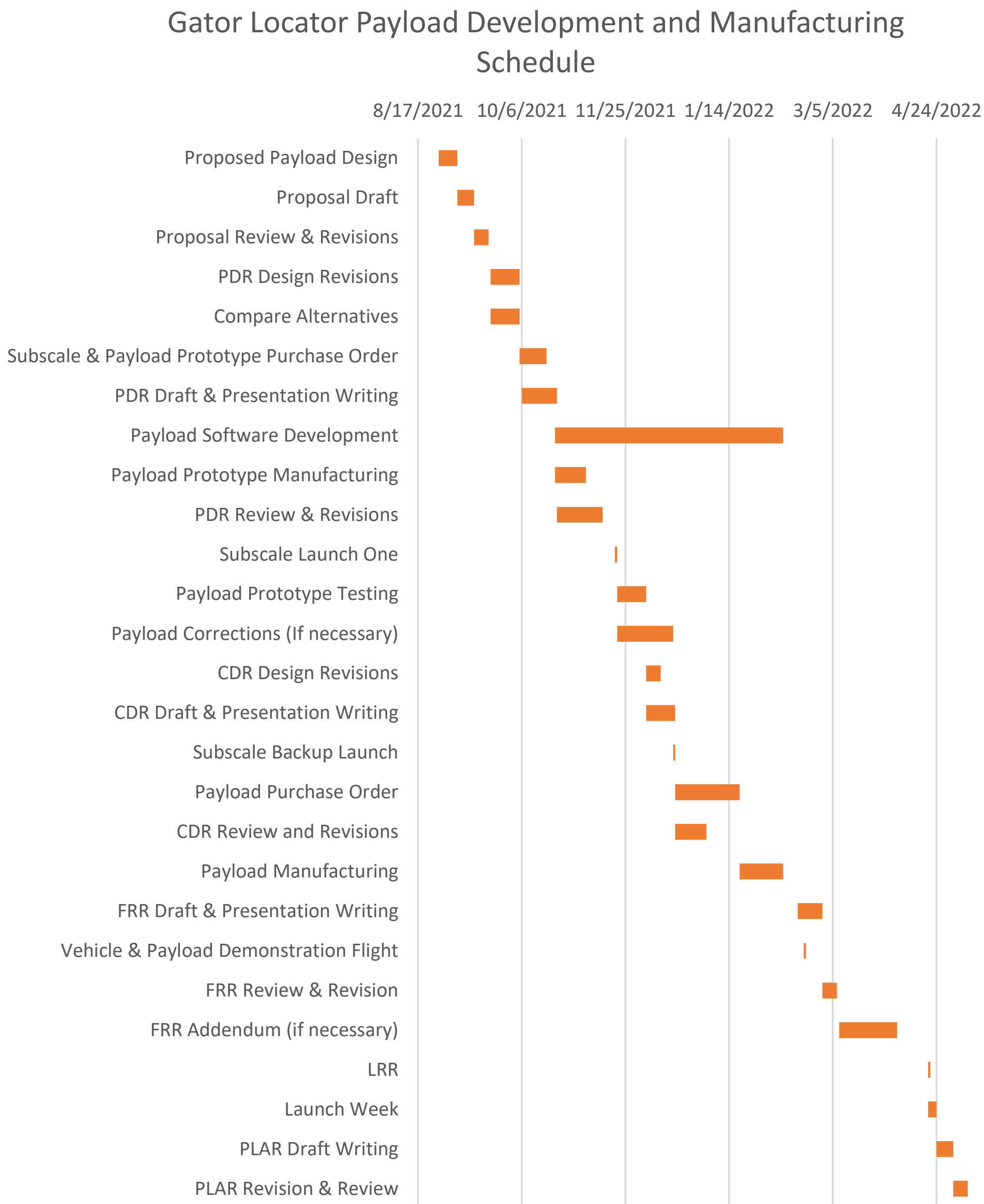

Figure 65: Gator Locator payload development and manufacturing schedule.

6.4.3.5 Testing Schedule

A testing schedule was developed to determine the time allotted to safely test the components aligned with each milestone (Figure 66).

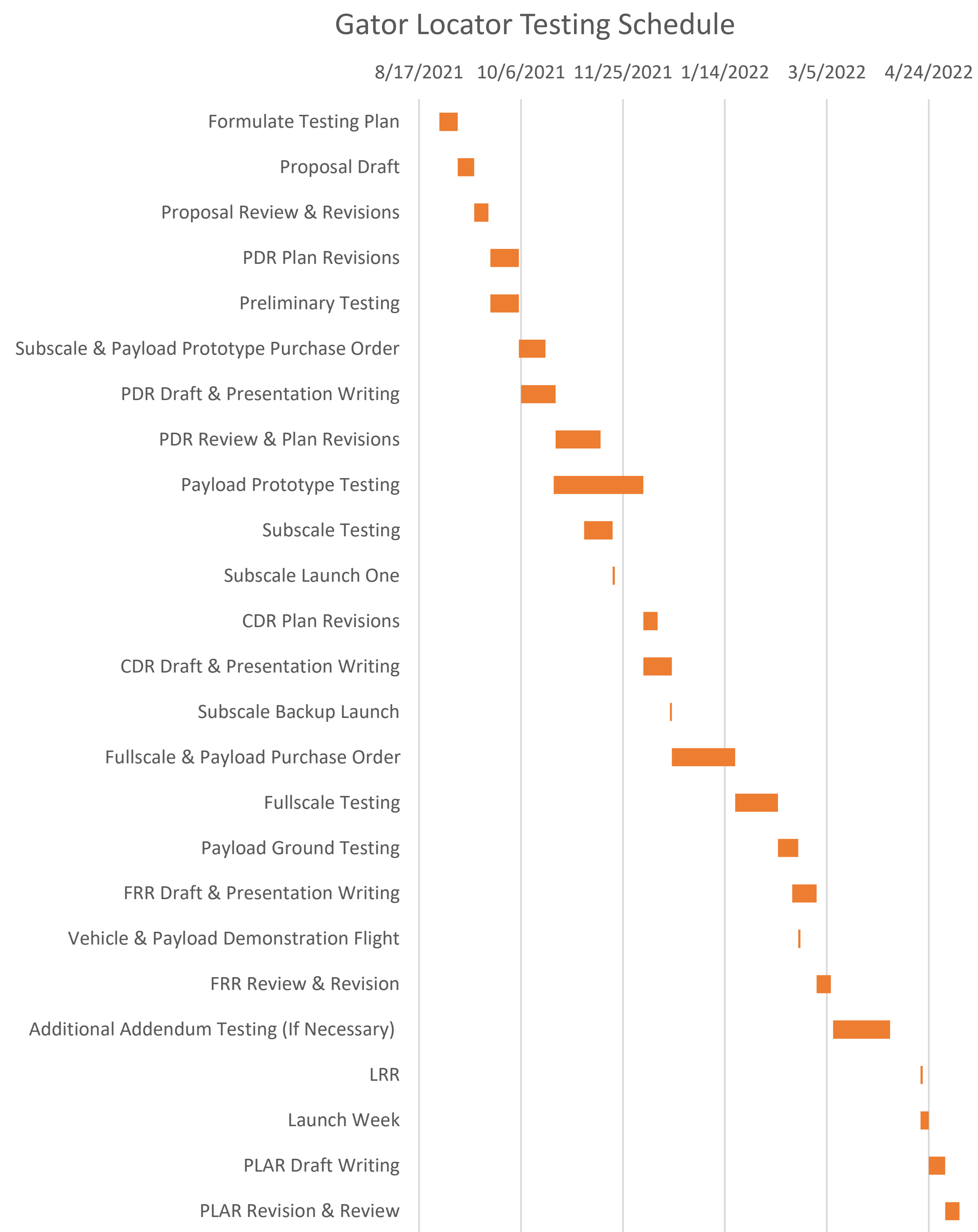

Figure 66: Gator Locator testing schedule.

6.5 Conclusion

In conclusion, Swamp Launch Rocket Team is confident in the capabilities of the leading designs identified during the Preliminary Design Review and their abilities to comply with all competition and team derived requirements.